GLOBAL JOURNAL OF GEOLOGICAL SCIENCES VOL. 6 NO. 2 2008: 95 - 104
 ISSN 1596 – 6798

STATISTICAL ANALYSIS OF TRACE ELEMENT CONCENTRATIONS IN SHALE – CARBONATE SEDIMENTS FROM NORTHEASTERN NIGERIA

E. E. NTEKIM, D. M. ORAZULIKE AND E.C. ASHANO

(Received 22 August, 2007; Revision Accepted 10 September, 2007)

ABSTRACT

Principal component and regression analysis of geochemical data in sampled shale – carbonate sediments in Guyuk, Northeastern Nigeria reveal enrichments of four predictor elements, Ni, Co, Cr and Cu to gypsum mineralisation. Ratios of their enrichments are Cu(10:1), Ni(8:1), Co(58:1) and Cr(30:1) The >70% intercorrelations between these elements plus >32% common factor loading and observed significant regression of Ca and Fe on Cu, Cr, Ni and Co depicts strong association between these trace elements and process of gypsum mineralisation.

KEYWORDS: intercorrelations, regression, factor analysis, predictor elements, gypsum, shale.

INTRODUCTION

Shale and carbonate rocks are common favourable sediments associated with sedimentary ores, including evaporites. This is principally due to the chemical nature of these sediments. Petrogenetically, carbonates and evaporites (commonly referred to as chemical precipitates) are closely related. These two, in turn, closely associate with shale due to progressive rhythmic carbonate sedimentation in regressive marine environments (Wilkinson, 1982; Boggs, 1987) and constituent clayey materials in the shale on which evaporites (especially gypsum) get adhered to. Repeated cyclic sequences of carbonate platforms are deposited during the quiet standstill phases and thick shale beds accumulation, occasioned by the pervasive low water energy conditions that follow periods of flooding during eustatic upheavals (Boggs, 1987). These "shorter-lived", fluctuations in sedimentation conditions is known to influence chemical sedimentation in evaporite basins through suspension mechanism, where thin gypsum laminations (of only few millimeters thickness) alternate with dark-gray laminae of carbonate and shaley rocks. Boggs (1987) suggests that the alternating gypsum (light) and lithologic (dark-gray) pairs of bands represent seasonal changes in water chemistry and temperature during the cyclic disturbances. These rhythmic sequences, which are observed in locations within the Upper Benue valley, Nigeria (Fig 1) reveals that the gypsum beds occur in shale strata adjoining limestone beds (Ntekim and Orazulike, 2003), especially at Dukul, Gudenyi, Lakoro, Gunda and Lamza. Vertical stratigraphic sequence examined along cuts on cliff slopes and stream courses in the study area is typical of carbonate sedimentation in marine environment (Boggs, 1987). The associated carbonate rocks (calcareous sandstones and limestone) with the shale attests to a carbonated environment, a necessary chemical condition for gypsum mineralisation (cf. Evans, 1978; Sonnenfeld, 1991; Uma, 1998). Probably the calcium carbonate minerals were altered in the adjoining limestone beds, and the Ca^{2+} ions were subsequently transported by the clay minerals into the shale where reaction with constituent free SO_4^{2-} ions produced the gypsum minerals.

Diagenesis of these typical marine chemical sediments (carbonates and evaporites), involve the breakdown and formation of various minerals and oxy-acid salts. Chemically the major cations in these rocks include Ca^{2+}, Mg^{2+}, Ba^{2+}, Sr^{2+}, Pb^{2+}, Fe^{2+}, Mn^{2+}, Zn^{2+}, Cu^{2+}, U^{2+}, Na^{+} and K^{+}, which are easily soluble in water. These, especially the major elements (Ca, Mg, Fe), participate in a wide range of geological processes during which isomorphic replacements between constituent cations take place. Such replacement is very pronounced in the various complicated sedimentation (both chemical and biochemical) processes during the formation of gypsum in enclosed sea basins (Milovsky and Kononov, 1985; Boggs, 1987). The relative concentrations of minor / trace elements, especially the base metals, are commonly used in geochemical exploratory studies to assess or delineate mineralisation, most especially ore bodies. Trace elements have great potential for use as mineralisation indicators or exploration pathfinders. They usually occur in trace amounts unless there is an anomaly hence; their determination can help detect abnormal chemical patterns, which may relate to mineralisation. In the present study, some major and trace element contents of the shale sediments were determined to examine their relationship to gypsum accumulation in the rock units.

E. E. Ntekim, Department of Geology, Federal University of Technology, Yola, Nigeria.
D. M. Orazulike, Geology Programme, Abubakar Tafawa Balewa University, Bauchi, Nigeria.
E. C. Ashano, Department of Geology and Mining, University of Jos, Nigeria.

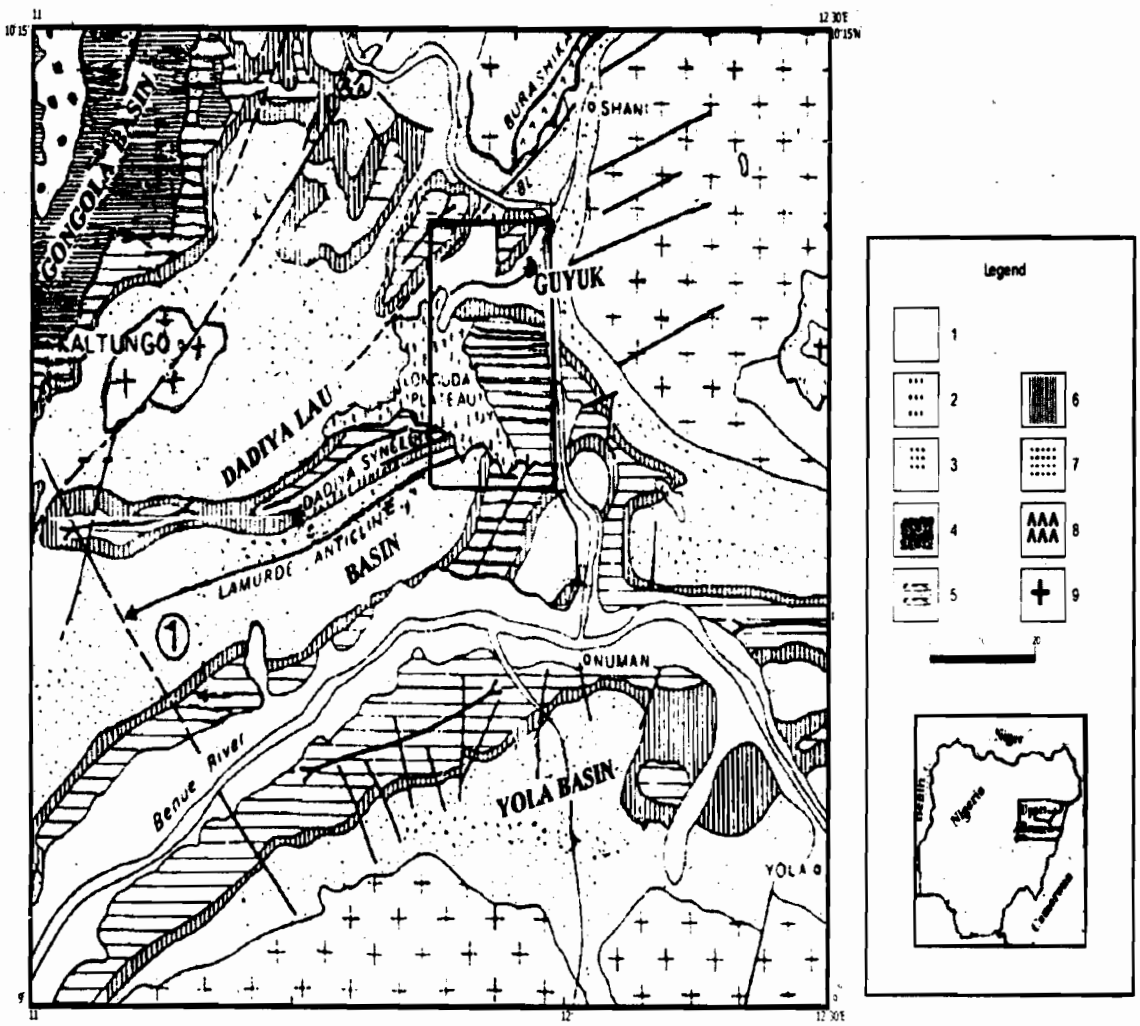

Fig. 1 Location of Guyuk within the Upper Benue Valley (Modified from Maurin et al, 1986)

1. Quaternary alluvium; 2. Tertiary to Recent volcanics; 3. Kerri Kerri Formation; 4. Gombe Formation; 5. Shale-limestone Formation; 6. Yolde Formation; 7. Bima Formation; 8. Burashika volcanics; 9. Undifferentiated Precambrian Basement. [Arean box is the Guyuk study area]

The purpose of this paper is to test statistically the abundance of trace elements in shale – carbonate rocks of Guyuk area in part of the lower Gongola basin of Nigeria and to develop a framework with which the likely gypsum mineralisation status of these rock types could be assessed on the basis of the distribution pattern of certain trace element contents.

Geology of the area

Several workers, including Opeloye (2002), Ntekim and Orazulike (2003) have studied the geology of Guyuk, the study area. Guyuk area (as part of the Upper Benue trough) has been affected by wrench faults and E – W trending submeridian normal faults, and has lithologic units that favour the formation of evaporites (Zaborski et al, 1997; Uma, 1998). The Late Cretaceous intense compressional earth movements, caused by deep-seated flexuring in the crystalline basement rocks determined the tectonic setting of the area (Carter et al, 1963; Benkhelil, 1986). Effects of these stresses produced narrow localised incipient basins, into which thick sedimentary sequences were later deposited. The sediments include detrital Bima sandstone, transitional Yolde, marine shale-limestone (Dukul, Jessu, Sekule and Numanha) units and partially continental Lamja sandstone, overlain by Tertiary Longuda basalts and a Quaternary river alluvium.

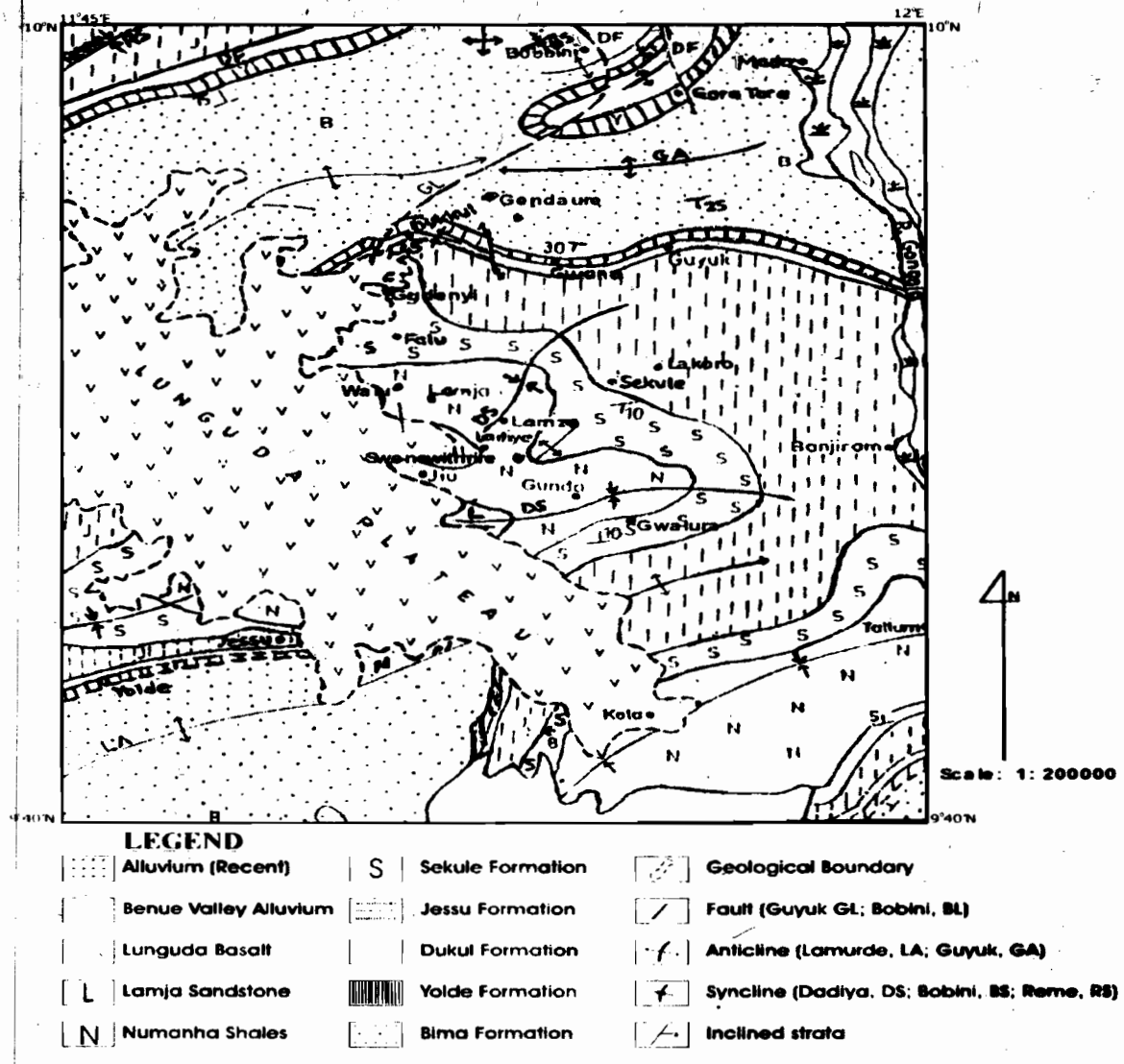

Fig. 2 Map of Guyuk Area showing Geology and Sample Locations (Modified from Carter et al, 1963)

The marine sediments consist of thick sequences of shale and fossiliferous limestone units and thin bands of siltstones and calcareous sandstone. The shale is black, carbonaceous and fossiliferous, and variously associated in the study locations. Encountered stratigraphic sections reveal shale – limestone – clay alternations at Gunda, Lamza, Walu, Dukul, Gudenyi, Bobini, Sukuliye and Lakoro; shale – mudstone alternations in Gwalura and Swenswithire; and sandy shale – clay alternations in Gwana. These associated stratigraphic sections reveal that Dukul, Sekule, Numanha and (lower parts of) Jessu Formations are enriched in gypsum in Guyuk area (cf. Braide, 1992).

METHOD

Principal component analysis (PCA) and regression statistical analyses were used to explore the data and establish statistical estimates of observed elemental distribution. Pearce (1976) suggests that statistical study of few analyses can be used to express the chemical variation in geological samples from particular sample locality. In this work, 40 shale samples and sixteen elements are used in the statistical analysis. The samples were selected after eliminating from the lists of collected samples, 10 outlier samples with much higher contents of the elements in relation to the rest of the samples. Concentration values used for the various analyses were log-transformed to reduce discrepancies between the values.

Beus and Grigorian (1975) submit that the ore producing (or mineralisation) potential in sedimentary formations can be assessed by various criteria, including abnormally high contents of principal metals, such as that make up the mineral deposit of interest, their association as well as increased variance in their distribution in rocks. In this work, the abundance and distribution variance of principal associated elements in shale and limestone samples collected from different localities in the study area were assessed. These include Ca, Fe, Mn, Cu, Zn, Ni, Co, Ba, Cr, As, Pb, Sr, Bi, Br, K and U.

RESULTS

Table 1 shows the indicator elemental concentration levels in the analysed shale – carbonate rocks. The population distribution of the relevant elements obtained from histogram plots, the correlation matrix from multiple correlation, PCA factor loadings and multiple regression obtained from the data are displayed in Figure 3 and Tables 2, 3 and 4. Most shale samples have concentration between 42.5 – 52.5ppm Ca. Fe(262.5 – 287.5ppm), Mn(1.5 – 2.5ppm), Cu(0.27

0.43ppm), Zn(0.22 - 0.28ppm), Ni(0.47 – 0.53ppm), Co(0.97 – 1.03ppm), Cr(2.38 – 2.62ppm), As(0.18 – 0.21ppm), Bi(0.13 – 0.16ppm). Average concentrations of the minor/trace elements vary within locations from 2610 – 8920 ppm Mn, Cu(300 – 670ppm), Zn(210 – 850ppm), Ni(380 – 1020ppm), Co(910 – 1590ppm), Cr(2250 – 4660ppm), As(160 – 300ppm), Pb(260 – 440ppm), Sr(790 – 3580ppm) and Ba(17750 – 31020ppm). In the limestone, mean concentrations of the minor/trace elements vary within the range Mn(6300 – 156030ppm), Cu(9820 – 29500ppm), Zn(310 – 1710ppm), Ni(630 – 1680ppm), Co(980 – 2560ppm), Ba(18440 – 61340ppm), Cr(2510 – 7150ppm), As(190 – 570ppm), Pb(300 – 860ppm) and Sr(720 – 4550ppm); and in clay samples, the average contents are Mn(1420 – 7580ppm), Cu(270 – 600ppm), Zn(180 – 690ppm), Ni(350 – 800ppm), Co(680 – 1450ppm), Ba(14720 – 33890ppm), Cr(1970 – 4460ppm), As(130 – 470ppm), Pb(180 – 710ppm) and Sr(1010 – 2680ppm). Generally, enhanced concentrations of the elements are observed at Lamza, Walu, Lakoro, Sukuliye, Gwalura and Gunda samples (Fig 4). The elements Ca, Fe, Mn, Sr, K and Ba are enriched in average shale and limestone rocks (Krauskopf, 1979; Mason and Moore, 1982) and Cr, Co, Cu, Ni, Zn, Pb, Bi, Br, U and As are normally in low concentrations in sediments, but are important constituents of both carbonate and clayey black shale that are concentrated in precipitating sulphide deposits (Milovsky and Kononov, 1985; Busek et al, 1991).

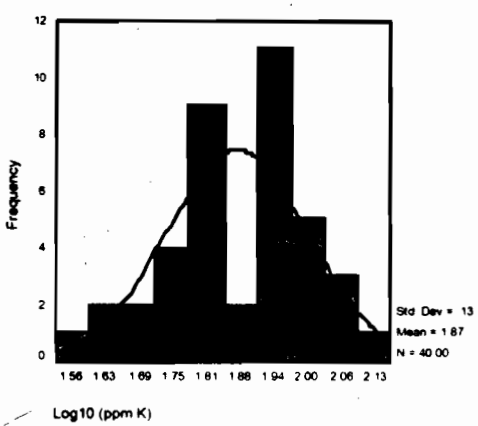

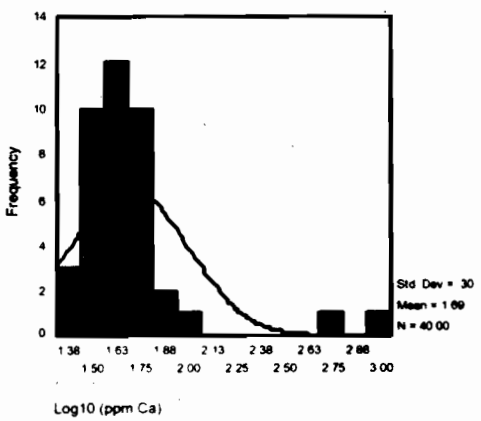

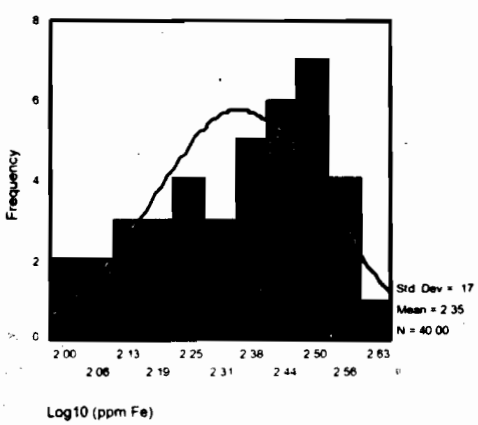

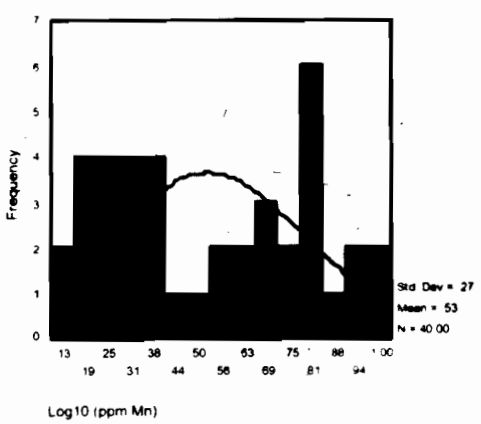

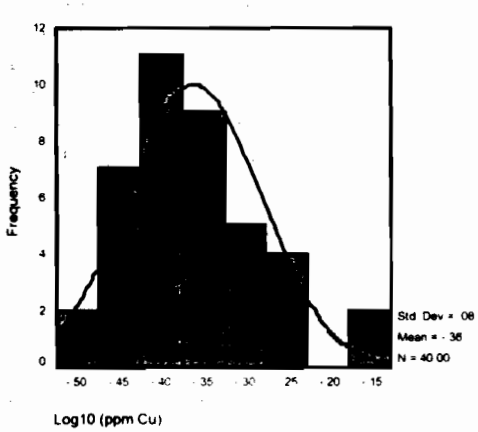

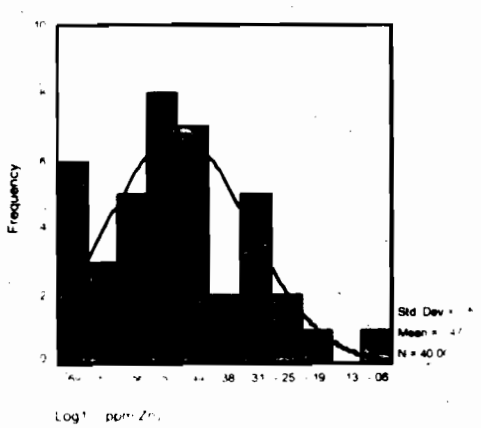

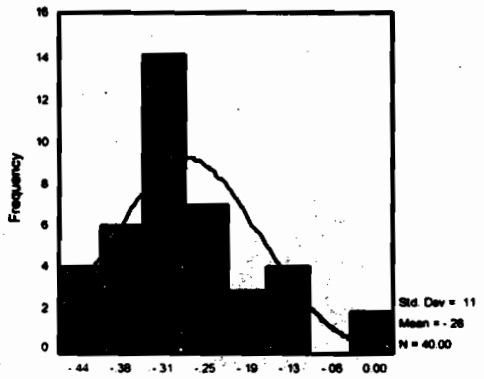

Log10 (ppm Ni)

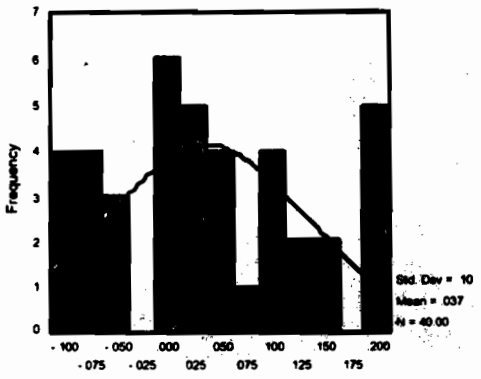

Log10 (ppm Co)

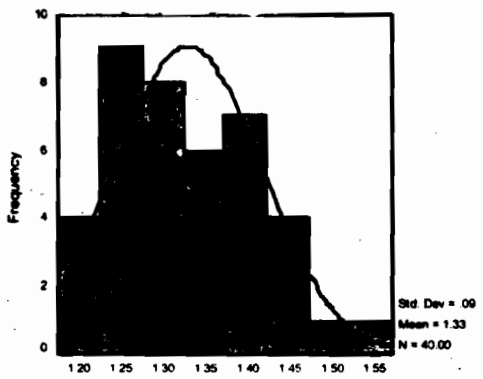

Log10 (ppm Ba)

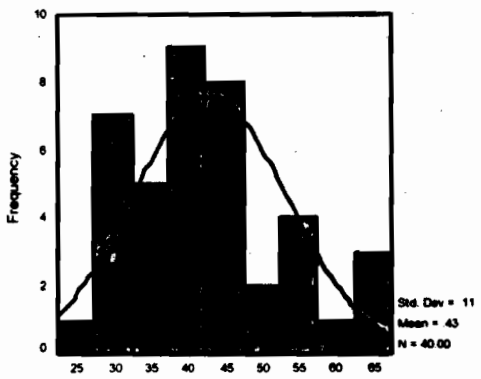

Log10 (ppm Cr)

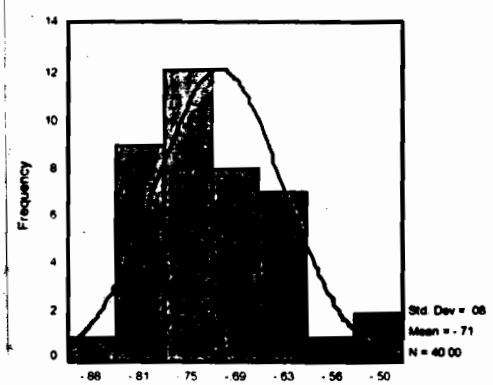

Log10 (ppm As)

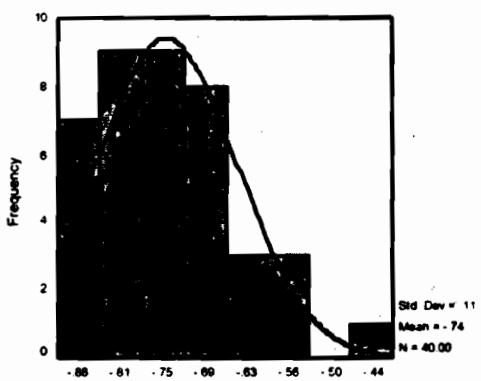

Log10 (ppm Bi)

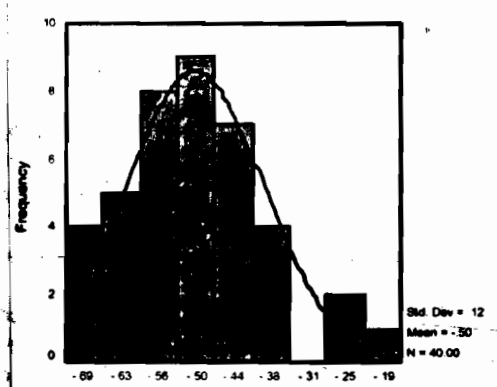

Log10 (ppm Pb)

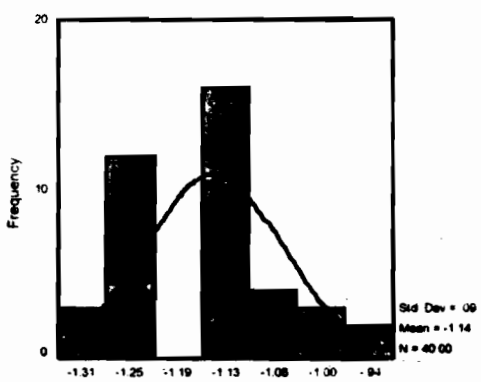

Log10 (ppm Br)

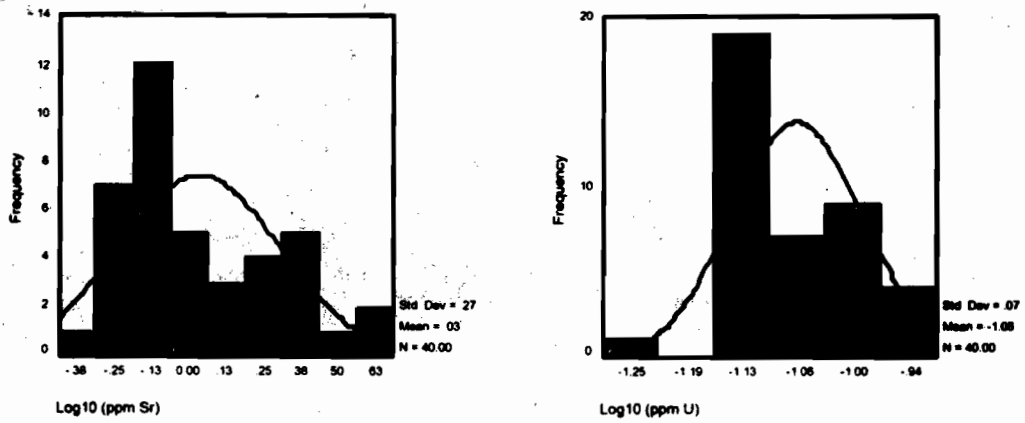

Fig. 3: Histogram plots of elemental concentrations in samples

Table 1: CONCENTRATION OF INDICATOR ELEMENTS IN SHALE SAMPLES (in $x10^3$ppm)

Element	STUDY LOCATION											A	Contrast
	1	2	3	4	5	6	7	8	9	10	Entire Area		
K	85.4	86.5	38.1	62.6	65.7	68.4	93.4	60.9	94.1	55.4	71.1		
Ca	45.4	43.8	41.6	400.0	50.5	39.7	57.1	488.2	75.6	357.9	159.9		
Fe	168.2	169.3	102.9	374.4	281.4	348.9	279.5	202.3	297.7	364.9	258.9		
Mn	2.61	4.70	1.59	11.66	3.72	14.40	3.60	9.70	6.99	15.70	7.50		
Ba	21.0	19.3	18.9	26.6	20.3	20.4	26.2	25.2	25.3	28.1	23.1		
Sr	1.02	1.02	0.79	1.86	0.95	0.83	1.87	2.98	2.43	1.98	1.60		
*Cu	0.41	0.40	0.37	0.52	0.36	0.45	0.55	0.53	0.61	0.76	0.49	0.046	11:1
*Zn	0.29	0.21	0.16	0.53	0.30	0.38	0.43	0.37	0.56	0.53	0.38	0.095	4:1
*Ni	0.48	0.44	0.35	0.77	0.45	0.63	0.52	0.65	0.71	0.87	0.59	0.072	8:1
*Co	0.90	0.98	0.65	1.23	0.99	1.24	1.31	1.27	1.41	1.46	1.14	0.019	60:1
*Cr	2.67	2.53	2.53	2.86	2.48	2.60	3.29	2.93	3.31	3.75	2.90	0.093	31:1
*As	0.19	0.17	0.13	0.23	0.16	0.19	0.22	0.22	0.26	0.28	0.21	0.012	18:1
*Pb	0.30	0.24	0.18	0.33	0.28	0.39	0.38	0.31	0.43	0.38	0.32	0.022	15:1
*Bi	0.17	0.16	0.13	0.21	0.14	0.18	0.21	0.22	0.25	0.27	0.19	0.005	38:1
*Br	0.07	0.06	0.05	0.08	0.06	0.07	0.09	0.09	0.10	0.10	0.08	0.045	1.8:1
*U	0.09	0.08	0.08	0.09	0.07	0.08	0.10	0.11	0.11	0.13	0.09	0.036	2.5:1

Key: 1 = Dukul; 2 = Gudenyi; 3 = Bobini; 4 = Lamza; 5 = Swenswithire; 6 = Walu;
7 = Lakoro; 8 = Sukuliye; 9 = Gwalura; 10 = Gunda.
A= Composite average in natural unmineralised shales (average of Krauskopf,1979; Rose et al,1979; Mason & Moore,1982 values)
* = Indicator elements
Contrast = Ratio of concentration in studied sediments to 'A' concentration.

DISCUSSIONS

Correlation coefficient of the data is determined to assess common intercorrelations between the constituent elements and principal component analysis is used to examine possible factors responsible for groupings of constituent elements. Correlation analysis of the analytical data confirmed this assertion. Table 2 shows significant correlation coefficients of the data set for shale samples. The analysis shows very high (>70%) intercorrelations between Ni, Bi, Cr, As, Cu, Br and U; and good (>50%) intercorrelation between other trace elements in the data set. Geochemically therefore, the environment is favourable for the simultaneous concentration of these elements. Principal component analysis of the data set shows that 72% of the proportion of variance for the 16 elements can be expressed in four R – mode factors (Table 3). Factor 1 has a high loading on Cu, Ni, Ba, As, Bi, Pb, Sr, Br, U, Co and Cr, and signifies the effect of gypsum mineralisation on the composition of the shale samples. These elements are closely associated with gypsum deposits (Boggs, 1987; Busek et al, 1991; Sonnenfeld, 1991). Factor 2 has a high loading on Fe, Cu, Zn, Ni, Co, Bi and Br, and represents the effect of petrogenetic late major and minor minerals (siderite, malachite, smithsonite, annabergite, erythrite, crocoite and associated alteration products rich in HBr and Bi_2O_3) that are commonly associated with the diagenetic alteration of carbonate rocks in oxidizing environments. Factor 3 has a high loading on K and negative loadings on the major petrogenetic and mineralisation indicator elements, signifying the effect of other minor minerals associated with gypsum e.g. polyhalite $[K_2Ca_2Mg(SO_4)_4]$. Factor 4 shows low factor loading on K, Mn, Cu and Pb, and negatively on all other elements in the data set, and can be interpreted to be other lithologic based geochemical signatures in the environment of deposition unrelated to gypsum mineralisation.

Table 2: Correlation Matrix For Elements in Shale Samples (40 – sample size)

	K	Ca	Fe	Mn	Cu	Zn	Ni	Co	Ba	Cr	As	Bi	Pb	Br	Sr	U
K	1.0															
Ca	-	1.0														
Fe	-	-	1.0													
Mn	-	-	-	1.0												
Cu	-	-	-	-	1.0											
Zn	-	-	.512	-	.587	1.0										
Ni	-	-	-	-	.644	-	1.0									
Co	-	-	.572	-	.696	.587	-	1.0								
Ba	-	-	-	-	-	-	.616	-	1.0							
Cr	-	-	-	-	.606	-	.701	-	-	1.0						
As	-	-	-	-	-	-	.621	-	.561	.508	1.0					
Bi	-	-	-	-	.741	.585	.737	.629	-	.657	.746	1.0				
Pb	-	-	-	-	-	-	-	.528	-	-	.625	-	1.0			
Br	-	-	-	-	.755	-	.674	.626	.658	.602	.670	.731	.585	1.0		
Sr	-	-	-	-	-	-	-	-	-	-	-	-	-	.570	1.0	
U	-	-	-	-	.644	-	.609	.523	.570	.563	.840	.749	.568	.804	.595	1.0

Note: - = value below 0.5 significance level

Table 3: Principal Component Analysis of Correlation matrix of Shale data (40 samples; samples 27, 36, 62, 81, 88, 92, 95, 96, 104, 105 omitted)

Element	Factors			
	1	2	3	4
K	0.264	-0.062	0.678	0.230
Ca	0.226	0.047	0.015	-0.901
Fe	-0.034	0.758	-0.413	-0.056
Mn	0.175	0.141	-0.845	0.185
Cu	0.559	0.630	-0.177	0.043
Zn	0 249	0.814	0.080	-0.089
Ni	0.604	0.402	-0.336	-0.379
Co	0.402	0.757	-0.044	-0.044
Ba	0.739	0.094	-0.335	-0.100
Cr	0.487	0.400	-0.201	-0.443
As	0.813	0.223	-0.009	-0.101
Bi	0.655	0 534	-0.074	-0.224
Pb	0.642	0 264	0 203	0.030
Br	0.819	0.363	-0.034	-0.164
Sr	0.640	-0.009	0.220	-0.290
U	0.876	0.255	0.149	-0.144
Cummulative %	32.4	19.8	11.1	9.1

Multiple regression analysis of the data is used to detect those samples in which element concentration is attributable to processes of mineralisation (Garrett, 1983; Howarth and Sinding-Larsen, 1983). Regression of the relevant major elements, Ca and Fe, against seven trace elements, Cu, Zn, Ni, Co, Cr, Pb and Sr reveals significant regression of Ca on Cu, Cr and Sr at 0.004, 0.033 and 0.048 values respectively; while Fe regressed on Ni, Co and Sr at 0.012, 0.001 and 0.021 values respectively. Other elements show values higher than the acceptable 0.05 significant levels (Table 4).

Table 4a **Shale Data: Regression of Ca on Cu, Zn, Ni, Co, Cr, Pb and Sr**
[Regression equation: Ca = 37.74 – 139.97Cu + 15.85Zn + 31.66Ni + 15.77Co + 10.20Cr – 16.06Pb + 5.57Sr]

Element	Coefficient	Std. Error	t ratio	Std. Coeff. Beta	Significance
Cu	-139.97	13.56	-3.08	-0.704	0.004
Zn	15.85	22.45	0.71	0.13	0.485
Ni	31.66	23.83	1.33	0.29	0.193
Co	15.97	15.59	1.01	0.22	0.319
Cr	10.19	4.57	2.23	0.44	0.033
Pb	-16.06	30.10	-0.0533	-0.09	0.597
Sr	5.57	2.71	2.06	0.32	0.048

F ratio for Cu, Zn, Ni, Co, Cr, Pb, Sr = 690.250/197.997 = 3.49

Table 4b: **Shale Data: Regression of Fe on Cu, Zn, Ni, Co, Cr, Pb and Sr**
[Regression equation: Fe = 28.94 – 272.72Cu + 133.76Zn + 283.77Ni + 249.49Co –16.42Cr – 189.16Pb – 29.35Sr]

Element	Coefficient	Std. Error	t ratio	Std. Coeff. Beta	Significance
Cu	-272.72	203.39	-1.341	-0.27	0.189
Zn	133.76	100.61	1.33	0.21	0.193
Ni	283.77	106.77	2.66	0.51	0.012
Co	249.49	69.85	3.57	0.69	0.001
Cr	-16.42	20.48	-0.80	-0.14	0.429
Pb	-189.16	134.91	-1.40	-0.21	0.170
Sr	-29.35	12.13	-2.42	-0.33	0.021

F ratio for Cu, Zn, Ni, Co, Cr, Pb, Sr = 23089.21/3976.08 = 5.81

From basic geochemical principles, the major probable indicator elements to gypsum mineralisation include Ca, Fe, Mn, Zn, Pb, Sr, Cu and Ba that participate in the various chemical processes during diagenesis of chemical precipitates (carbonates and evaporites) and Ni, Co, As and Cr, which are important constituents of both carbonate and clayey black shale that are notably concentrated in precipitating sulphide deposits (Keith and Degens, 1959; Milovsky and Kononov, 1985; Boggs, 1987; Busek et al, 1991). Considering the fact that major elements are not very indicative of environment of deposition (Ernst, 1970) and the petrogenesis of some of these elements, gypsum mineralisation indicators in this study area would include Ni, Co, As, Cr, Cu, Zn, Bi, Br, U and Pb. These indicator elements naturally occur in low concentrations in limestones and shale. When compared with research findings, their concentrations (Table 1) are several times more in studied sediments than in global natural unmineralised sediments, as obtained from Krauskopf (1979); Rose et al (1979); and Mason and Moore (1982).

Mean compositions of these indicator elements were examined in both the gypsum bearing and litho-beds that do not host gypsum bodies on the basis of obtained statistical data. Examination of the concentration levels using the standard (mean + 2 standard deviation) threshold mark reveal that about 4.6% of the samples contain anomalous concentrations of the elements. Using determined threshold value of each of the elements, about 2.9 – 8.6% of the gypsum-bearing shale samples are correctly identified as anomalous and about 91.4 – 97.1% are missed; and of the background values, 100% are correctly identified as non-gypsum bearing (Table 5). Of interest is that concentrations of K and Fe in all the samples were below the threshold mark and concentrations of Cu, Co and Cr statistically identified one Lakoro sample (no.31) to be gypsum bearing, against its non-gypsum bearing status in the field. The Cu, Co and Cr elements are therefore, probably closely related to gypsum hosted in the sediments (hence, are good predictor elements), and the Lakoro sample could possibly be mineralised at other unexposed sections of the location. On the other hand, K and Fe elements are not very necessary indicators of gypsum occurrence.

Table 5: Measure of Concentration levels of Elements

Element	Sample Size	Prime range (ppm)	m + 2d value (ppm)	A %	B %
K	40	85.0 – 95.0	122.66	0	2.9
Ca	40	42.5 – 52.5	80.23	8.6	0
Fe	40	262.5 – 287.5	412.23	0	0
Mn	40	1.5 – 2.5	9.10	5.7	0
Cu	40	0.27 – 0.43	0.61	2.9	2.9
Zn	40	0.22 - 0.28	0.63	5.7	0
Ni	40	0.47 – 0.53	0.86	5.7	0
Co	40	0.97 – 1.03	1.58	2.9	2.9
Ba	40	17.0 – 19.0	31.21	2.9	0
Cr	40	2.38 – 2.62	4.23	5.7	2.9
As	40	0.18 – 0.21	0.28	5.7	0
Bi	40	0.13 – 0.16	0.29	2.9	0
Pb	40	0.22 – 0.28	0.52	8.6	0
Br	40	0.06 – 0.08	0.11	5.7	0
Sr	40	0.5 – 0.75	3.27	8.6	0
U	40	0.06 – 0.08	0.12	8.6	0

Note: A% = anomalous samples correctly identified;
B% = background values mistakenly identified as anomalous

On the basis of the regression equation (Table 4), concentration of a negligible -139.97ppm of Cu, 10.2ppmCr and 5.57ppm of Sr could be used to predict the presence of Ca in gypsum mineralised region; and about 283.77ppm of Ni, 249.49ppm of Co and -29.35ppm of Sr would serve to predict for Fe content. However, on simple linear regression of Ca on individual predictive element, Ni, Bi, U and Br (with 0.010, 0.042, 0.034 and 0.019 values respectively) could be good predictors for Ca content in the environment. From the analysis therefore, Cu, Cr, Ni, Co and Sr elements are good predictors (at 0.05 significance level) for Ca and Fe in gypsum – rich areas. Ca is the major cation in gypsum deposit and Fe is usually mobilised under

reducing and precipitated under oxidizing conditions; and show strong presence and influence in early sulphide (pyrite) and carbonates (siderite) and secondary sulphates (melanterite) during the diagenetic process of gypsum formation. Elements that can predict enrichments of these two major cations are seen as geochemical tracers or pathfinder elements. Hence Cu, Cr, Ni and Co are good pathfinder elements to gypsum mineralisation. Under normal conditions, these trace elements would be mobile in the strongly acidic solutions during the oxidation of pyrites and other sulphide ores. However, the diffusion of the organic waters through organic – rich and unconsolidated sediments rich in Fe possibly generated $Fe(OH)_3$, which provide a good adsorptive surface (scavenger) for these elements (Maynard, 1983). Also, interaction between the diffused water (which are low in oxygen) with oxygenated surface water (common in environment of gypsum formation) would trap these elements (Beus and Grigorian, 1975), and incorporate them into the gypsum precipitated during interaction of the sulphate and carbonate – rich waters during the diagenetic processes. These geochemical processes must have worked simultaneously to produce the distribution and dispersion patterns of the elements in the Guyuk area as illustrated in Figure 4.

The observed high intercorrelations between the identified seven trace elements (Ni, Bi, Cr, As, Cu, Br and U) and their collective intercorrelation with Fe signifies their close affinity to the processes involving Fe. Iron is seen as a vital element in the various geochemical processes namely sedimentation, diagenetic alteration and adsorption within the environment of gypsum formation and accumulation.

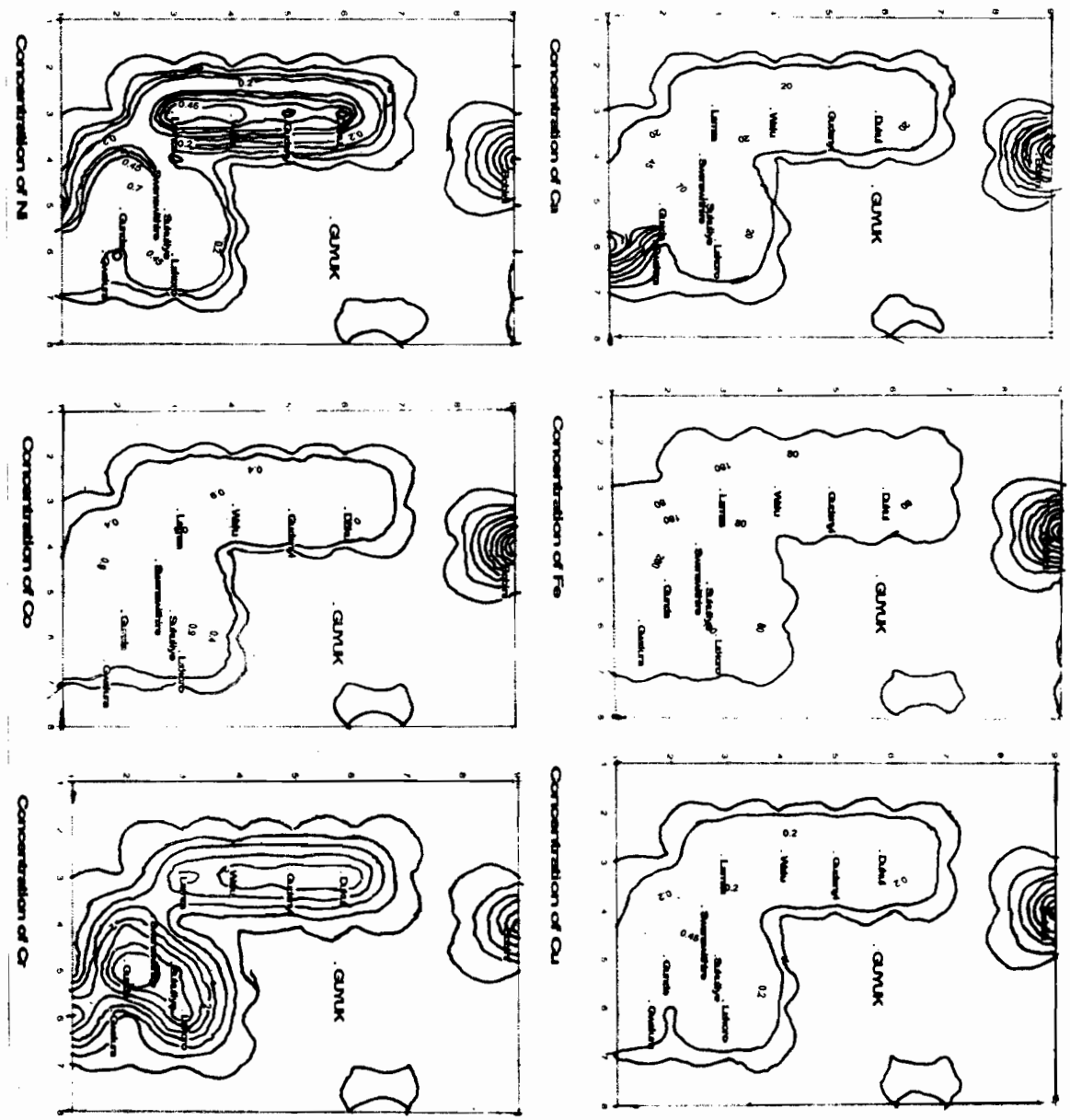

Fig. 4 Contours of some elemental contents in shale samples

CONCLUSIONS

Study of the geochemical pattern in sampled sediments identifies and distinguishes enrichments of four predictor elements, Ni, Co, Cr and Cu to be related to gypsum mineralisation. The ratios of the enrichments of these elements to gypsum in the studied shale sediments are Cu(11:1), Ni(8:1), Co(60:1) and Cr(31:1). These concentrations are anomalously higher relative to natural unmineralised shale materials and are well

above the 2:1 contrast value recommended by Hawkes (1959) as useful anomaly. Similarly, the high (>32%) loading of a single factor on a group of mineralisation indicator elements including these four (Cu, Cr, Ni and Co) and the observed significant regression of Ca and Fe on them depicts the strong bond between these trace elements to process of gypsum mineralization. Hence their common trend of variance marks mineralisation of gypsum in the study area.

ACKNOWLEDGEMENTS

The authors acknowledge the critical comments of colleagues during the course of this work, and that of the anonymous reviewers.

REFERENCES

Benkhelil, J., 1986. Structure and geodynamic evolution of the intracontinental Benue Trough, Nigeria. Elf Nig. Ltd., Nigeria. Bull. Centres Rech. Explor. Prod. Elf- Aquitaine (BCREDP), 12: 29 – 128.

Beus, A. A. and Grigorian, S. V., 1975. Geochemical Exploration Methods for Mineral Deposits. Applied Publishing Co., Wilmette, 287p.

Boggs, S., (Jnr), 1987. Principles of Sedimentology and Stratigraphy. Macmillan Publishing Company, New York, 784p.

Braide, S. P., 1992. Studies on the sedimentary and tectonics of the Yola Arm of the Benue Trough: Facies Architecture and their tectonic significance. J. Min. Geol., 28: 23-31.

Busek, F., Cerny, J. and Sramek, J., 1991. Sulphur isotope studies of atmospheric S and the corrosion of monuments in Prayne, Czechoslovakia. In: Krouse, H.R. and Grinenko, V.A. (Eds.), Stable Isotopes – Natural and Anthropogenic Sulphur in the Environment. John Wiley & Sons, England, pp 399 – 408.

Carter, J. D, Barber, W., Tait, E. A. and Jones, J. P., 1963. The Geology of parts of Adamawa, Bauchi and Bornu provinces of Nigeria. Geol. Surv. Nig. (GSN) Bull., 30: 1- 109.

Ernst, W., 1970. Geochemical Facies Analysis. Elsevier, Amsterdam, 152p.

Evans, R., 1978. Origin and significance of the Evaporites in basins around Atlantic margin. Bull. Assoc. Amer. Petrol. Geologists (AAPG), 62: 223 - 234.

Garrett, R. G., 1983. Mathematical and Statistical activity in North America, In: Howarth, R.J. (Ed.), Statistics and Data Analysis in Geochemical Prospecting. Elsevier Scientific Publishing Co., Amsterdam, pp341 – 350.

Hawkes, H. E., 1959. Geochemical Prospecting, In: Abelson, P.H. (Ed.), Researches in Geochemistry. John Wiley, New York, 2: 62 – 78.

Howarth, R. J. and Sinding-Larsen, R., 1983. Multivariate Analysis, In: Howarth, R.J. (Ed.), Statistics and Data Analysis in Geochemical Prospecting. Elsevier Scientific Publishing Co., Amsterdam, pp207 – 283.

Keith, M. I. and Degens, E. T., 1959. Geochemical indicators of marine and freshwater sediments. In: Abelson, P.H. (Ed.), Researches in Geochemistry. John Wiley, New York, 2, pp 38 – 61.

Krauskopf, K. B., 1979. Introduction to Geochemistry (2nd ed.). McGraw-Hill Kogakasha Ltd., London, 617p.

Mason, B. and Moore, C.B., 1982. Principles of Geochemistry (4th ed.). John Wiley & Sons Inc., NewYork, 344p.

Maynard, J. B., 1983. Geochemistry of Sedimentary ore Deposits. Springer-Verlag, New York, 305p.

Milovsky, A. V. and Kononov, O. V., 1985. Mineralogy. Mir Publishers, Moscow, 320p.

Ntekim, E. E. and Orazulike, D. M., 2003. Structural and Lithologic characteristics of Lamurde – Lau area in Upper Benue Trough, N.E. Nigeria: A strategy for Gypsum Prospecting. Nig. J. Pure & Appl. Sci., 19: 1692 – 1697.

Opeloye, S. A., 2002. Some Aspects of Facies Architecture, Geochemistry and Paleoenvironments of Senonian Formations in Yola Arm, Upper Benue Trough (Nigeria). Unpl. Ph.D. Thesis, Abubakar Tafawa Balewa University, Bauchi, Nigeria, 160p.

Pearce, J.A., 1976. Statistical Analysis of major element patterns in Basalts. J. of Petrology, 17(1): 15 – 43.

Rose, A.W., Hawkes, H.E. and Webbs, J.S., 1979. Geochemistry in Mineral Exploration (2nd ed.). Academic Press Ic. (London) Ltd., London, 657p.

Sonnenfeld, P., 1991. Evaporite Basin Analysis. Reviews in Economic Geology, 5: 159-168.

Uma, K.O., 1998. The brine fields of the Benue Trough, Nigeria: A comparative study of geomorphic, tectonic and hydrochemical properties. J. Afri. Earth Sc., 26(2): 261-275.

Wilkinson, B. R., 1982. Cyclic Cratonic Carbonates and Phanerozoic Calcite Sea. J. Geol. Education, 30: 189 – 203.

Zaborski,P., Ugodulunwa,F.,Idornigie,A . Nnabo,P. and Ibe, K., 1997. Stratigraphy and Structure of the Cretaceous Gongola basin, Northeast Nigeria. Elf Nig. Ltd., Bull. Centres Rech. Explor. Prod. Elf-Aquitaine (BCREDP), 21 153 – 185.

GLOBAL JOURNAL OF GEOLOGICAL SCIENCES VOL. 6 NO. 2 2008: 105 - 112
 ISSN 1596 – 6798

STREAM SEDIMENT GEOCHEMICAL SURVEY OF AN AREA AROUND DASS, N.E. NIGERIA

I. V. HARUNA, S. S. DADA AND Y. D. MAMMAN

(Received 22 March, 2007; Revision Accepted 14 April, 2008)

ABSTRACT

Stream sediment geochemical survey was carried out in Dass area to determine possible dispersion train for Pb, Cu, Co, Ni and Zn. A total of 114 active stream sediment samples were collected over an area of 60km^2. The samples were treated with hot HNO_3 and analysed for Pb, Cu, Co, Ni, Zn, Mn, Mg, Ca, and Fe.The results indicated high concentration of Zn (81.3µg/g), Cu (10.8µg/g), Pb (50.0µg/g), Ni (20.0µg/g) and Co (51.6µg/g) in the area. Descriptive statistical method together with element distribution maps, employed in the presentation of the result, point to a dispersion train for anomalous Pb, Zn, Cu, Co, and Zn in the western flank of the study area. The underlying geology probably played a major role in the distribution of the anomalies.

KEYWORDS: Dass, Dispersion train, Stream sediment.

INTRODUCTION

Attention in exploration is increasingly being directed to the poorly out cropping regions of the world. In such regions, ore deposits are concealed beneath thick lateritic cover, which are products of intense weathering processes. This type of setting renders geological methods ineffective for mineral exploration.

Though rocks of the Dass area are well exposed at the far northern and southeastern parts of the area, they are unfortunately covered by thick laterites in the other parts. Consequently, prospecting for mineral deposits in a large part of the area is made difficult and is only confined to the far isolated hills of the northern part which are not easily accessible.

Specifically, the area extends from around river Bagel through Kagadama broad plains to Dott-Bagel-Lir area. It consists of steep-sided, round top hills that stretch from south to north in the western part. Isolated flat-topped hills are scattered in the far eastern part of the area. The northern part is a region of dissected uplands. The central section comprising Kagadama may be said to consist of a relatively elevated broad plains that form the watershed between Bagel and Dott river systems. These river system and their numerous tributaries made stream sediment geochemical survey the most convenient tool for mineral prospecting in the area.

Geological Setting

The study area (Fig 1) forms part of the Nigerian Basement Complex, which is underlain by gneisses, migmatites and metasediments of Pre-Cambrian age. The lithology varies considerably. The major rock units of the area include granite gneiss, migmatite gneisses, charnockitic gneisses and charnockites.

Others include pegmatites and dolerites. Migmatite gneiss occur in the northcentral and northeastern parts of the area. Texturally, they are medium to coarse grained, dark to light coloured and occur as low-lying outcrops. Granite gneiss covers almost the whole of the eastern and southern parts and extends through Kagadama westward to Lir and Bajar to the far north at Layi. The gneisses are generally medium to coarse grained and strongly foliated. The charnockitic gneiss occupies the area south of Jahun extending for about one kilometer southwards to around Dajim where it grades into the banded gneisses. It also occurs as discrete individual hills in the granite gneiss complex west of the study area.

Pegmatites ranging from a few meters to tens of meters in length and oriented SW-NE are concentrated in the western part of the area. They are mostly tourmaline- and amethyst-bearing. Charnockites are restricted to the western part where they occur as coarse grained bouldery rocks that form parts of the Bajar and Lir hills in the granite gneiss terrane.

Sampling Method and Analysis

Stream sediment samples were collected at the mouths of tributaries discharging into major streams in the area (Fig 2). At each sample point, active stream sediments weighing about 50g was collected bearing in mind the factors that could affect elemental distribution such as dilution effect and factors that could cause contamination such as collapsed bank materials. The samples were prepared using the method described by Smith et al (1976). This involved sun drying, disaggregating in a porcelain mortar and sieving to minus 80 mesh fraction. The samples were then decomposed using hot HNO_3 and the concentrations of Copper, Lead, Zinc, Nickel, Cobalt, Cadmium, Magnesium, Manganese and iron in the various samples determined using atomic absorption spectrophotometer. Routine rechecking of the standard working range of the machine was conducted at regular intervals to minimise errors.

The large numbers of analytical results were condensed into tables (Table 1) by grouping the values into

I. V. Haruna, Department of Geology, Federal University of Technology, Yola, Nigeria.
S. S. Dada, Abubakar Tafawa Balewa University, Bauchi, Nigeria.
Y. D. Mamman, Department of Geology, Federal University of Technology, Yola, Nigeria

adequate number of classes and calculating their cumulative frequency distributions. To ease determination of the characteristic parameters of the distributions and comparison between various population types, the cumulative frequency of occurrence in each class was plotted as ordinate on a probability graph paper against the class midpoint to give a cumulative frequency curve represented by more or less straight lines.

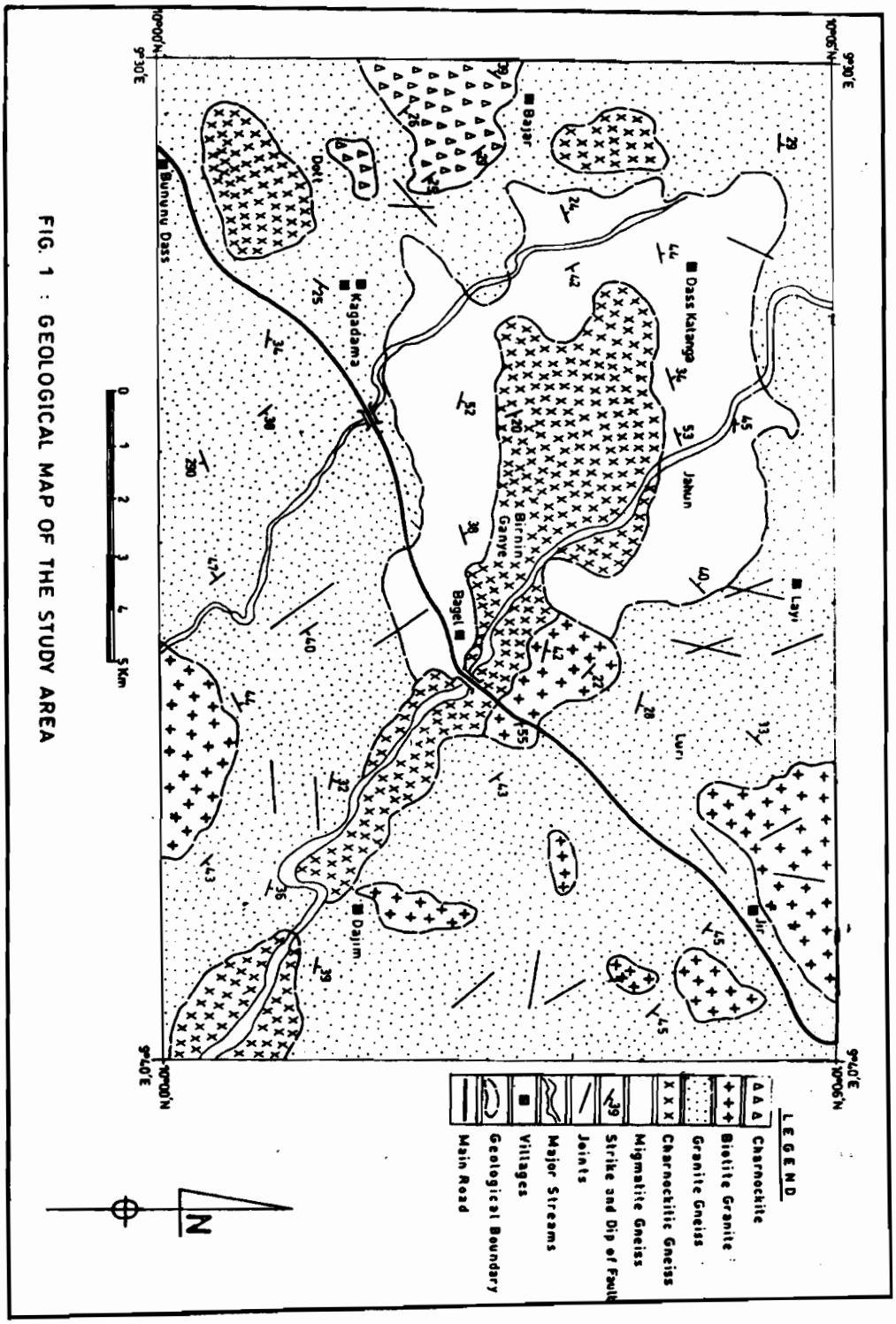

FIG. 1 : GEOLOGICAL MAP OF THE STUDY AREA

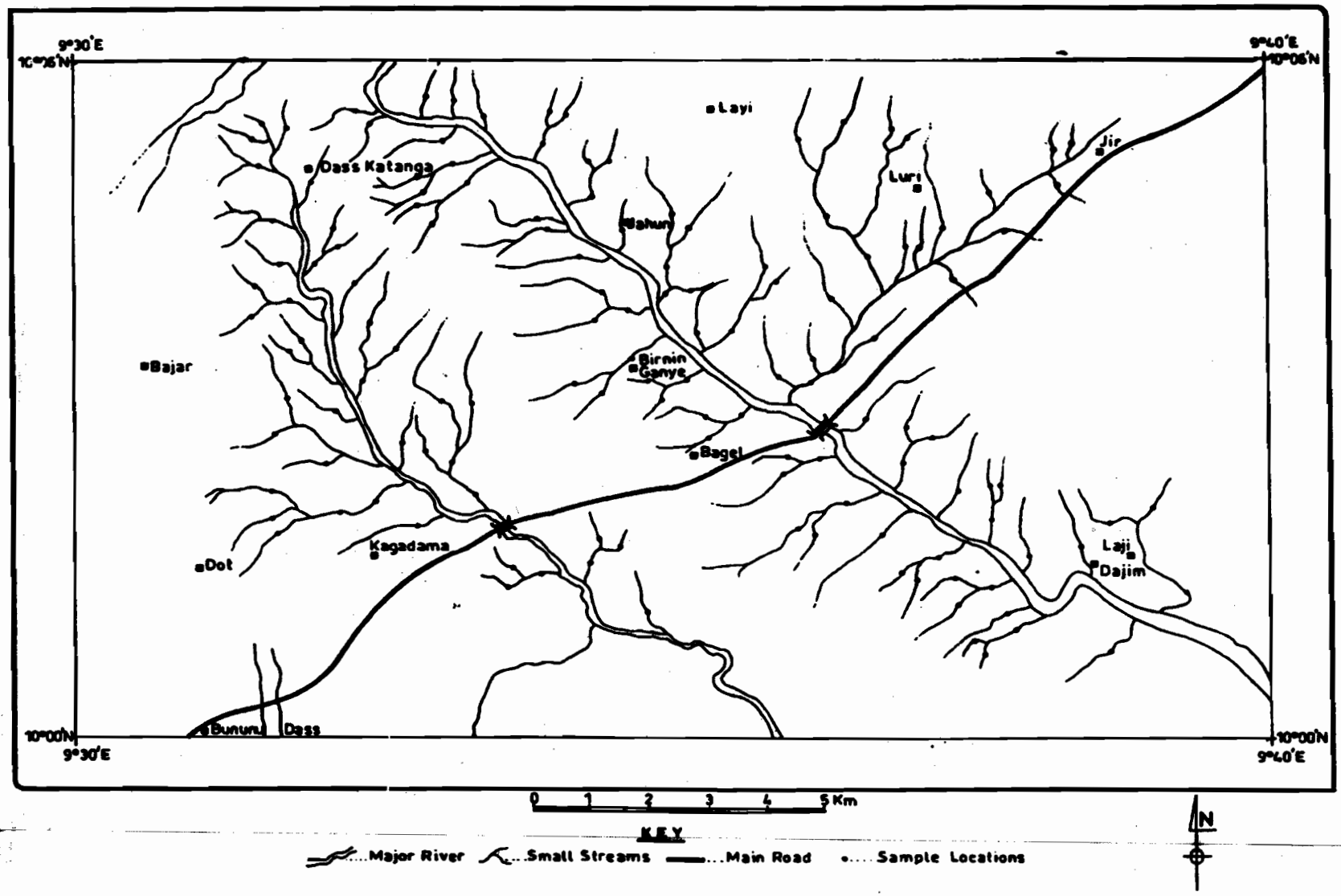

Fig. 2 : Geochemical Sample Locations of the Study Area.

Table 1. Some statistical parameters of extractable metal content from stream sediment

Interval of element concentration (µg/g)					Internal mid point					Frequency					Relative frequency (%)					Relative Cumulative frequency (%)				
Zn	Cu	Pb	Co	Ni	Zn	Cu	Pb	Co	Ni	Zn	Cu	Pb	Co	Ni	Zn	Cu	Pb	Co	Ni	Zn	Cu	Pb	Co	Ni
20-25	3-4	3-7	8-12	6-9	22.5	3.5	5	10	7	6	9	4	5	9	10.53	15.79	7.02	8.77	15.79	99.99	99.99	99.99	100.00	100.00
25-30	4-5	7-11	12-16	9-10	27.5	4.5	9	14	9	9	9	6	7	15	15.79	15.79	10.53	12.28	26.32	89.46	84.2	92.96	91.23	84.21
30-35	5-6	11-15	16-20	10-12	32.5	5.5	13	18	11	5	11	7	5	5	8.77	19.30	12.28	8.77	8.77	73.67	68.41	82.43	78.95	57.89
35-40	6-7	15-19	20-24	12-14	37.5	6.5	17	22	13	10	12	10	2	13	17.54	21.05	17.54	3.51	22.81	64.9	49.11	70.15	70.18	49.12
40-45	7-9	19-23	24-28	14-16	42.5	7.5	21	26	15	4	5	3	8	7	7.02	8.77	5.26	14.04	12.28	47.36	28.06	52.61	66.67	26.31
45-50	9-9	23-27	28-32	16-18	47.5	8.5	25	30	17	6	3	9	5	3	10.53	5.26	15.79	8.77	5.26	40.34	19.29	47.35	52.63	14.03
50-55	9-10	27-31	32-36	18-20	52.5	9.5	29	34	19	9	6	7	11	5	15.79	10.53	12.28	19.30	8.77	29.81	14.03	31.56	43.86	8.77
55-60	10-11	31-35	36-40		57.7	10.5	33	38		3	1	7	8		5.26	1.75	12.28	14.04		14.03	3.5	19.28	26.56	
60-65	11-12	35-39	40-44		62.5	11.5	37	42		1	1	1	2		1.75	1.75	1.75	3.51		8.76	1.75	7.00	10.52	
65-70		39-43	44-48		67.5		41	46		1		1	1		1.75		1.75	1.75		7.01		5.25	7.01	
70-75		43-47	48-52		72.5		45	50		1		1	3		1.75		1.75	5.26		5.26		3.5	5.26	
75-80		47-51			77.5		49			0		1			0		1.75			3.51		1.75		
80-85					82.5					2					3.51					3.51				

Interval of element concentration (µg/g)				Internal mid point				Frequency				Relative frequency (%)				Relative Cumulative frequency (%)			
Mg	Ca	Fe	Mn	Mg	Ca	Fe	Mn	Mg	Ca	Fe	Mn	Mg	Ca	Fe	Mn	Mg	Ca	Fe	Mn
200-300	000-200	000-1000	15-30	250	100	500	17.5	24	19	1	1	42.12	33.33	1.75	1.75	99.99	99.97	100.00	99.92
300-400	200-400	1000-2000	30-35	350	300	1500	22.5	17	26	3	1	29.82	45.61	5.26	1.75	57.87	66.64	98.25	98.17
400-500	400-600	2000-3000	35-30	450	500	2500	27.5	7	3	12	1	12.28	5.26	21.05	1.75	28.05	21.03	92.99	96.42
500-600	600-800	3000-4000	30-35	550	700	3500	32.5	3	3	5	3	5.26	5.26	8.77	5.26	15.77	15.77	71.94	94.67
600-700	800-1000	4000-5000	35-40	650	900	4500	37.5	1	1	3	4	1.75	1.75	5.26	7.02	10.51	10.51	63.17	89.41
700-800	1000-1200	5000-6000	40-45	750	1100	5500	42.5	1	2	8	14	1.75	3.51	14.04	24.56	8.76	8.76	57.91	82.39
800-900	1200-1400	6000-7000	45-50	850	1300	6500	47.5	0	1	8	14	0	1.75	14.04	24.56	7.01	5.25	43.87	57.83
900-1000	1400-1600	7000-8000	50-55	950	1500	7500	52.5	2	1	2	16	3.51	1.75	3.51	28.02	7.01	3.5	29.83	33.77
1000-1100	1600-1800	8000-9000	55-60	1050	1700	8500	57.5	1	1	6	1	1.75	1.75	10.53	1.75	3.5	1.75	26.32	5.25
1100-1200		9000-10000	60-65	1150		9500	62.5	1		9	1	1.75		15.79	1.75	1.75		15.79	3.5

The various central tendency parameters (Table 2) were estimated following the method described by Lepeltier (1969)

Table 2: Estimates of statistical parameters from the graphs

Element	Range(µg/g)	Mean(µg/g)	Threshold(µg/g)
Zn	23.1 - 81.3	41.2	45.0
Cu	3.0 - 10.8	6.3	6.5
Co	8.4 - 51.6	31.0	24.0
Ni	6.0 - 20.0	12.0	17.0
Pb	3.3 - 50.0	23.0	23.0
Mg	270 – 1116	380	800
Mn	15.0 - 73.5	49.0	43
Fe	870 – 9960	6200	4500
Ca	48 – 1700	380	500

N.D = not detectable

The pH of sediments determined in a 1:5 sediment distilled water slurry by means of standardized pH meter gave a range of 5.8 – 6.3 for the western flank and 6.1 – 6.8 for areas around river Bagel

RESULTS

Result of analysis of the stream sediments as condensed in Table 1 are presented in Fig. 2. The forms of cumulative frequency curves shown by almost all elements of economic importance (Pb, Zn, Ni, Cu, Co) are characteristic of two populations (Fig. 3). In other words, the curves show two breaks suggesting bimodal density distribution. Individually however, the elements behave differently. For Copper, the positively broken line is an expression of an excess of low values in bimodal population distribution. An estimate of their proportions is given at 48 percentile. This indicates the presence of 48% higher population and 52% of lower population. The threshold taken at the abscissa of this breaking point corresponds to 6.5µg/g.

In the probability plot for Zn distribution, a smooth curve through the data points has the form of a bimodal density distribution with an inflection point at the 44 cumulative percentile. The positive branch towards lower values corresponds to the normal population while the negative branch corresponds to a population of higher concentrations. The central branch corresponds to a mixture of the two populations. Threshold taken at the middle of this branch corresponds to 45.0:g/g. The probability of finding values higher than 72.5:g/g in the area is 0.05%.

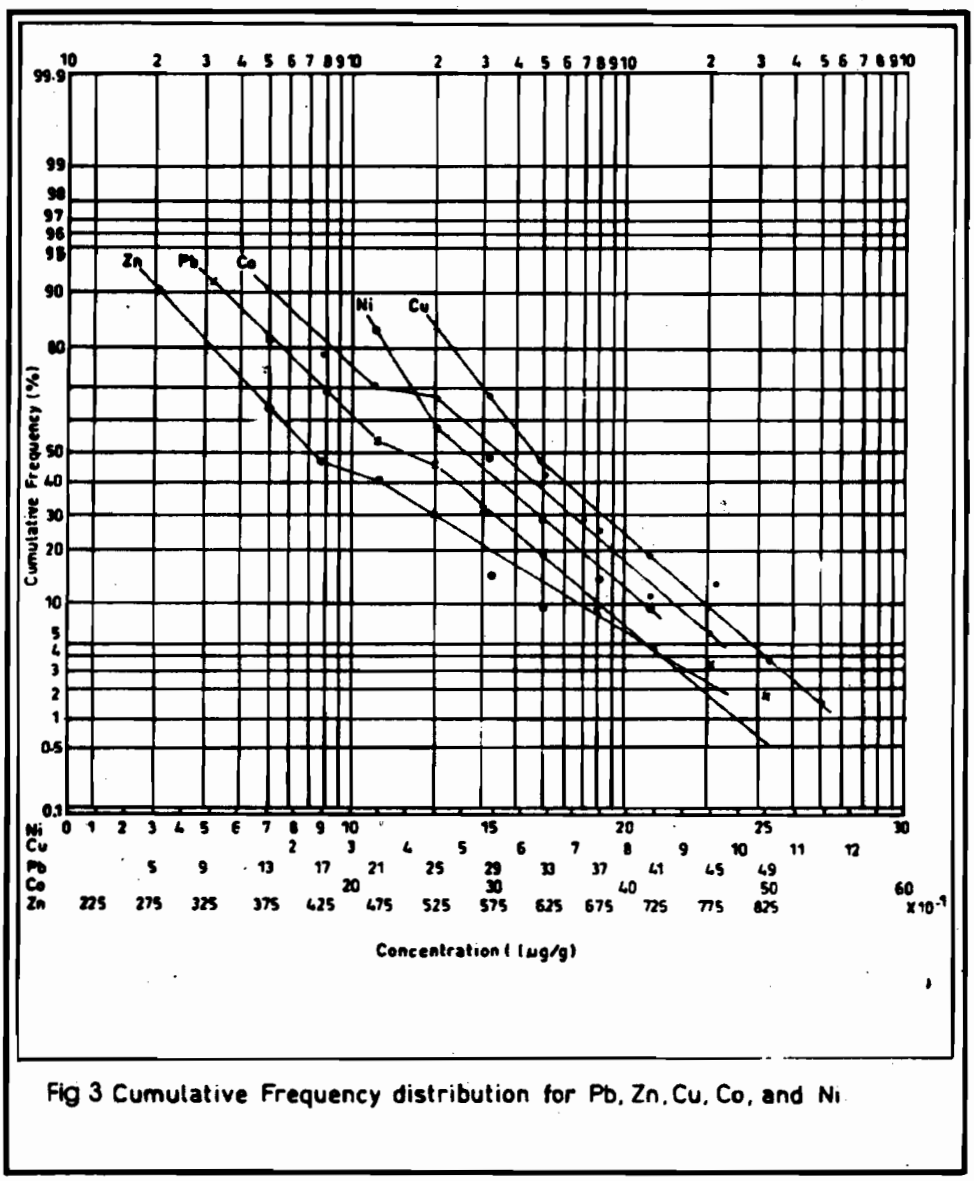

Fig 3 Cumulative Frequency distribution for Pb, Zn, Cu, Co, and Ni

The cumulative distribution curve for Ni shows positive skewness. A histogram would give a frequency curve skewed to the right in the direction of high values. Break of the distribution line occurs at 58% level. The abscissa of the breaking point indicates the limit above which there is departure from normal distribution. This

breaking point occurs above the normal threshold level of 2.5%. Threshold taken at the abscissa of this breaking point corresponds to 13.0µg/g.

The form of cumulative distribution curve for Co is similar to that of Pb but with inflection points at 68 cumulative percentile indicating, the presence of 68% higher populations and only 32% lower population. Abscissa of the midpoint of the central segment indicates a threshold of 24.0µg/g.

The form of curve shown by Pb is characteristic of two populations with the central segment indicating considerable overlap of the two. The inflection point at 50% cumulative percentile indicates the presence of equal proportions of high and low populations. Abscissa of the midpoint indicates a threshold of 23.0µg/g.

In summary, a greater percentage of the data falls within the background and threshold values whereas the anomalous values are few and scattered.

Summary of their range, mean, ratio and thresholds is presented in Table 2.

DISCUSSION

Copper - Zinc

In general terms, most of the anomalous values of the elements lie in the western flank of the study area (Fig 4) and conforms with the chain of uplifted basement that run from south to north.

Relatively high values are scattered in the northwestern part of the area under consideration. The low values of Cu are related to the bedrock lithology and suggest the near absence of basic and ultrabasic rocks in the entire study area. Cu is one of the chalcophile elements concentrated in pyroxenes and amphiboles, as well as, magnetite and biotite in intrusive rocks (Krauskopf, 1979). In basic and ultrabasic rocks, pyroxenes, amphiboles and to a lesser extent, olivines are strongly indicated by Cu among other elements (Beus and Grigorian, 1977). The bulk of the Cu in the basement is therefore incorporated in silicate minerals, the most important of which being pyroxenes. As a result of oxidation and weathering, Cu is liberated from the Cu-bearing minerals in the country rocks as a soluble sulphate under acid to near neutral conditions. Its divalent ion is then adsorbed and co-precipitated with, or adsorbed to sediment particles (Boyle et al 1996). Alternatively, Cu may be adsorbed by organic matter and co-precpitated with Fe-Mn oxides, but is less readily scavenged by Fe-Mn oxides than other base metals, such as Co, Zn and Ni.

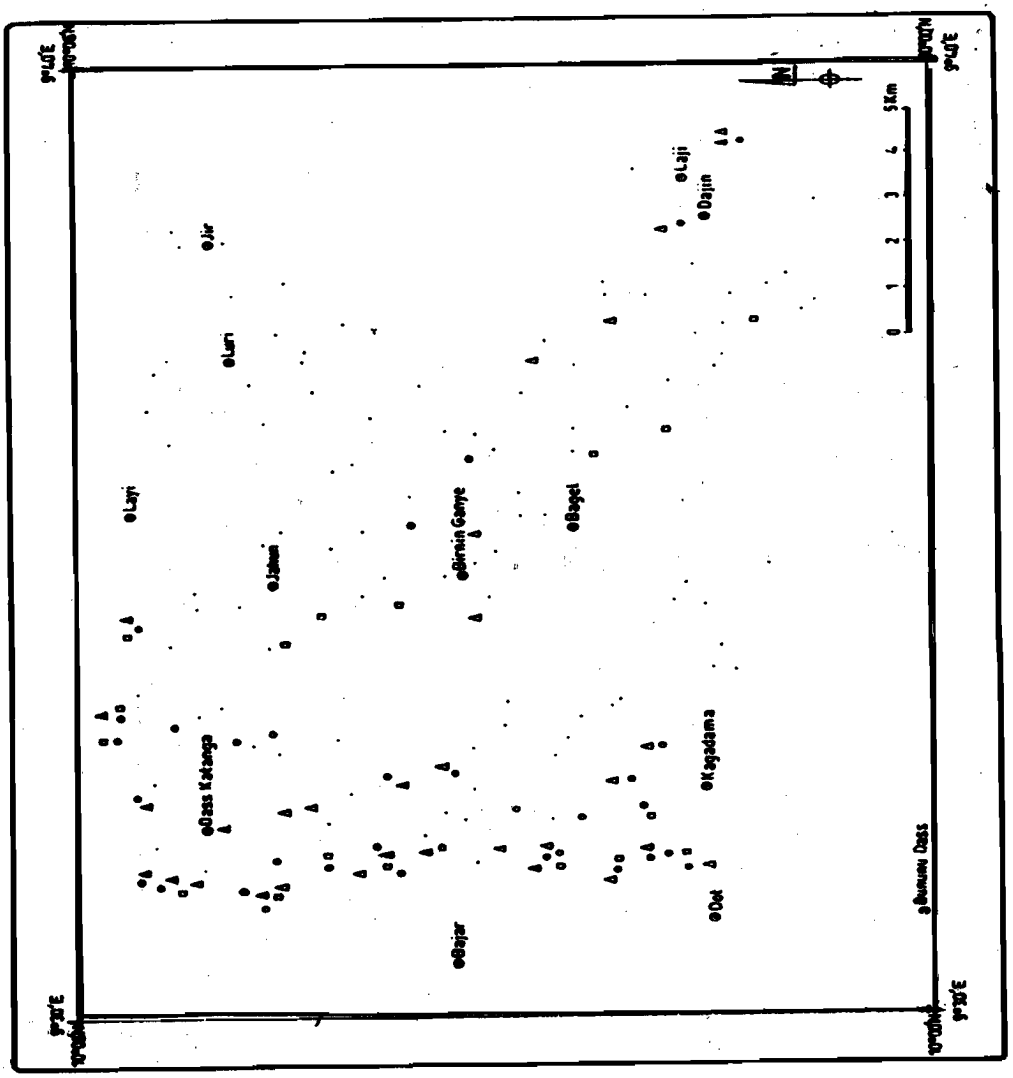

Fig. 4 : Geochemical Anomalies of Dass Area

Zn has a close affinity with Pb in its distribution in the stream sediments. Like Pb, the anomalous values (80µg/g) of Zn lie on the western flank of the area with low values (≤ 50µg/g) recorded along river Bagel and its tributaries in the east.

The distribution of Zn is controlled by lithology. Zn is one of the chalcophile elements that substitutes for the major cations of Mg and Fe in silicate structures (Krauskopf, 1979). However, for the most part, the metals are left to accumulate in the residual solutions that eventually form sulfide ores. The traces of chalcophile metals commonly reported in ordinary igneous rocks may be present in large part as tiny sulfide grains rather than as substitute for major elements. The concentration of high values of Zn in the western flank coincides with the distribution of charnockites, charnockitic gneiss and granite gneiss.

The Zn-bearing minerals in these rocks weather, releasing Zn, which pass through underground water into streams, where it is co-precipitated in the sediments. Average background content of Zn in stream sediments range between 10-200µg/g and values greater than 200µg/g may indicate mineralization (Reedman, 1980).

Low values of Zn (mostly <60µg/g) are recorded along River Bagel and its tributaries in the east. These low values may not be unrelated to the dilution effects and chemical characteristics of Zn. Although Zn has high mobility, it is often absorbed by organic matter.

Nickel – Cobalt - Lead

Fairly high values of Ni are sparsely distributed in the western, northwestern and southeastern part of the study area while background values are recorded north of Bagel Bridge. This distribution can be interpreted in terms of the bedrock lithology underlying the sampled areas. Ni has intermediate radii and is abundant in the earlier members of differentiation sequence as a result of ready substitution for Fe and Mg, with some strongly enriched with magnesium in ultramafic rocks (Krauskopf,1979). Ni is concentrated in magnesium pyroxenes and olivines (in ultrabasic and basic rocks), and biotite in intermediate and acid rocks (Beus and Grigorian, 1977). The fairly high (about 20µg/g) and sparsely distributed values in the west, northwest and southeast can be attributed to contributions from the biotite granites and the granite gneisses. In granites, such as those present in the study area, almost all the Ni is contained in the biotite, and in such environment, which practically, has no ultrabasic rocks economic Ni minerlization is rare.

The low values (6-20µg/g) of nickel content in the stream sediments is probably due to the paucity of basic and ultrabasic rocks in the area, its relatively high mobility not withstanding. The average background content of nickel in stream sediments is between (5-50µg/g). The low values of between 6-20µg/g are well within this range.

Cobalt content in the area ranges between 8.4-51.6µg/g with minimum anomalous value graphically estimated at 24.0µg/g. Most of the anomalous values are scattered in the western, northwestern and southeastern parts of the area, with background values distributed in an area north of the Bagel river bridge.

The source of the Co is attributed to crystalline rocks in the west and northwestern part of the area. Co is one of the elements occurring in the transition group, and like Ni, has intermediate radii and substitute readily for Fe and Mg, hence it is abundant in the earlier members of the differentiation sequence. Co is therefore concentrated in magnesian pyroxenes and olivine and in biotite in intermediate and acid rocks such as found in the area under consideration. However, economic Co deposits in the area can not be expected.

Average background content of Co in stream sediments normally range between 5-50 µg/g with anomalous concentrations over mineralization always more than 100-500µg/g (Reedman, 1980). The low values of Co can therefore be explained in terms of the paucity of basic and utrabasic rocks, and its chemical behavior during transportation. Co has relatively high mobility but readily scavenged and held by Fe-Mn oxides (Reedman, 1980).

Most of the high values of Pb lie on the western flank of the study area, while low or background values are recorded along river Bagel and its tributaries in the east.

The underlying geology plays a major role in the distribution of Pb anomalies. Pb is one of the elements belonging to "large-ion lithophile" group (LIL). It has cations with large radii and low electric charge, which tend to substitute for K, hence it is concentrated in felsic rather than mafic rocks (Krauskopf, 1979). Abundance of Pb in a rock series is a good indication of the extent to which differentiation has sorted out constituents of the original igneous material. Pb is concentrated in orthoclase, which is the mineral indicator of the geochemical characteristic of acid and intermediate rocks. Maximum concentrations are found in zircon and in some other accessory minerals (Beus and Grigorian, 1977). The concentration of high values of Pb in the western flank is therefore not surprising, but serves to confirm the presence of plutonic acidic rocks such as charnockite and charnockitic gneisses, which consist of mineral such as biotite, hornblende, zircon and microcline.

As a result of weathering, Pb is released from the various Pb- bearing minerals in the charnockites and charnockitic gneisses. It then passes into the soil where it co-precipitates with or gets absorbed by clay minerals and organic matter. Subsequently, it passes directly through underground water into streams where it is co-precipitated in the sediments. The values range between 5-50µg/g. The low values (<30µg/g) for Pb recorded along river Bagel and its tributaries in the east are probably due to its low mobility and the dilution effects.

Manganese – Iron – Calcium - Magnesium

Although the association of Fe – Ca – Mg has been used as a lithological index reflecting the geology of the underlying rocks (Ojo, 1988), these elements are often used by most authors to aid interpretation of minor and trace elements. Hydrous oxides of these elements can be sorbents i.e. carriers of trace elements in surface and ground waters. For example, Fe is said to be very effective trap for trace metals such as Cu, Pb, Zn (Lecomte and Sondag 1980). The precipitation of a trace element along the paths of its aqueous migration sequence does not depend on its solubility product or on its activity in the solution rather it is controlled by the precipitation of a sorbent, which is capable of being a carrier of this trace element. For majority of trace elements whose concentrations in waters in the supergene zone is very low, and which almost reaches

values necessary to ensure precipitation from the solution, the sorption precipitation (co-precipitation) together with the sorbent – carrier is the principal mode of precipitation.

Mn does not occur in significant amounts in the area. The low content of Mn is attributed to the acid bedrock lithology of the area. Mn, like Co, Ni and Cr falls in the group of elements with intermediate radii; it is therefore abundant in the earlier members of the differentiation sequence as a result of its substitution for Fe and Mg. It has its maximum abundance in gabbros and basalts. Its low mobility is probably one of the limiting factors to its distribution.

CONCLUSION

Interpretation of trace element composition of the stream sediment has pointed to a dispersion train for anomalous Cu, Zn, Pb, Co and Ni, in the western flank of the area. Pb, Co and Ni are indicator element for Cu-Zn minaralisation while Pb, Zn, Cu may be suggestive of hydrothermal uranium deposits. The western flank of the area is criss-crossed by pegmatite and aplite veins along the flank of Dott, Lir and Bajar hills. The veins might have acted as traps for ore-bearing fluids migrating from the subajacent charnockites and charnockitic gneisses.In fact, amethyst, tourmaline and beryl have been visually identified from heavy mineral sampling in this area. Detail geochemical survey is therefore recommended in the western flank of the study area.

REFERENCES

Beus, A. A. and Grigorian, S. V., 1977. Geochemical Exploration Methods for Mineral Deposits. Applied Publishing Ltd. USA. 31-270pp.

Boyle, R. W., Tupper, W. M., Lynch, J., Friedrich, G., Ziauddin, M; Shafiqullah, M; Carter, M, and Bygrave K., 1996. Geochemistry of Pb, Zn, Cu, As, Sb, Mo, Sn, W, Ag, Ni, Co, Cr, Ba and M, in the waters and stream sediments of the Bathurst-Jaquet River District, New Brunswick. GSC paper. pp. 41 - 65.

Krauskopf, K. B., 1976. Introduction to Geochemistry. Mc Graw-Hill, New York, 72pp.

Lecomte, P. and Sondag, G., 1980. Regional geochemical reconnaissance in the Belgian Ardennes: Secondary dispersion patterns in stream sediments. Mineraluim Deposita. 15:47-60.

Lepeltier, C., 1969. A Simplified Statistical Treatment of Geochemical Data by Graphical Representation. Journ. Economic Geology 64: 536-550pp.

Ojo, O. M., 1988. Stream sediment geochemistry of Guburunde Horst, "Gongola Basin", Upper Benue Trough, Nigeria. Journ. of African Earth Sciences. 7: 91-101.

Reedman, J. H., 1980, Techniques in Mineral Exploration. Applied Science Publishers, London. 25-455pp.

Smith, A. Y., Cameron, J. and Baretto, P.M., 1976. Uranuim Geochemical Prospecting in Australia. I.A.E.A. Sym. Vienna. pp. 657-670

GLOBAL JOURNAL OF GEOLOGICAL SCIENCES VOL. 6 NO. 2 2008: 113 - 122
 ISSN 1596 – 6798

PETROCHEMISTRY AND TECTONIC SETTING OF METABASIC ROCKS OF ISANLU, SOUTHWEST NIGERIA

S. B. OLOBANIYI

(Received 27 December, 2007; Revision Accepted 10 June, 2008)

ABSTRACT

The geochemistry of amphibolite of the Isanlu area of southwest Nigeria was studied and its petrotectonic setting evaluated. Amphibolite occurs as small outcrops and residual hills that are conformably interbanded with a suite of meta-volcanosedimentary rocks. The rock reveals a mid-amphibolite facies assemblage of hornblende (magnesio and pargasitic compositions), plagioclase (oligoclase – labradorite) with small amounts of quartz and biotite. Locally, this assemblage has suffered retrogression into the greenschist facies and preserve the metamorphic assemblage actinolite + chlorite + epidote + quartz ± titanite.

Amphibolite in the study area is characterized by a moderate SiO_2 (46.50-53.74 wt. %), moderately high FeO_{tot} (8.78-14.41 wt. %), low Fe_2O_3/FeO (average 0.22), low MgO (6.18-10.56 wt. %), low to high CaO (8.60-18.20 wt. %) and low alkalis. Trace elements including Nb, Y and Rb are low in abundance while Sr and Ba show marked enrichment reflecting the abundance of modal plagioclase. Refractory elements including Ni, Co, Cr and V also show enhanced values probably reflecting the fairly primitive nature of its mafic ancestry. The rock classifies as high-Fe tholeiite with plume-type mid-oceanic ridge and volcanic arc tectonic affinity. However, the interbanded nature of the rock with the enclosing metasediment suggests that it was emplaced in a continental setting. This rock was probably emplaced in an ensialic basin developed on rift-controlled grabens, where the crust is sufficiently attenuated by rising mantle plumes resulting in ocean floor – type contamination-poor magmatism.

KEYWORDS: Petrochemistry, Tectonic setting, Amphibolite, Ensialic basin, Egbe-Isanlu schist belt

INTRODUCTION

The Nigerian schist belts are a series of narrow northerly trending and metasediment-dominated troughs of Precambrian age. In addition to metasediments these troughs host metaigneous and granitic intrusives. A volumetrically minor but important component of the metaigneous unit are metabasites, mostly occurring as amphibolites. The chemistry of basic rocks has often been used in tectonic environment discrimination. This is predicated on the assumption that basaltic rocks are geochemically sensitive to changes in tectonic framework (Floyd and Winchester, 1975; Pearce, 1982; Myers and Breitkopf, 1989), and that many of the elements employed as parameters are relatively insensitive to secondary processes (Winchester and Floyd, 1977). This technique has been employed with remarkable success in several terrains of the world (Rahaman et al., 1988; Frimmel et al, 1996), and most significantly in areas where the present state of preservation and poor exposures precludes an unambiguous identification of the palaeotectonic environment using other geological data (Wood et al., 1979).

In Nigeria, several workers have attempted to characterize the environment of segments of the basement complex rocks. Interpretations emanating from such studies have implied ensialic (Bafor, 1988; Olade and Elueze, 1979) or ensimatic (Rahaman et al., 1988) settings or even an agglomeration of exotic terrains (Ajibade and Wright, 1989). These results suggest that varying tectonic regimes may have been operative in different segments of the basement complex of Nigeria. Consequently, a wider investigation of the tectonic setting of the different segments of the basement rocks is desirable. This paper examines the petrochemistry and petrogenetic affinity of amphibolite from Isanlu in southwestern Nigeria and attempts deducing the palaeotectonic environment of its emplacement.

GEOLOGICAL SETTING

The Nigerian basement complex can broadly be classified into three units; the gneiss-migmatite complex, the metasedimentary schist belt and the Older Granite suite. The migmatite-gneiss complex consists of Archean (ca. 3000Ma) and Palaeoproterozoic (ca. 2000Ma) components (Oversby, 1975; Dada and Briqueu, 1996) which form the floor on which supracrustals (the schist) were deposited. Both 'basement' and 'cover sequence' were subsequently deformed by the Pan-African thermotectonic event (ca.600Ma) (Ajibade et al., 1987), to produce conformable structural relationships (Annor et al., 1996; Olobaniyi, 1997). This effectively obscured the age relationship between the two units and hinders definitive conclusions on the origin of the schist belts. As a result of the Pan-African thermotectonic event (Kennedy, 1964), huge volumes of discordant granitiods, termed the Older Granites, of varying compositions including granites, granodiorites, syenites and adamellites were emplaced.

The Egbe-Isanlu schist belt is located in southwest Nigeria (Fig. 1) and forms one of the numerous linear metasedimentary belts. This belt consists predominantly of semi-pelitic metasediment, and minor occurrences of

S. B. Olobaniyi, Department of Geology, Delta State University, P.M. B. 1, Abraka, Delta State Nigeria

psammite, banded iron formation with metaigneous rocks including talc schist and amphibolite (Olobaniyi, 1997). Both metasedimentary and metaigneous suites are concordantly interbanded and bear similar greenschist to mid-amphibolite metamorphic imprint, and north-southerly trending structural features. These metamorphic tectonites are intruded in places by coarse grained and porphyritic granites that constitute prominent topographic features in the area.

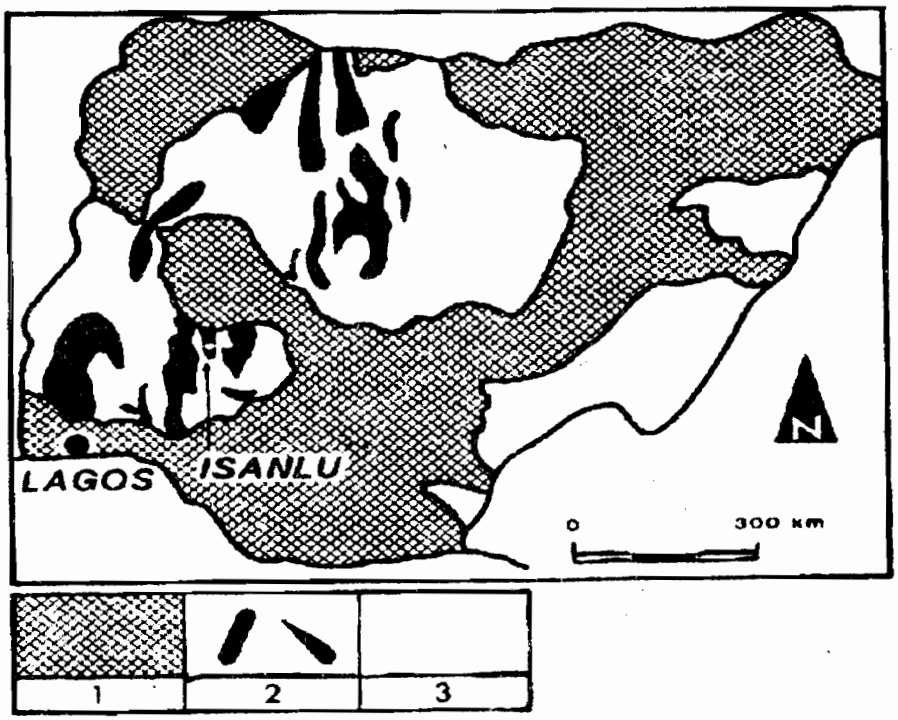

Figure 1: simplified geological map of Nigeria showing the location of Isanlu within the Egbe-isanlu Schist belt. 1: Phanerozoic sedimentary rocks; 2: Schist belts; 3: Undifferentiated basement complex.

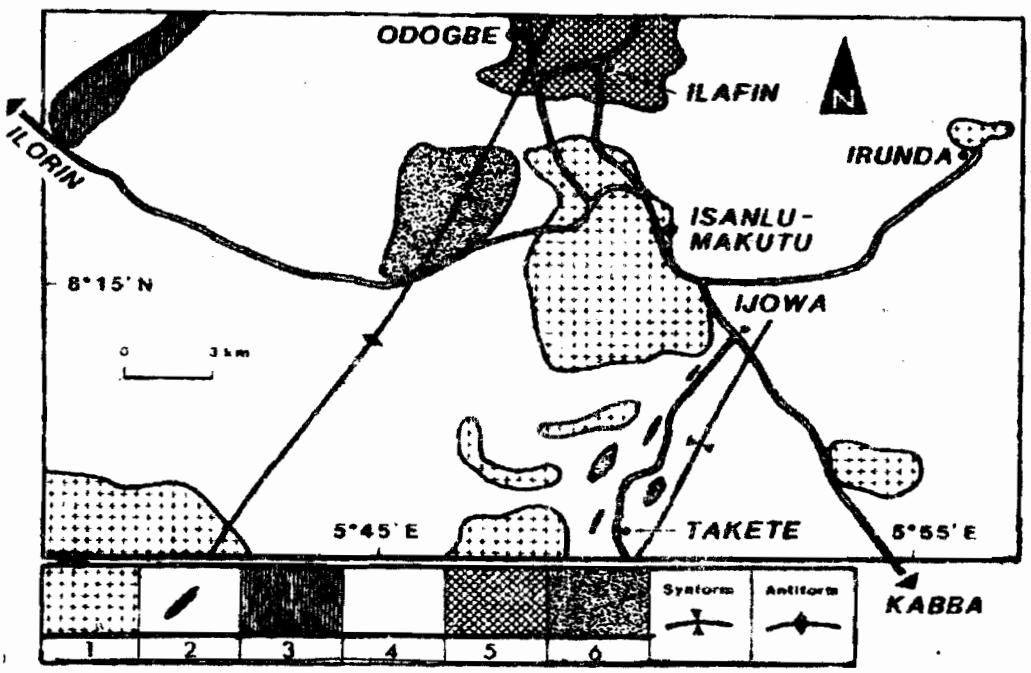

Figure 2: geological map of Isanlu showing Amphibolite and the associated rocks, 1: Granite; 2: Iron-formation; 3: Amphibolite; 4: Quartz mica schist; 5: Talc schist; 6: Quartzite
(after Olobaniyi, 1997).

FIELD OCCURRENCE AND PETROGRAPHY

Amphibolite occurs in this area essentially as residual hills and to a lesser extent as small outcrops which appear to be remnants of originally tabular bodies that were fractured or boudinaged. It also occurs as small concordant sheets that are conformably interbanded with the other components of the metasedimentary and metaigneous rocks of the area. Locally amphibolite is intensely migmatized by invading granitiods.

The Isanlu amphibolite is black to dark green and coarse to medium grained in texture. It commonly appears massive in hand specimen but reveals a well-defined penetrative fabric under the microscope. This rock consists of a matrix of green to deep- green hornblende (60-70 vol.%) of actinolitic, magnesio-hornblendic and pargasitic compositions, and plagioclase (10-30 vol.%) that varies in composition from oligoclase to labradorite. Flakes of biotite (0-5 vol %) and small amounts of quartz (0-2 vol. %) also occur in the assemblage. This rock reveals various stages of retrogression from the amphibolite through to the greenschist facies. Indeed, the common assemblage of the highly altered (retrograded) amphibolite consists of a matrix of actinolite, chlorite, epidote, albite, quartz, titanite and iron oxides. Details of the petrology and mineral chemistry of this rock is presented in Olobaniyi (1997 and 2006).

GEOCHEMISTRY

Analytical Techniques

Eleven representative samples of amphibolite from Isanlu were selected and analyzed for both major and trace element composition. The bulk of these elements were measured by XRF using a Philip PW 1480 automated sequential spectrometer at the Geochemistry Institute of Georg August University, Gottingen, Germany. Discs for both major and trace elements determination were prepared at 1100^{0}C using spektoflux 100 containing lithium tetraborate. For the determination of Fe^{2+}, a titration method was used.

Elemental Abundance and Petrogenetic Affinity

Table 1 presents the analytical result of the selected amphibolite samples. Its statistical summary is indicated in Table 2 and compared this with the compositions of modern and ancient analogues in Table 3. This rock is characterized by a moderate SiO_2 content with a narrow range of 46.5-53.74 wt. %, a moderately high FeO_{total} (8.78-14.14wt.%) coupled with low MgO (6.18-10.56 wt.%). Amphibolite has Mg# varying from 46.86 to 63.22 and a low Fe_2O_3/FeO ratio averaging 0.22, consistent with the composition of poorly evolved tholeiitic basalts. FeO_{total} shows enhanced mean value relative to MORB and oceanic tholeiite but comparable to Archean and Proterozoic Birrimian tholeiite (Table 2). The CaO content is low to high increasing from 8.60 to 18.20 wt.% while Al_2O_3 content is in the range 10.24 to 15.60 wt.% (mean CaO/Al_2O_3 = 0.89). The mean normative hy:di ratios (1.18) (Olobaniyi,1997), is comparable to most tholeiites (≤1). Alkalies, including Na_2O (0.55-2.70 wt. %) and K_2O (0.15-0.99 wt.%) are depleted indicating its sub-alkalic nature. On the Silica versus Zr/TiO_2 diagram of (Winchester and Floyd, 1977), (Fig. 3) the rock plots predominantly in the field designated for sub-alkalic basalt. On the AFM scheme of Irvine and Barager(1971), (Fig. 4) this composition defines a tholeiitic trend with strong iron enrichment. A further appraisal of its petrogenetic character using the Jensen cation plot (Jensen, 1976) (Fig. 5) indicates that the rock is a high iron tholeiite (HFT).

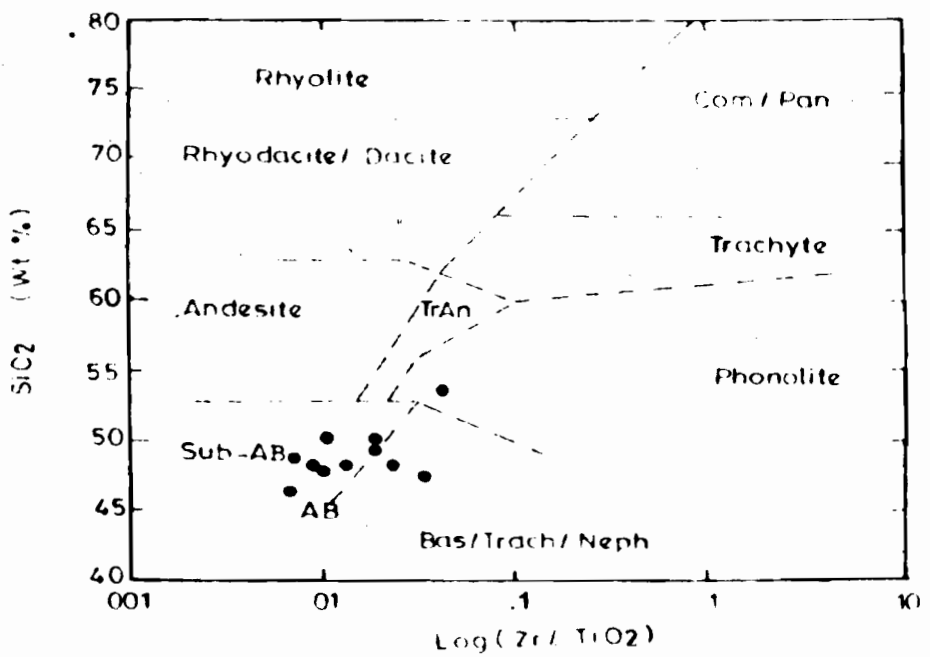

Figure 3: Classification of Isanlu Amphibolite on the SiO_2 versus Zr/TiO_2 scheme of Winchester and Floyd (1977)

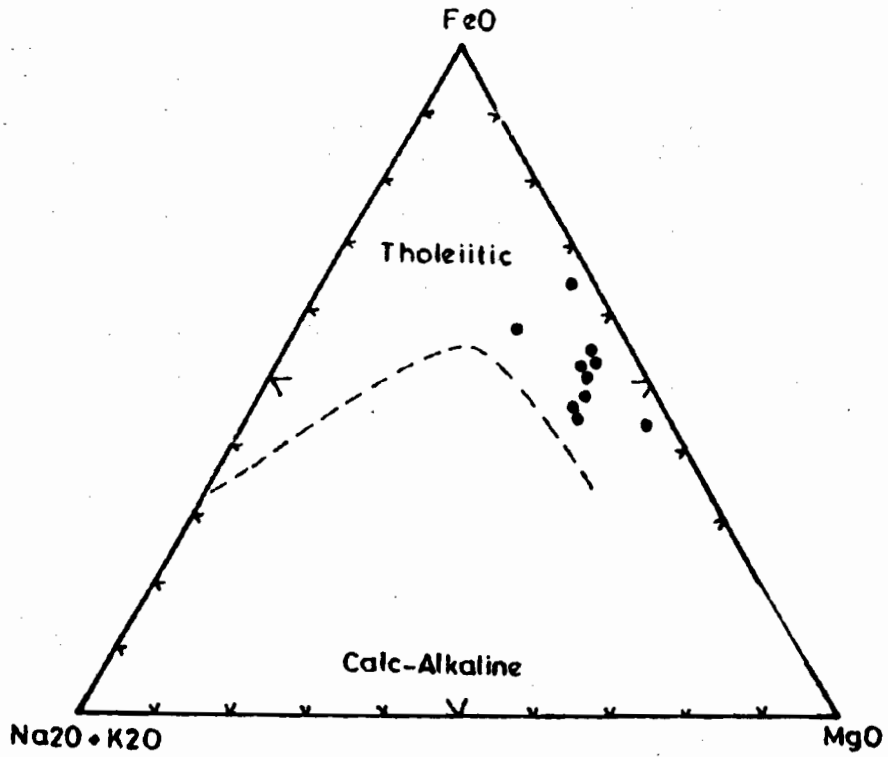

Figure 4: Chemical characterization of Isanlu Amphibolite on the AFM Scheme of Irvine and Baragar (1971)

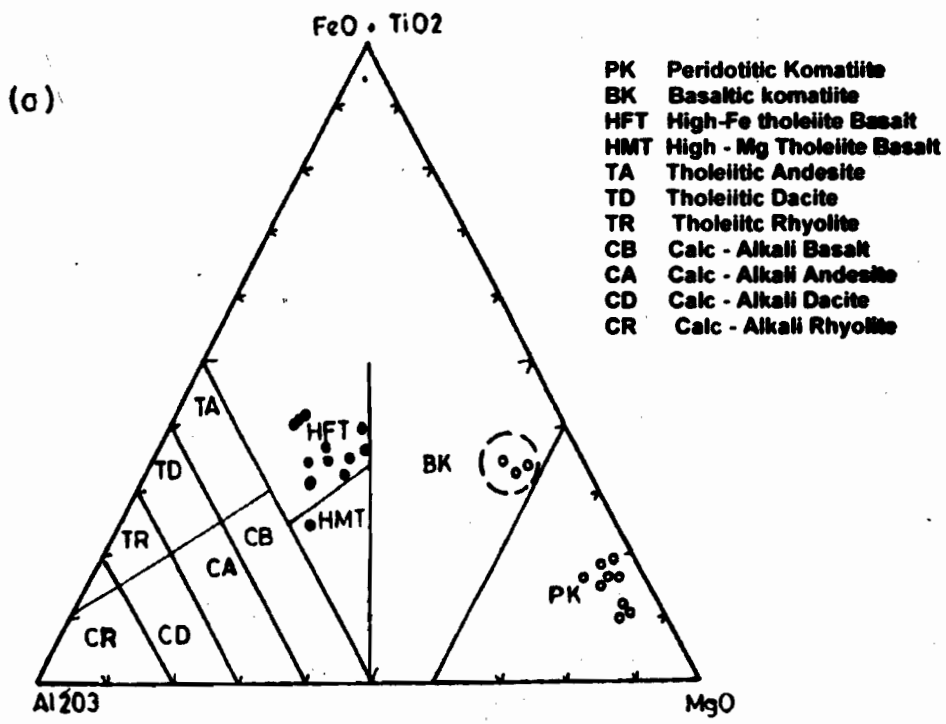

Figure 5: Chemical characterization of Isanlu Amphibolite on the Jensen plot

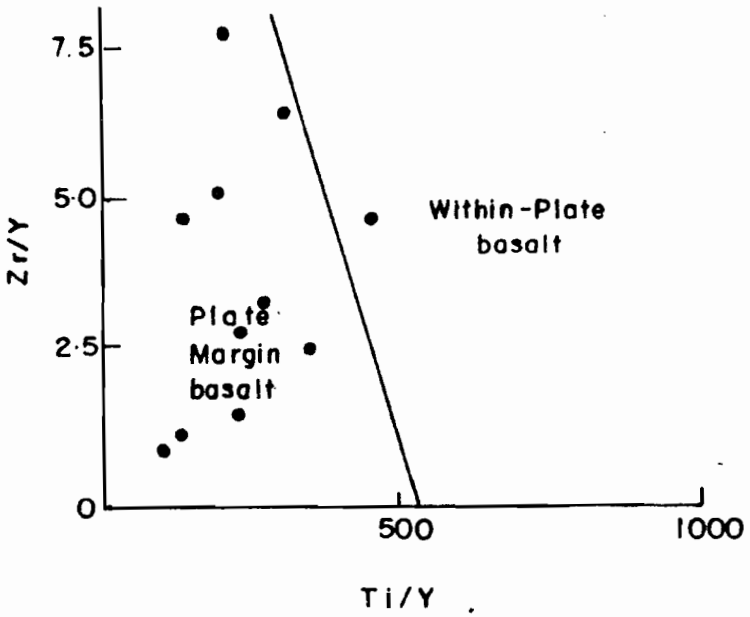

Figure 6: Tectonic discrimination of Isanlu Amphibolite on the Zr/Y versus Ti/Y diagram of Pearce & Gale (1977)

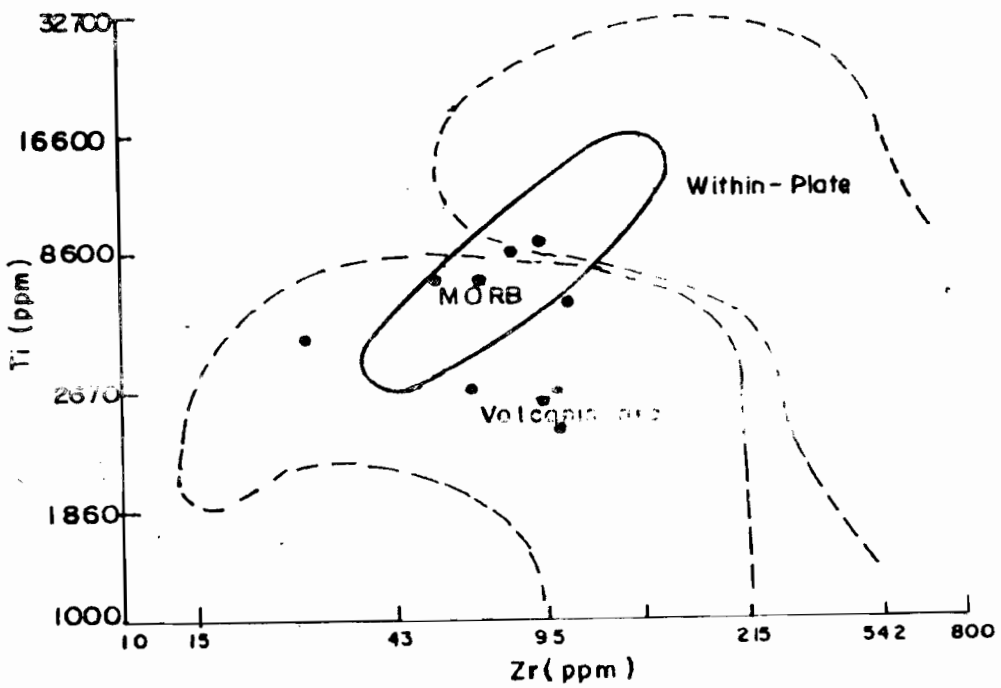

Figure:7: Tectonic discrimination of Isanlu Amphibolite on the Ti-Zr diagram of Pearce and Cann (1973)

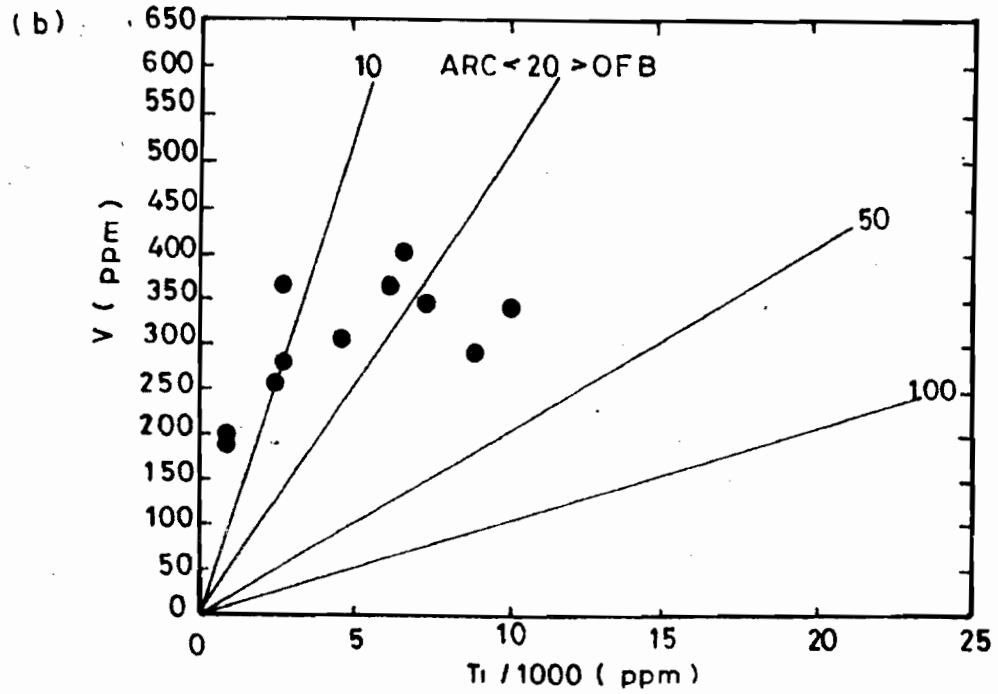

Figure 8: Tectonic discrimination of Isanlu Amphibolite on the V-Ti Scheme of Shervais (1982)

Table 1: Chemical Analysis of Amphibolite From Isanlu

	1	2	3	4	5	6	7	8	9	10	11
SiO_2 wt. %	48.10	50.20	49.60	48.30	46.50	48.94	50.03	53.74	47.48	48.48	47.83
Al_2O_3	15.60	13.80	14.90	15.10	14.10	14.14	12.74	10.24	10.56	12.56	14.66
Fe_2O_3	1.01	2.32	1.91	0.91	1.49	11.95*	11.62*	11.27*	12.93*	10.13*	10.66*
FeO	13.40	10.40	8.72	7.87	10.90	nd	nd	nd	nd	nd	nd
CaO	9.97	10.20	12.20	13.60	13.20	12.12	8.64	11.19	13.49	12.76	12.32
MgO	7.24	6.18	8.51	10.50	8.94	9.43	10.56	9.93	9.66	9.77	8.13
Na_2O	0.63	2.06	1.25	0.55	0.99	1.13	2.70	1.53	1.40	1.80	1.13
K_2O	0.15	0.97	0.39	0.24	0.25	0.18	0.30	0.80	0.60	0.99	0.66
TiO_2	1.68	1.09	0.15	0.15	1.21	0.79	1.01	0.42	0.47	0.47	1.43
P_2O_5	0.19	0.10	0.02	0.01	0.09	0.18	0.20	0.53	1.48	0.84	1.55
MnO	0.25	0.24	0.20	0.20	0.21	0.01	0.20	0.21	0.23	0.23	0.23
H_2O-	0.05	0.08	0.12	0.09	0.06	nd	nd	nd	nd	nd	nd
LOI	nd	0.52	0.64	0.56	0.61	nd	nd	nd	nd	nd	nd
	98.27	**98.16**	**98.61**	**98.07**	**98.56**	**99.27**	**98.15**	**99.86**	**98.30**	**98.03**	**98.60**
Nb ppm	12	6	7	6	9	1	12	16	15	21	32
Zr	94	71	17	12	49	33	117	107	97	68	88
Y	32	25	20	12	19	19	18	14	21	13	18
Sr	246	110	86	43	165	128	210	233	423	312	410
Rb	6	13	8	8	6	6	nd	nd	nd	nd	nd
Pb	9	10	9	13	6	7	nd	nd	nd	nd	nd
Ga	22	17	11	9	16	12	nd	nd	nd	nd	nd
Zn	112	105	72	53	82	77	75	100	120	87	87
Ni	114	34	63	63	99	120	260	150	320	290	120
Co	59	40	52	46	56	38	59	66	35	41	62
Cr	223	147	540	907	309	241	110	216	130	260	314
V	338	399	199	185	344	304	360	385	290	285	298
Ba	40	128	151	149	90	25	84	120	99	210	56
Sc	39	45	62	65	49	52	nd	nd	nd	nd	nd
Cu	nd	nd	nd	nd	nd	nd	110	245	220	120	167

nd = not determined, * = FeO (total)

Table 2: Statistical Summary of Isanlu Amphibolite Chemistry

SiO_2 wt %	53.74	46.50	49.02	1.92
Al_2O_3	15.60	10.24	13.49	1.79
Fe_2O_3	12.93	0.91	1.53	5.23
FeO	13.40	7.87	10.26	2.14
CaO	13.60	8.64	11.79	1.61
MgO	10.56	6.18	8.99	1.37
Na_2O	2.70	0.55	1.38	0.63
K_2O	0.99	0.15	0.50	0.32
TiO_2	1.68	0.15	0.81	0.52
P_2O_5	1.55	0.01	0.47	0.57
MnO_2	0.25	0.01	0.20	0.07
H_2O-	0.12	0.05	0.08	0.03
LOI	0.64	0.52	0.58	0.05
Nb ppm	32	1	12.45	8.55
Zr	117	12	68.45	36.29
Y	32	12	19.18	5.67
Sr	423	43	236.40	126.36
Rb	13	6	7.83	2.71
Pb	13	6	9.00	2.45
Ga	22	9	14.50	4.76
Zn	120	53	88.18	19.60
Ni	320	34	148.45	97.40
Co	66	35	50.36	10.80
Cr	907	110	308.82	230.64
V	399	185	307.91	68.62
Ba	210	25	104.73	54.37
Sc	65	39	52.00	9.96
Cu	245	110	172.40	59.59

The mean values of trace elements including, Nb (12.45ppm), Y (19.18ppm) and Rb (7.83ppm) are low in abundance levels compared to Archaean tholeiites and Phanerozoic oceanic tholeiites (Condie, 1981). Sr (236ppm) and Ba (104 ppm) show enhanced values relative to Archean and Phanerozoic oceanic tholeiites (Table 2) but probably reflect the abundance of modal plagioclase (10-30 vol.%) (Olobaniyi, 1997) or crustal contamination. Refractory trace metal including Ni (148.45 ppm), Co (50.36 ppm), Cr (308.82 ppm) and V (307.91ppm) show marked enrichment in mean values apparently reflecting the fairly primitive nature of its mafic parentage. Trace element ratios of Rb/Sr (0.08), Ni/Co (1.7), Ti/Zr (130), Zr/Y (3.7), and Ti/V (24.9) bear general resemblance to those of Archaean and Proterozoic Birrimian tholeiites (Table 3).

Table 3: Comparison of Mean Composition of Isanlu Amphibolite with Archean and Modern Tholeiites (Condie, 1976; 1981) and Birrimian Tholiites, Ghana (Leube et al., 1990).

		Archaean		**Preterozoic**	**Phanerozoic**		
	Average Isanlu Amphibolite	Depleted Archaean Tholeiite	Enriched Archaean Tholeiite	Birrimian Tholeiites, Ghana	MORB	Arc	Continental Rift
SiO_2 wt. %	49.02	50.2	49.5	48.7	49.8	51.1	50.3
Al_2O_3	13.49	15.5	15.2	13.7	16.0	16.1	14.3
Fe_2O_3	1.53	1.63	2.8	13.79	2.0	3 0	3.5
FeO	10.26	9.26	9 17	-	7.5	7 3	9.3
CaO	11.79	11.6	8.79	9 41	11.2	10 8	9.7
MgO	8.99	7.53	6.82	6.53	7.5	5 1	5.9
Na_2O	1 38	2 15	2.70	2.45	2.8	2 0	2.5
K_2O	0.50	0.22	0.69	0.34	0 14	0.30	0.8
TiO_2	0.81	0.94	1 49		1.5	0.83	2.2
P_2O_5	0.47	0.10	0.17	0.15	0.20	0.15	0.16
MnO	0.20	0.22	0.18	0.21	0.17	0.17	0.2
Zr ppm	68.45	53	135	72	100	60	200
Y	19.18	20	30	34	30	20	350
Sr	236 40	100	190	161	135	225	350
Rb	7.8	4	10	-	-	5	30
Zn	88.18	80	120	102	75	80	90
Ni	148.45	140	125	111	100	25	100

Co	50.36	52	55	62	32	20	40
Cr	308.82	490	250	184	300	50	100
V	307.91	260	365	299	300	270	300
Ba	104.73	80	90	98	11	60	350
CaO/Al_2O_3	0.89	0.75	0.58	0.70	0.70	0.67	0.68
Ba/Sr	0.84	-	-	-	-	-	-
Rb/Sr	0.08	0.04	0.06	-	0.0074	0.02	0.08
Ni/Co	1.7	2.7	2.3	1.8	3	1.3	2.5
Ti/Zr	130	106	66	104	90	83	66
Zr/Y	3.7	2.7	4.5	2.3	3.3	3.0	6.7
Ti/V	24.9	22	24	26	30	18	44

Tectonic Affinity

In determining the tectonic environment of emplacement of the metabasic rock, two factors are paramount. These are its chemistry and field structural relationship with other lithologies. The basic rock under study is not extensively fractionated at crystallization and as such is suitable for tectonic modeling. Several discrimination schemes that rely on presumed immobile elements in basic rocks and their metamorphic derivatives have been suggested as tools for tectonic environment prediction (Floyd and Winchester, 1975; 1978; Pearce and Norry, 1979; Wood, 1980; Pearce, 1982; Shervais, 1982; Meschede, 1986). For this investigation only high field strength (HFS) elements including, Ti, Zr, Y and V that are relatively immobile at mid-amphibolite facies condition (Rollinson, 1991) have been used. On the Zr/Y versus Ti/Y diagram of Pearce and Gale (1977) (Fig. 6) the rock plots dominantly in the field designated for plate margin basalts. An appraisal of the type of plate margin environment in which the rock was emplaced, using the Ti-Zr diagram of Pearce and Cann (1973) (Fig. 7), suggests a mid-oceanic ridge and volcanic arc setting. Further investigation on the V-Ti scheme of Shervais (1982) (Fig. 8) corroborates its ocean floor-type chemistry. Wood et al. (1979) have discriminated between normal (N)- and plume(P)-type MORB N-type MORB have Zr/Nb ratios > 30 whereas P-type MORB and oceanic island tholeiites have low ratios ≈≈ 10 The Isanlu metabasic rocks have values between 2-9 suggesting compatibility with P-type MORB

Although the trace element geochemistry of the mafic rock suggests an oceanic origin, its field and structural relationship with other lithologies indicate otherwise. Field evidence unambiguously shows that this rock originated as sills or sub-concordant intrusives into the original sediments of the basin. The interlayered nature of this rock with metasediments indicates that no fully developed oceanic crust existed. According to Green (1992), such chemistry can also be associated with plume-induced continental rifts, where the crust is sufficiently thinned resulting in minimal crustal contamination. Its chemistry may rather suggest that the tectonic setting is comparable with respect to the degree of depletion, especially in trace elements, to Phanerozoic ocean-floor basalts (Leube et al. 1990). A more plausible model would be an ensialic basin developed on rift-controlled grabens in which sedimentation and magmatism was contemporaneous. The genesis of this rift can be related to the activity of mantle plumes causing crustal thinning and melting of mantle materials below the thin crust (at shallow levels) resulting in their emplacement as dykes and sills

DISCUSSION AND CONCLUSIONS

The preceding sections suggest that the amphibolite of Isanlu bear tholeiitic petrogenetic affinity and are emplaced in a plume-induced rifted basin. Such basins now represented by schist belts are numerous in the Precambrian terrain of Nigeria (Elueze, 1992). This may imply the activity of several contemporaneous plumes in the Precambrian of Nigeria. The genesis of such plumes is still not well understood, but it has been speculatively linked to back-arc activities, in response to plate margin processes at the boundary of the West African craton and Benin-Togo-Nigeria shield (Burke and Dewey, 1972). Recently, Courtillot et al. (2003) recognized the activity of superplumes in the antipolar regions of the world namely, Africa and the Central Pacific Ocean. According to Gurnis et al. (2000), these plumes are evidenced by superswells (high crustal elevations) and by corresponding regions of low S-wave velocity in the mantle. The African superplume possibly included a number of secondary plumes acting on various parts of the African plate for long periods of geological time (Pijarno, 2004), initiating basins and possibly instigating orogenic activities within the geological domain.

The geochemistry of mafic rocks could be useful benchmarkers for assessing the extent of lateral continuity or heterogeneity of the subcontinental mantle (Tommasini et al., 2005). The chemical nature of the Isanlu amphibolite is comparable to most other amphibolites found in other schist belts of Nigeria (Olade and Elueze, 1979; Elueze, 1985; Elueze and Okunlola, 2003; Okunlola et al., 2006). Generally, this rock constitutes a fairly uniform suite and only minor variations are observed between the belts. Such minor variations probably reflect varying degrees of crustal contamination during magma ascent through somewhat unequally attenuated crust. Significantly, this implies a regionally homogeneous subcontinental mantle within the Precambrian domain of Nigeria. It may also reflect a consistent petrogenetic process within the domain in the Precambrian.

REFERENCES

Ajibade, A. C., and Wright, J. B., 1989. The Togo-Benin-Nigerian shield: evidence of crustal aggregation in the Pan-African belt. Tectonophysics, 165: 125-129.

Ajibade, A. C., Rahaman, M. A. and Woakes, M., 1987. Proterozoic crustal development in the Pan-African regime of Nigeria. In: Proterozoic

Lithospheric Evolution (Kroner, A. editor). American Geophysical Union. 17: 259 - 271

Annor, A. E., Olobaniyi, S. B., Mucke, A., 1996. A note on the geology of Isanlu area in the Egbe – Isanlu schist belt, southwest Nigeria. Journal of mining and Geology, 32(1): 47- 51

Bafor, B. E., 1988. Some geochemical considerations in the evolution of the Nigerian basement in the Egbe area of southwestern Nigeria. In: Precambrian Geology of Nigeria (Oluyide P.O. et al. editors) Geological Survey of Nigeria 277-288.

Burke, K. C. and Dewey, J. F., 1972. Orogeny in Africa. In: African Geology (Dessauvagie T.F. and Whiteman, A.J. editors.). University of Ibadan. 583-608

Condie, K. C., 1976. Trace element geochemistry of Archean greenstone belts. Earth Science Review 12(4): 393-417.

Condie, K. C., 1981. Archean greenstone belts.

Courtillot, V., Davaille, A., Besse, J. and Stock, J., 2003. Three distinct types of hotspots in the Earth's mantle. Earth and Planetary Science Letters 205: 295 – 308

Dada, S. S. and Briqueu, L., 1996. Pb-Pb and Sm-Nd isotopic study of metaigneous rocks of Kaduna: implication for the Archaean mantle in northern Nigeria. 32rd Annual Conference Nigerian Mining and Geosciences Society, Benin. Abstract 57p.

Elueze, A. A., 1985. Petrochemical and petrogenetic characteristics of Precambrian amphibolites of Alawa district, northwestern Nigeria. Chemical Geology 48: 29 - 41.

Elueze, A. A. 1992. Rift systems for Proterozic schist belts in Nigeria. Tectonophysics 209. 167-169.

Elueze, A. A. and Okunlola O. A. 2003. Geochemical features and petrogenetic affinity of Precambrian amphibolites at Burum area central Nigeria. Journal of Mining and Geology 39(2): 71 - 78.

Floyd, P.A. and Winchester, J.A., 1975. Magma-type and tectonic setting discrimination using immobile elements. Earth and Planetary Science Letters 27: 211-218.

Floyd, P. A. and Winchester, J. A., 1978. Identification and discrimination of altered and metamorphosed volcanic rocks using immobile elements. Chemical Geology 21: 291-306.

Frimmel, H. E., Hartnady, C. J. H. and Koller, F. 1996. Geochemistry and tectonic setting of magmatic units in the Pan-African Gariep belt, Namibia. Chemical Geology 130: 101-121.

Green, J. C., 1992. Proterozoic rifts. In: Proterozoic Crustal Evolution (Condie, K.C. ed). Developments in Precambrian Geology 10: 97 - 147.

Gurnis, M, Mitrovica, J. X, Ritsema, J, van Heijst, H. J. 2000. Constraining mantle density structure using geological evidence of surface uplift rates: the case of the African Superplume. Geochem Geophys Geosyst 1, pap no 1999GC000035

Irvine, T.N. and Baragar, W. R. A., 1971. A guide to the chemical classification of common volcanic rocks. Canadian Journal of Earth Science 8: 523 - 548.

Jensen, L.S., 1976. A new cation plot for classifying subalkalic volcanic rocks. Ontario Division of Mines. Miscellaneous Paper 66, USA

Kennedy, W. R. 1964. The structural differentiation of Africa in the Pan-African (+500my) episode. Research Institute for African Geology (Leeds). 8th Annual Report 48-49.

Elsevier, Amsterdam

Leube, A., Mauer, R. and Kesse, G.O., 1990. The early Proterozoic Birrimian Supergroup of Ghana and aspects of its associated gold mineralization. Precambrian Research 46: 139 -165.

Meschede, M., 1986. A method of discriminating between different types of mid-oceanic ridge basalts and continental tholeites with the Nb-Zr-Y. Chemical Geology 56: 207 - 218.

Myers, R. E. and Breitkopf, H., 1989. Basalt geochemistry and tectonic setting: a new approach to relate tectonic magmatic process. Lithos 23: 53 - 62.

Okunlola, O. A., Akintola, A. I. and Egbeyemi, R. O., 2006. Compositional features and petrogenetic affinity of Precambrian amphibolitic schist of Sepeteri area southwestern Nigeria. Global Journal of Geological Sciences 4(2): 199-208

Olade, M. A. and Elueze, A. A. 1979. Petrochemistry of the Ilesha amphibolites and Precambrian crustal evolution in the Pan-African domain of SW. Nigeria. Precambrian Research 8: 303-318.

Olobaniyi, S. B., 1997. Geological and geochemical studies of the basement rocks and associated iron formation of Isanlu area in the Egbe-Isanlu schist belt, southwest Nigeria. Ph.D Thesis, University of Ilorin, Nigeria. 240pp.

Oversby, V.M., 1975. Lead isotopic study of aplites from the Precambrian basement rocks near Ibadan, southwestern Nigeria. Earth and Planetary Science Letters 27: 177-180

Pearce, J. A., 1982. Trace element characteristics of lava from destructive plate boundaries. In: Andesites (Thorpe, R.S. editor) Wiley Chester 525-548.

Pearce, J. A. and Cann, J. R., 1973. Tectonic setting of basic volcanic rocks determined using trace element analysis. Earth and Planetary Science Letters 19: 290-300.

Pearce, J. A. and Gale, G. H., 1977. Identification of ore deposition environment from trace element geochemistry of associated igneous host rocks. Geological Society Special Publication 7: 14-24.

Pearce, J. A. and Norry, M. J. 1979. Petrogenetic implication of Ti, Zr, Y and Nb variations in volcanic rocks. Contributions to Mineralogy and Petrology 69: 33 - 47.

Pirajno, F., 2004. Hotspots and mantle plumes: global intraplate tectonics, magmatism and ore deposits. Mineralogy and Petrology, 82: 183-216.

Rahaman, M. A., Ajayi, T. R., Oshin, I..O. and Asubiojo, F. O. I., 1988. Trace element geochemistry and geotectonic setting of Ife-Ilesha schist belt. In: Precambrian Geology of Nigeria. (Oluyide P.O. et al. editors). Geological Survey of Nigeria. 241-256.

Rollinson, H. 1993. Using geochemical data: evaluation, presentation, interpretation. Longman. London.

Shervais, J. W., 1982. Ti-V plots and the petrogenesis of modern and ophiolitic lavas. Earth and Planetary Science Letters 59: 101-118.

Tommasini, S , Manetti, I. P., Innocenti, F., Abebe1, T., Sintoni1, M. F. and Conticelli1, S., 2005. The Ethiopian subcontinental mantle domains: geochemical evidence from Cenozoic mafic lavas. Mineralogy and Petrology 84: 259-281

Winchester, J. A. and Floyd, P. A. 1977. Geochemical discrimination of different magma series and their differentiation products using immobile elements. Chemical Geology 21: 291-306.

Wood, D.A., 1980. The application of a Th-Hf-Ta diagram to problems of tectonomagmatic classification and to establishing the nature of crustal contamination of basaltic lavas of the British Tertiary volcanic provinces. Earth and Planetary Science Letters 50: 11-30.

Wood, D. A., Jornon, J.L and Trevil, M., 1979. A re-appraisal of the use of trace elements to classify and discriminate between magma series erupted in different tectonic settings. Earth and Planetary Science Letters 45: 326-336.

GLOBAL JOURNAL OF GEOLOGICAL SCIENCES VOL. 6 NO. 2 2008: 123 - 127
 ISSN 1596 – 6798

A TECTONIC IMPLICATION OF THE ERUPTION OF PYROCLASTICS IN UTURU, SOUTHERN BENUE TROUGH, SOUTHEAST NIGERIA

V.U. UKAEGBU

(Received 11 May, 2007; Revision Accepted 1 July, 2008)

ABSTRACT

The origin of the Benue Trough is linked to rifting associated with the separation of South America from Africa in the Cretaceous times. The vast igneous activities in the trough are thought to either precede the separation of the two continents or post-date Albian sediments deposited in the trough after the separation. Exposures of pyroclastics within flatland in Uturu, east of Okigwe, were studied with a view to determining the implication of the eruption that emplaced the pyroclastics on the tectonic evolution of the Lower Benue Trough. Field expressions show that the pyroclastics erupted parallel to the axial plane of the Abakiliki anticlinorium in NE-SW direction and are spatially associated with shales of the Asu River Group and Nkporo Shale. Mud fragments of diverse sizes (1cm-20cm) and shapes of the host Asu River Group are incorporated in the pyroclastics. The sizes of the fragments of the pyroclastics fall mainly within the range of tuff and lapilli composed of mainly pyroxene, plagioclase, melilite and opaque minerals. The Nkporo Shales form cover unit over the pyroclastics and do not show any effect of the volcanism on them. The stratigraphic relationship between the pyroclastics and the surrounding sedimentary units shows that the pyroclastics erupted after the deposition of Asu River Group shales (mid-Albian) but terminated before the deposition of the Nkporo Shales. This corresponds to period between Cenomanian and Santonian and suggests a link to the tectonic events that post-dated the separation of South America from Africa.

KEYWORDS: Benue Trough, Tectonism, Abakiliki anticlinorium, pyroclastics, lapilli.

INTRODUCTION

The origin and evolution of the Benue Trough are believed to be related to an aulacogen (Olade, 1975) or rift formed during the separation of South America from Africa in the Cretaceous (Okereke, 1988; Okeke et al. 1988; Freeth, 1990; Nwachukwu, 1990). Benkhelil (1989) was of the view that transcurrent faulting through an axial fault system, which developed local compressional and tensional regimes that resulted in basins and basement horsts, controlled the tectonic evolution of the Benue Trough. Benkhelil (1989) further posited that magmatism in the Cretaceous times was restricted to main fault zones in most of the trough, especially in the Abakaliki Trough, where it has alkaline affinities. However, in general, these igneous activities are thought to either precede the separation of South America from Africa (Uzuakpunwa, 1974; Ekwueme, 1994; Olade, 1979; Amajor and Ofoegbu, 1988) or post-date Albian sediments in the trough.

A study of one of the igneous activities at Uturu, 8km east of Okigwe, within the foot of the Okigwe-Awgu escarpment in the Lower Benue Trough was undertaken. Literature indicates that four lithologic units of Cretaceous ages have been recognized in Uturu (Simpson, 1955; Reyment, 1965), with the marine shale of the Asu River Group forming the oldest unit and the Ajali Sandstone, the youngest unit. The Santonian tectonism appears to have been accompanied by development of major faults and spates of volcanic activities (Hoque, 1980). Among the products of the volcanic activities are pyroclastics, which are associated with the Cretaceous sedimentary series, where the Nkporo Shale oversteps the Asu River Group unconformably. Pyroclastics are known to be important constituents of vapour-rich magma phases, and their eruption usually gives rise to a variety of fragments.

The pyroclastics outcrop in three low hills in Amanyanwu village of Uturu (Fig. 1), covering a total area of about 22,000m^2, and trend in a NE-SW direction, parallel to the Abakiliki anticlinorium (Fig. 1). The area forms an uneven relief, with the pyroclastic hills showing pronounced erosional features that impact smooth surfaces, devoid of thick vegetation, to the rocks (Fig. 2) and separated by low-lying Nkporo Shale. Lying at the foot of these pyroclastic bodies are ferruginous sands and dislodged boulders of the pyroclastics. Amajor et al. (1988) interpreted the Uturu pyroclastics as intra-continental plate alkaline basaltic volcanic rocks. This research is an attempt to use the mode of field occurrence, mineral paragenesis and textural characteristics deduced from petrography to suggest a regional tectonic model for the Lower Benue Trough.

V. U. Ukaegbu, Department of Geology, University of Port Harcourt, Port Harcourt, Nigeria

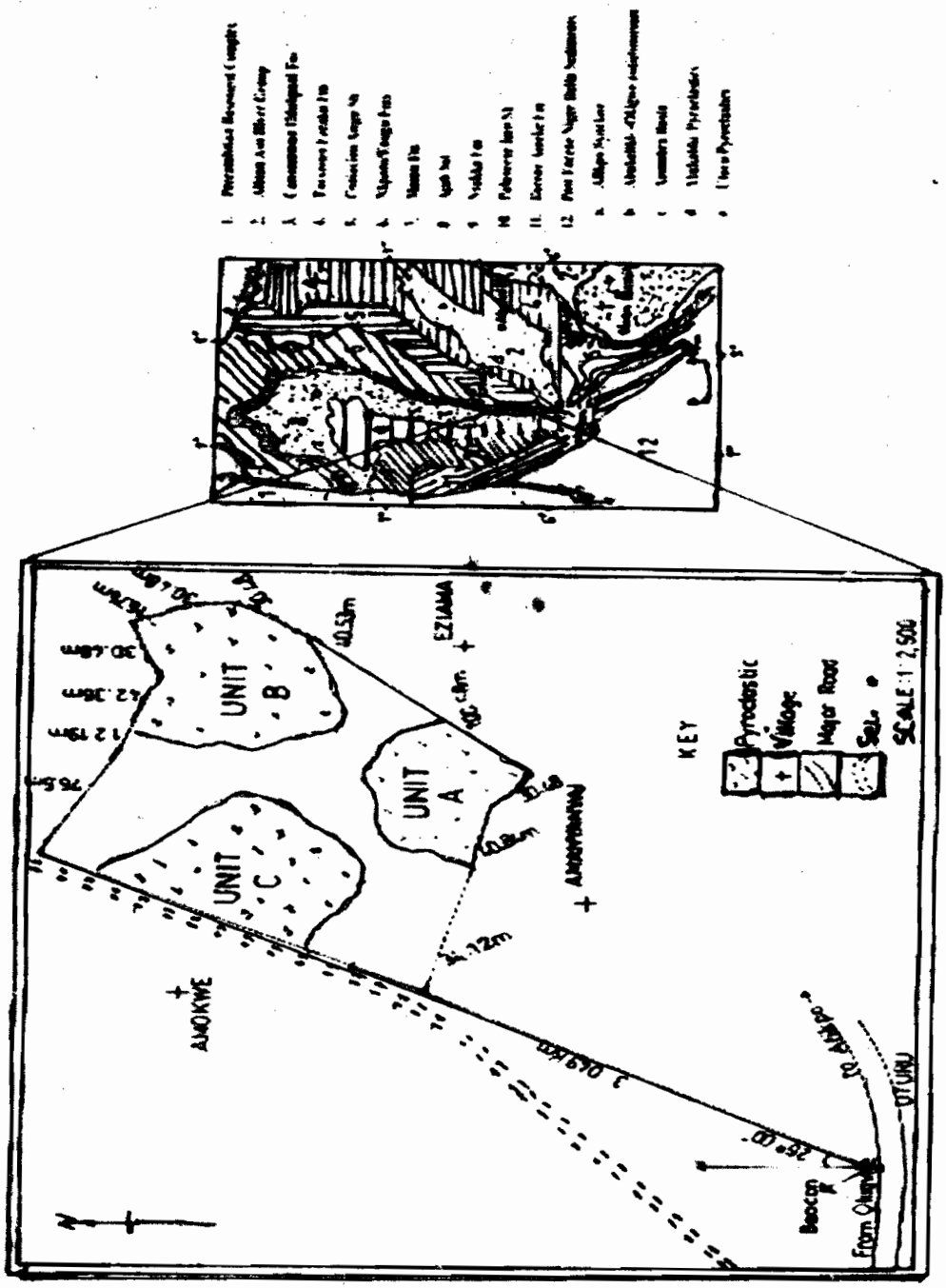

Fig. 1: Geologic map of the Study area showing the outcrops of the pyroclastics at Uturu. Inset: Geologic map of part of southeastern Nigeria showing the Abakiliki anticlinorium (adopted from Amajor and Ofoegbu, 1988).

METHOD OF STUDY

Field studies of three units of the pyroclastics were undertaken to evaluate their spatial expressions such as aerial extent, exposed sections, contact relationships, structural trends and some special features like sizes and shapes of fragments. Samples were randomly collected vertically and across the exposures for microscopic studies to determine their mineralogy and textures in order to properly classify them and infer their petrogenetic and geothermal characters.

RESULTS AND ANALYSIS

Field Relations

The three units are essentially similar in mineralogy, texture, contact relationship and layering pattern. There are also other smaller units scattered around and between these principal units. The pyroclastics intruded the Asu River Group but are overlain in some parts by Nkporo Shale. Mamu and Ajali Formations are not associated with the pyroclastics. The Asu River Group, through which the pyroclastics extruded, is low-lying. The pyroclastics form maximum relief of up 7m above the flatland of Nkporo shales. Excellent exposures of the pyroiclastics are displayed by massive quarry activities

in the area. There are some distinctive layers from base to top (Fig. 3) and alternation of thick (0.75-1.5m) and thin (about 0.15m) layers in all the three locations of 7,500m^2, 8,438m^2 and 6,250m^2, respectively. When fresh, the rocks are greenish to dark colour and light to brownish colour when weathered. Large rounded, spindle-shaped fragments (agglomerate bombs) of the pyroclastics are embedded in fine matrix components.

Mineral Composition

Mineralogy of the pyroclastics is uniform. In thin section, the constituent minerals are mainly euhedral pyroxene (augite), plagioclase and melilite. Quartz, pyroxene, plagioclase and melilite occur as phenocrysts. The groundmass minerals show interference colours from colourless to dark-grey, blue or brown, and are also largely pyroxene, plagioclase and melilite. Opaque minerals are present in varying amounts.

Fragments and Textures

Pyroclastics in the Benue Trough have been variously described as pyroclastic flows, breccias, tuffs, agglomerates (Okezie, 1965; Uzuakpunwa, 1974 and Olade, 1979). Field studies indicate that all the fragments are highly angular except for a few agglomerate bombs in matrix of tuff or lapilli. Thus, most of the fragments appear to have been emplaced in solid condition. There are a few blocks of older rock components of sedimentary origin, whereas majority of the fragments fall under lapilli size. Thus, the pyroclastics are principally composed of lapilli breccia. Some few sections are composed of entirely volcanic tuff. In some places, lapilli are moderately scattered in the tuff to form lapilli-tuff. The Uturu pyroclastics compare with the Abakiliki pyroclastics described by Olade (1979). Most of the large fragments are mixtures of both angular and rounded fragments (Fig. 4). Some of the fragments show chilled margins (Fig. 5), while the vitric tuff shows vitroclastic texture (Fig. 6). Vesicles are common features of most parts of the pyroclastics.

Fig.2. Sparse vegetation within the pyroclastic bodies

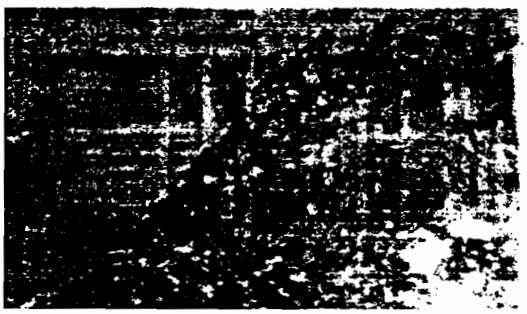

Fig.5. Chilled margin between layers of the pyroclastics rich in volcanic bombs and ash breccia

Fig.3. The pyroclastics showing well defined layering

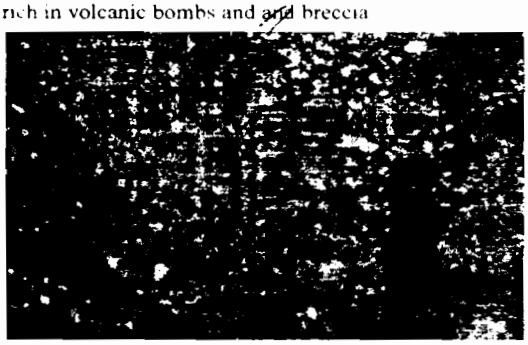

Fig.6. Vitric textures of the pyroclastics in the Study Area

Fig.4. Porphyritic textures of the pyroclastics in the Study Area

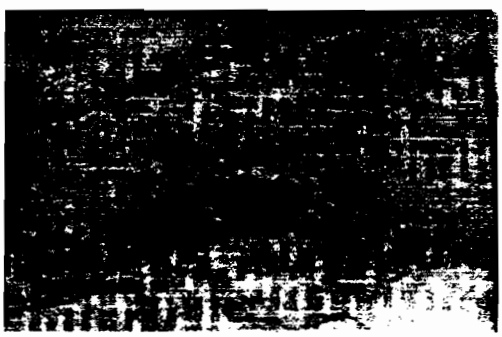

Fig.7. Shaly fragment of the older Asu River Group in the pyroclastics.

GEOTECTONIC IMPLICATIONS

Earlier workers relate the origin of the Benue Trough to the separation of South American continent from the African continent in early Cretaceous (Burke *et al.* 1971; Wright, 1981). Many scholars believe that South America finally separated from Africa in Santonian times and that the high level tectonic activities that occurred in Santonian times may be related to the separation of these two continents (Wright, 1968, 1972; Burke *et al.* 1971; Nwachukwu, 1972; Hoque, 1980). The swinging back of Africa due to the final separation from South America formed compression zones, which may have been responsible for the intense folding, faulting and volcanism in the Benue Trough, during the Santonian times (Ekwueme, 1994). Burke and Whiteman (1973) believed that the magmatism in the Benue Trough was andesitic due to sea floor spreading.

The basaltic mineral compositions of mainly pyroxene, plagioclase and melilite, and the dominance of fine to glassy texture and eruption along the axis of the Abakiliki anticlinorium suggest deep-seated source, which exploited the fissures created by the Cenomanian or Santonian tectonism resulting from separation of South America from Africa in the Cretaceous times (Beka and Ukaegbu, 2006). The interactions of these two continents may have resulted to fluid accumulation in the axis of their stress field, along the Abakiliki Anticlinorium, giving rise to explosive eruption of the magma from beneath. Thus, the pyroclastics appear to be products of widespread tectonism, which accompanied the separation of South America from Africa. However, the pyroclastics do not show any evidence of tectonic deformation

The pyroclastics seem to be controlled by the NE-SW trending axis of the Abakiliki Anticlinorium, suggesting that the Santonian (or earlier Cenomanian) tectonic event might have formed a fracture system that trends parallel to the axis of the Abakiliki Anticlinorium, in the Benue Trough. This evidence is collaborated by Hoque (1984), who said, "the pyroclastics are much younger (late Santonian) than the Benue Trough (early Cretaceous)". The fracture system may have provided the pathway for the magma that eventually erupted explosively due to huge accumulated gas phase. If the extrusion was consequent to the Cenomanian or Santonian event, then it explains the presence of near-vertical aligned mud rocks of the pre-Santonian shale of the Asu River Group in the pyroclastics. The time of the magmatism can be deduced from the stratigraphic relationship between the pyroclastics and surrounding sedimentary sequences (Table 1). Since the Asu River Group (Albian) is older than the pyroclastics as supported by inclusions of its fragments in the pyroclastics (Fig.7), and, on the other hand, the pyroclastics are older than the overlying Nkporo Shale (Campo-Maastitchian), then the pyroclastics were emplaced between the Albian and Campanian times However, because there were two tectonic episodes between the Albian and Campanian times (Reyment, 1965; Nwachukwu, 1972; Uzuakpunwa, 1974; Olade, 1975), the eruption could have taken place during one of these two events.

CONCLUSION

Petrological investigation revealed basaltic source, dominated by pyroxene, plagioclase, melilite and opaque minerals and the pyroclastics show primary structures such as xenoliths of mud rocks derived from the older shales of the Asu River Group, and parallel layering. The stratigraphic relationship between the pyroclastics and the surrounding shales of the Asu River Group suggests a post-Albian but pre-Campanian age for the pyroclastics. The eruption may be related to the separation of South America from Africa. The interactions of these two continents may have resulted to fluid accumulation in the axis of their stress field, parallel to the axis of the Abakiliki Anticlinorium, resulting in explosive eruption of the magma from beneath. The swinging back of Africa due to the final separation from South America formed compression zones, which may have been responsible for the intense folding, faulting and volcanism in the Benue Trough, during the Santonian times.

REFERENCES

Amajor, L.C. and Ofoegbu, C.O, 1988. Intra-continental Plate Alkaline Basaltic volcanism, Uturu, Southern Benue Trough, Nigeria. Acta Universitatis Carolinae-Geologica. 2: 233-242.

Beka, F.T. and Ukaegbu, V. U., 2006. Trace and Rare Earth Elements as petrogenetic and geotectonic indicators for dolerite dykes in Obudu Plateau, Bamenda Massif, southeastern Nigeria.

Benkhelil, J., 1989. The Origin and Evolution of the Cretaceous Benue Trough (Nigeria). Journal of African Earth Sciences 8: 251-282.

Burke, K.C. and Whiteman, A. J., 1973. Uplift, rifting and the break up of Africa. In: Tarling and Runcorn (Eds): Implications of Continental Drift to the Earth Sciences, 735-55, Academy Press, London.

Burke, K., Dessauvagie, T.F.J. and Whiteman, A.J., 1971. Opening of the Gulf of Guinea and the geological history of the Benue depression and Niger Delta Nature Phys. Sci. 233, 51-5.

Ekwueme, B N., 1994 Basaltic magmatism related to the early stages of rifting along the Benue Trough: the Obudu Dolerite of southeast Nigeria. Geol. Journ., 29: 269-276.

Freeth, S.J., 1990 The origin of the Benue Trough. In: Oforgbu, C. O., (Ed) The Benue Trough Structure and Evolution Friedr Vieweg and Sohn, Braunschweig/Wiesbaden, pp 217-227.

Hoque, M., 1980. Pyroclastics Volcanism ant Tectonics of S. E. Benue trough, Nigeria TAVCE I Symposium, Arc Volcanism, Tokyo Pp134-136.

Hoque, M. 1984. Pyroclastics from the Lower Benue Trough of Nigeria and their tectonic implications. Journ. Africa Earth Sci., 2(4): 1-358.

Nwachukwu, J., 1990. Petroleum Resources of the enue Trougfh. In: Oforgbu, C.O. (Ed.). The enue Trough Structure and Evolution. Friedr. ieweg and Sohn, Braunschweig/Wiesbaden, p 217-227.

Nwachukwu, S.O., 1972. The Tectonic Evolution of the outhern Portion of the Benue Trough, Nigeria. Geol. Mag. 109 (5): 411-419.

Okeke, P.O., Ofoegbu, C.O., Amajor, L.C., 1988. On the origin of the highly altered basalts, Southern Benue Trough, Nigeria. Bulgarian Academy of Sciences. Geochemistry, Mineralogy and Petrology, 24, Sofia. Pp55-67.

Okereke, C.S., 1988. Contrasting Models of rifting: The Benue Trough and Cameroon Volcanic Line, West Africa. Tectonics, 7(4): 775 - 784.

Okezie, C.N., 1965. A preliminary report on the igneous rocks of Abakiliki town and environs, and their relation to lead- zinc mineralization. Unpubl. Geol. Surv. Report No. 1349.

Olade, M. A., 1975. Evolution of Nigeria Benue Trough Aulacogen): A Tectonic Model. Geol. Mag. 112: 575-583.

Olade, M. A., 1979. The Abakaliki pyroclastics of southern Benue Trough Nigeria: their petrology and tectonic significance.

Reyment, R.A., 1965. Aspects of the Geology of Nigeria. Ibadan University Press. Pp23-70.

Simpson, R., 1955. The Nigeria Coal Fields. The Geology of parts of Owerri and Benue Provinces. Geol. Surv. Nigeria Bull. 24: 83-86.

Uzuakpunwa, A. B., 1974. The Abakiliki pyroclastics – Eastern Nigeria: new age and tectonic implications. Mag. III (1): 65 - 70.

Wright, J. B., 1968. South Atlantic Continental drift and the Benue Trough> Tectonophysics 6: 301-310.

Wright, J. B., 1972. High pressure phases in Nigerian Cenozoic lavas: distribution and setting. Bull. Volcanol. 34: 833 - 847.

Wright, J. B., 1981. Review of the origin and evolution of the Benue Trough in Nigeria. Earth Evolution Sciences, 2: 98-103.

GLOBAL JOURNAL OF GEOLOGICAL SCIENCES VOL. 6 NO. 2 2008: 129 - 137
 ISSN 1596 – 6798

SEQUENCE STRATIGRAPHIC APPRAISAL: COASTAL SWAMP DEPOBELT IN THE NIGER DELTA BASIN NIGERIA

N. O. UNUKOGBON, G. O. ASUEN AND W. O. EMOFURIETA

(Received 7 February, 2008; Revision Accepted 30 July, 2008)

ABSTRACT

Mid-Lower Miocene Agbada sedimentary intercalations of "AB" Field in the coastal swamp depobelt, Western Niger-Delta, were evaluated to determine their sequence stratigraphic character. The analysis was based on a combination of data sets including logs of six wells to describe lithic variations of the Agbada Formation within the 'AB' Field. These well logs were integrated with biostratigraphic data to develop a sequence stratigraphic framework. The results revealed two maximum flooding surfaces dated 10.4Ma and 9.5Ma. A sequence boundary dated at 10.35Mya was also identified across the field. The strata in the study area were divided into lowstand system tracts (basin floor fan, slope fan and prograding wedge), transgressive and highstand systems tracts. Biostratigraphic data suggested that these sediments were deposited in coastal deltaic to bathyal marine environments. Basal deposits directly overlying sequence boundaries where formed by the migration of large distributary channels. Upward coarsening sets of inclined beds, hundreds of feet thick, record progradation of deltas into slope. Blocky and upward fining well-log patterns are interpreted to reflect deposition in shoreline, paralic, and fluvial environments. The thick sequences of highly microfossiliferous are the probable petroleum source rocks. The massive sand formation of the basin floor fan, the sand-rich prograding wedge and the highstand sands as well as the transgressive sands constitute good reservoirs. The distal shale toes of the prograding wedge and transgressive shales as well as highstand shales form seals for the stratigraphic traps formed in the study area.

KEYWORDS:- Sequence stratigraphic tool, system tract deposits.

INTRODUCTION

The Tertiary Niger Delta Basin is a prolific oil province within the West African subcontinent (Fig. 1). The basin covers an area of some 70,000km^2 area within the Gulf of Guinea in Western Africa. Its origin is associated with the failed arm of a rift triple junction associated with the opening of the South Atlantic during the late Jurassic that persisted into the Middle Cretaceous (Lehner and De Ruiter, 1977).

Three formations are defined (Short and Stauble, 1967) within the 4km (13,000 ft) thick Niger delta clastic wedge based on sand/shale ratios estimated from subsurface logs: (1) Basal offshore-marine and prodelta shale of the Akata Formation, (2) Interbedded sandstone and shale of the dominantly deltaic Agbada Formation and (3) The fluvial continental sands of the Benin Formation.

Sequence stratigraphy offers a model in which a series of system tracts within a depositional sequence is deposited in response to a cycle of relative fall and rise of sea level. The analysis of these cycles can be used to explain how the mechanisms of sediment accumulation, erosion and inter-related processes produced the current configuration of these rocks, and the time involved in their deposition, as each layer is bounded by surfaces that transgress time (Wheeler, 1958; Middleton, 1973; Vail et al 1977; Galloway, 1989; Catuneanu, et al, 1988; Catuneanu, 2002; Embry, 2002; Mitchum, 1977; Fischer & McGowan 1967; Van Wagoner et al; 1990; Van Wagoner et al; 1988; Kerans & Tinker, 1997; and Mitchum & Van Wagoner, 1991).

Sequence stratigraphy was applied to sedimentary analysis of 'AB' Field of the Niger Delta Basin using well logs integrated with high resolution biostratigraphic data of six wells to develop a sequence stratigraphic framework for the field. This was done by ascertaining the major bounding surfaces, their age relationships as well as depositional environments.

The study area described as 'AB' Field is on the onshore part of the Western Niger Delta Basin. The delta is composed of mega units coastal swamp depobelts (Fig.3). It is described as a shelf-contained entities with respect to stratigraphy, structure-building, and hydrocarbons distribution. The field covers an area of 450km square. The six exploration wells studied are all deviated (Fig. 4). The major producing Agbada Formation has an average depth of 5,700ft in 'AB' Field.

The aim of this appraisal is to subdivide the stratigraphic column of the "AB" Field into sequences and systems tracts based on the integration of available well logs and high resolution biostratigraphic data. This will help to delineate potential reservoirs, source rocks and stratigraphic traps, by identifying facies and their associations as a tool for the development of a sequence stratigraphic framework of the field. This is done through the identification of parasequence and establish parasequence set stacking pattern major bounding surfaces, system tracts and predict field wide sequence stratigraphical relationships.

N. O. Unukogbon, Department of Geology, University of Benin, Benin City, Nigeria
G. O. Asuen, Department of Geology, University of Benin, Benin City, Nigeria
W.O. Emofurieta, Department of Geology, University of Benin, Benin City, Nigeria

Fig.1: Global position of the Niger Delta

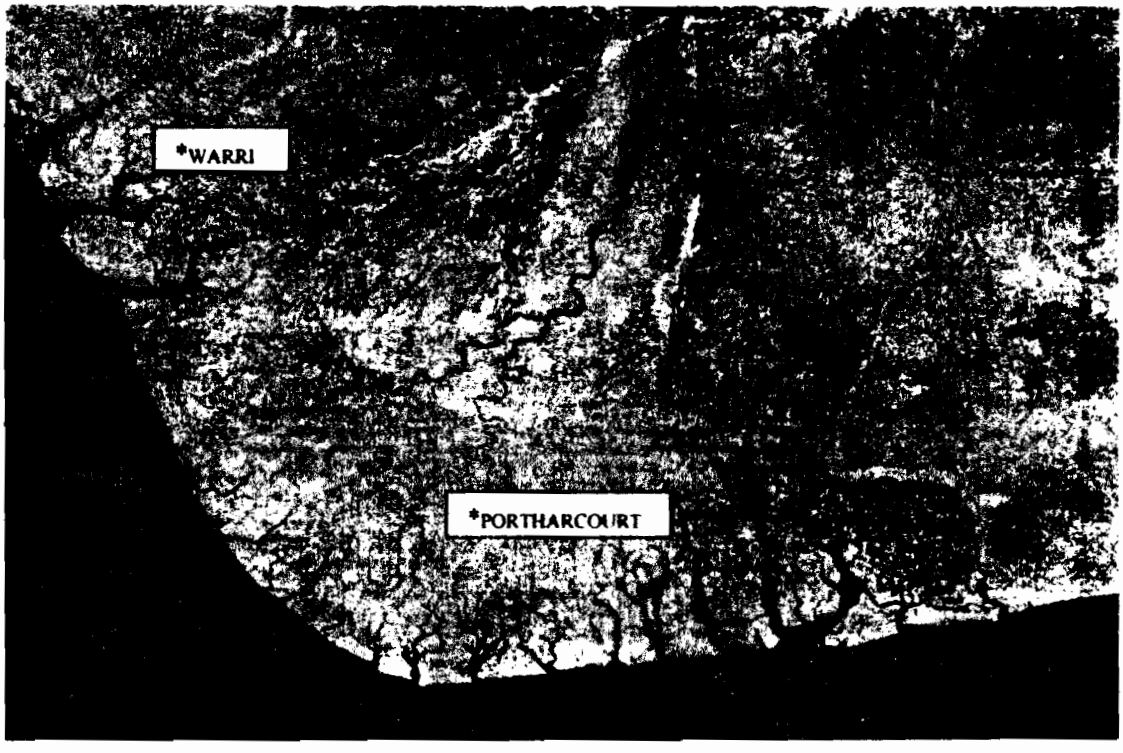

Fig.2: Satellite image of the Niger Delta Basin

Fig. 3: Stratigraphy and Depobelts of the Niger Delta Basin.

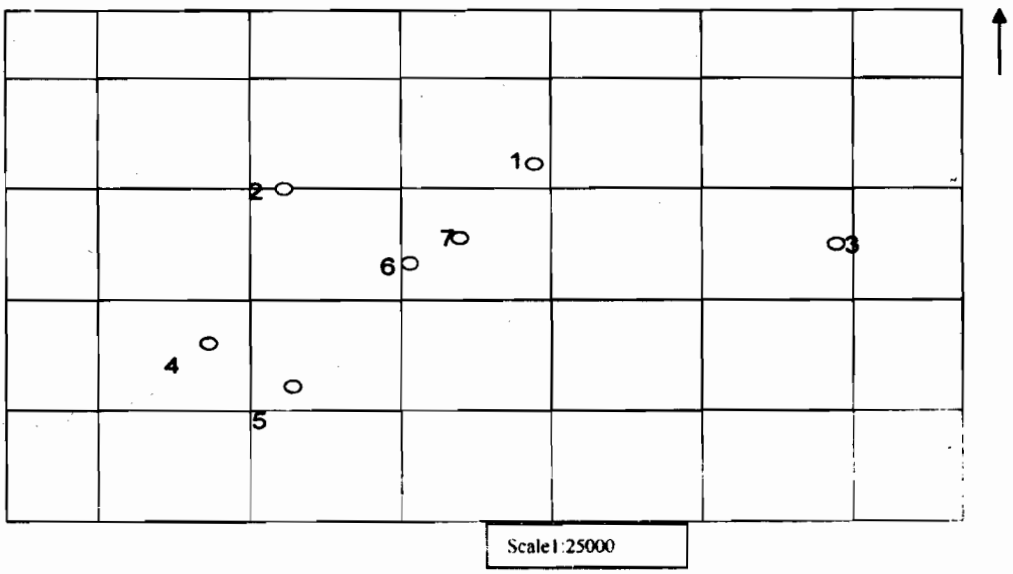

Fig. 4: Well locations within AB Field

METHODOLOGY

The study focuses on the interpretation of depositional processes within the Niger Delta clastic wedge in 'AB' Field. Stratigraphic surfaces observed were correlated between wells mapped across a 400 square km area. Sequence stratigraphy is best determined when well logs are tied to biostratigraphic markers. Using these two combination, it is possible to identify, match and tie sequence stratigraphic surfaces as well as interpret the stacking patterns of the vertical sedimentary sequences. The character of electric logs of wells that penetrate the clastics often reflect changes in grains size and so was easily applicable to use in this process.

- Interpret lithology from log character, confirm with cores and ditch cuttings where possible.
- Interpret depositional environments from micropaleontology, palynology or from paleoecology and then from well log character.
- Interpret condensed sections from faunal abundance and diversity to recognise:

(a) Major condensed sections associated with maximum flooding surfaces.
(b) Secondary condensed sections not associated with maximum flooding surfaces.

(c) Base of lowstand prograding wedges.
(d) Base of lowstand slope fans.
(e) Minor condensed sections between attached lobes in slope fans.

- Age date with high resolution biostratigraphy and correlate with global/company sequence cycle chart.
- Interpret sequence and system tract boundaries, from log character.
- Identify and correlate parasequence and marker beds.
- Construct well log sequence stratigraphic cross-sections.
- Prepare a chronostratigraphic chart from key cross sections to summarize stratigraphic framework.
- Predict the source rock, reservoir rock and seal for any potential petroleum accumulation.

The data base made available for this study were supplied by Shell Petroleum Development Company and they include; Base map of six well locations, Structural map, well log data: Gamma ray, Spontaneous potential, Resistivity, Neutron (CNL), and Density (FDC), Biofacies data, Pollen/faunal zonations and Global/company sequence cycle chart.

RESULTS AND DISCUSSION

Lithostratigraphy

The lithological profile of AB-1 derived from gamma ray log signature of the subcrop has the following key lithological units within the Tertiary Agbada Formation of AB Field.

Retrogradational facies (11,670 – 9,850 ft AHD): This lithologic unit is dominantly composed of marine shale, 70% and sandstone 30%. The marine shale units are fine-grained with a dark to medium grey or dark brown colouration in which siderite cements may be common. The sandstones are transgressive marine sands. Biostratigraphic analysis indicates that these facies were deposited in an inner to middle neritic zones.

Progradational facies (9,850 – 7,720 ft AHD): This lithologic unit is dominated by sand, which accounts for about 60% and 40% shales. Biostratigraphic analysis indicates that they were deposited in inner neritic to bathyal zones.

Progradational facies (7,720 – 6,900 ft AHD): This lithologic unit is dominantly composed of sand, which accounts for about 70% while shales make up 30%. Biostratigraphic analysis indicates that these facies were deposited in middle neritic to bathyal zones.

Retrogradational facies (6,900 – 6,500 ft AHD): This lithologic unit is dominated by marine shale, which accounts for about 70% and 30% sandstone. The marine shale units are fine-grained deposits comprising of shales and silty shales in which siderite cements may be common with a dark to medium grey or dark brown colouration. The sandstones are transgressive marine sands. Biostratigraphic analysis suggests that these facies were deposited in middle neritic to bathyal zones.

Progradational facies (6,500 – 5,110 ft AHD): This unit is dominated by sand 60% and 40% shales.
Biostratigraphic analysis indicates that these facies were deposited in proximal fluvial marine to bathyal zones.

Biostratigraphy

High-resolution biostratigraphic data were analysed for faunal abundance and diversity, condensed sections where identified by stacks of biofacies populations. Maximum flooding surfaces were identified by peaks in micro faunal abundance and diversity. Faunal diversity minima were used to pick sequence boundaries. Micro-flora/fauna zonations were used to establish age relationship. The biofacies signatures revealed condensed sections at 5110-5261ft AHD, 6200-6681ft AHD and 8780-9652ft AHD in AB-1.

Table 1: Microfaunal Zonation Of AB-1

					OML XXX
TOP	***BOTTOM***	***F.ZONE***	***RELIABILITY***	***REMARKS***	***DATE***
DEPTH	***DEPTH***		***GRADIENT***		***REVISED***
0	4200			No Data	02/03/2006
4256	4483			Barren	
4509	6233	F9600/F9700			
6320	12980	F9600	1	Top Nonion 4	
13040	13760			Undiagnostic	
	MICROFAUNAL MARKER				
	6440	F9650	3	No Uvigerina 8 Ass. Fauna only	

Table 2: Palynological Zonation of AB-1

			AB-01		
P ZONE	TOP	BOTTOM	RELIABILITY	REMARKS	DATE
	DEPTH	DEPTH	GRADIENT		REVISED
					12/04/2002
	0	4250		No data	
P830	4256	5628	4	q.b. 45	
P820	5660	6720	2	q.b. 292	
P788	6800	6980		Negative	
P784	7046	11210	3	t. reg. 250	
P770	13610	13700	2	t. 440	

Sequence Stratigraphy

The lithology of the AB-Field was dominated by alternating intercalations of sand and shale. The parasequences identified from well log characters were of the coarsening upward cycles, consisting of shale at the base and sand at the top. From the parasequences, parasequence sets stacking patterns were built. The parasequence stacking patterns identified were aggrading, prograding and retrograding. Parasequence set cycle order was on the average of 5,000 years for the deposition of each cycle deposit. The first major bounding surface identified down hole was the maximum flooding surface (MFS) occurring at 9,850 ft along hole depth (AHD) which formed when the last fine-grained widespread transgressive sediment was deposited. The MFS is within a condensed section composed of sediments rich in the tests of micro-fossils that were not buried by sediment deposition because sedimentation rates were slow in comparison to the area of sea floor available for sedimentation. The MFS was age dated with biostratigraphy at 10.4Ma. Beneath the MFS, is the transgressive system tracts (TST) formed during a rise in sea level, above the shelf margin as eustasy began to rise rapidly. The TST is associated with a ravinement erosion surface formed when the transgressing sea reworks either the prior sequence boundary or the sediments that may have collected during the regression that followed the formation of the sequence boundary. The system tracts above the MFS was observed from log signatures to be the high stand system tracts (HST) which was interpreted to have been deposited at a time of still stand of base level. Parasequence sets identified include progradational and aggradational sets. The HST was associated with a slow rise of relative sea level followed by a slow fall when the slower rate eustatic change balances that of tectonic motion resulting in sedimentation outpacing accommodation space. The prograding highstand clinoforms developed in the process capped by aggrading parasequences that thin upward. The SB at the base of the LST occurs at 7,720 ft AHD and was age dated at 10.35Ma biostratigraphically. The lowstand system tract (LST) occurred with a fall in sea level induced by eustasy falling rapidly, causing fluvial incision up dip with formation of a sequence boundary focusing sediment input at the shoreline. Basin floor fans (BFF) resulting from slope instability were deposited as sediments transported from the fluvial systems are rejuvenated by the forced regression. The top of the (BFF) was identified at 7,340 ft AHD. The slope fans (SF) formed when sedimentation rates slowed as reduction in slope instability prevented sediments from being displaced far down slope. The top of the SF was identified at 7,110 ft AHD. With slow relative sea level rise induced by a rise in eustasy there was an increase in accommodation space relative to sedimentation resulting in lowstand prograding wedge (LPW) characterised by parasequences that aggraded. The top of the LPW was identified at 6,900 ft AHD. A final TST with a condensed section developed above the LST terminating in an MFS at 6,500 ft AHD age dated with biostratigraphy at 9.5Ma. The top of the final HST was not covered by petrophysical well log data.

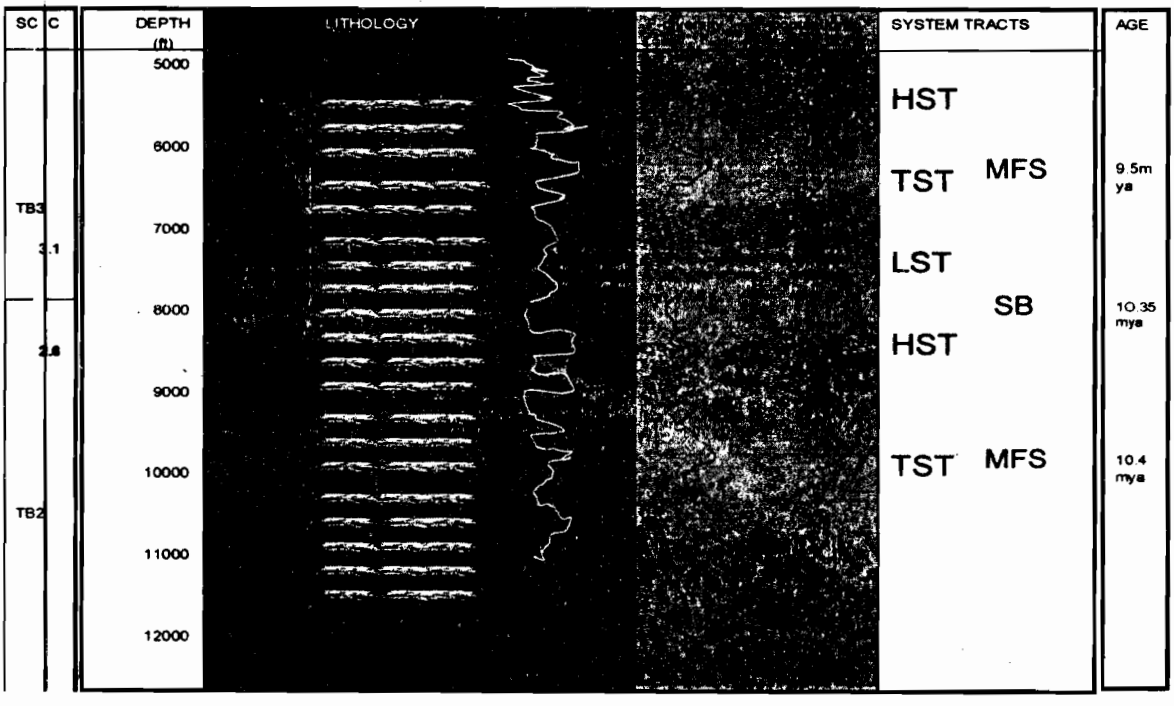

Fig. 5: Stratigraphic summary model of AB-1

KEY: HST: Highstand system tracts MFS: Maximum flooding surface
TST: Transgressive system tracts
LST: Lowstand system tracts SB: Sequence boundary

DISCUSSION

The AB stratigraphic intervals fall within the parelic sequence of alternating sand and shale bodies of variable thicknesses. The sand/shale ratios generally decrease with depth suggestive of a fining downward motif. The entire sequence constitutes an overall prograding delta with some periods of transgression.

Integrated results of well log and biofacies interpretations revealed that the paleoenvironment of deposition of the sediment, in 'AB' Field ranged from inner neritic to deep marine; Three stacking patterns – progradational, aggradational and retrogradational patterns were identified, Two maximum flooding surfaces and a 3RD order sequence boundary were delineated. The basin floor fan, the sand-rich prograding wedge, the transgressive sands and the highstand sands constitute good (potential) reservoirs. The distal shale toes of the prograding wedge as well as highstand shales and transgressive shales form seals for stratigraphic traps formed in the study area. Possible migration pathways include carrier beds and faults. The reservoir units include; Channel Sandstone, Channel Heterolith, Upper Shoreface Sandstone, Lower Shoreface Heterolithic, and coastal Plain Sandstone. Stratigraphic traps identified include submarine fan and lowstand wedge.

Sequence stratigraphic correlation of AB Field was achieved through the identification and correlation of flooding surfaces (chronostratigraphic lines) across the wells. The intervening stratigraphic units were thereafter correlated within the time lines defined by flooding surfaces, thus revealing two maximum flooding surfaces (MFS) and a third order sequence boundary (SB) across the field. The log character is of upward-coarsening sandstone successions that generally correlate across AB Field to mostly blocky and upward-fining successions that are less continuous between adjacent well. Progression from prograding delta deposits to delta top and fluvial facies was recognised.

Sequence boundaries within the Agbada Formation, in the area of AB Field, are defined by channel-form deposits observed to directly overly the sequence boundaries and these are deposits of the "Lowstand Rivers". Vertical logtrends within these sequences are similar to those predicted by the standard models for prograding deltaic shorelines. Deposits directly above sequence boundaries are coarse grained, and generally fine upward. Log trends generally change from thicker, sandier, blocky and upward-fining successions to thinner upward-coarsening successions, suggesting a progression from channel deposits to dominantly offshore prograding lobes. This reflects deepening upward from the sequence boundary to maximum flooding surface characterised by (retrogradational parasequence set) depositional shoaling. The Agbada Formation is generally interpreted to contain fluvial-deltaic deposits (Weber and Daukoru, 1975). Well logs through the sequences clearly show an up-section progression from blocky upward fining successions (channel deposits) to upward-coarsening successions (prograding lobes) which reflects a progression from fluvial depositional settings to pro-delta and deltaic shorelines. Eustatic Sea level variations during the Middle to Late Miocene correlates with sequences in AB Field. Lowstand shelf exposure occurred when incised fluvial valleys carried sediments directly to the slope edge depositing facies directly above sequence boundaries. As accommodation filled, the locus of sediment deposition and loading would also have shifted seaward. The evolution of channel meanders appear to be similar to fluvial meandering channels in terms of direction and geometry of channel migration channel fills are coarse-grained. Well log correlations indicate that most reservoir sandstones are associated with the sequence boundary.

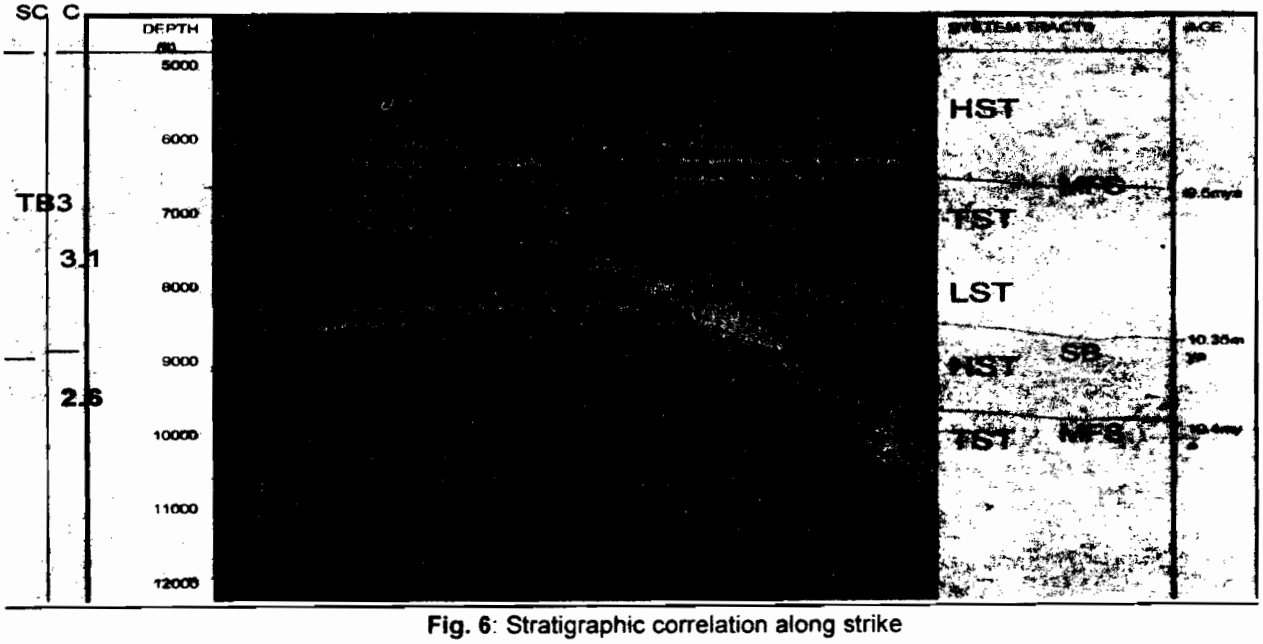

Fig. 6: Stratigraphic correlation along strike

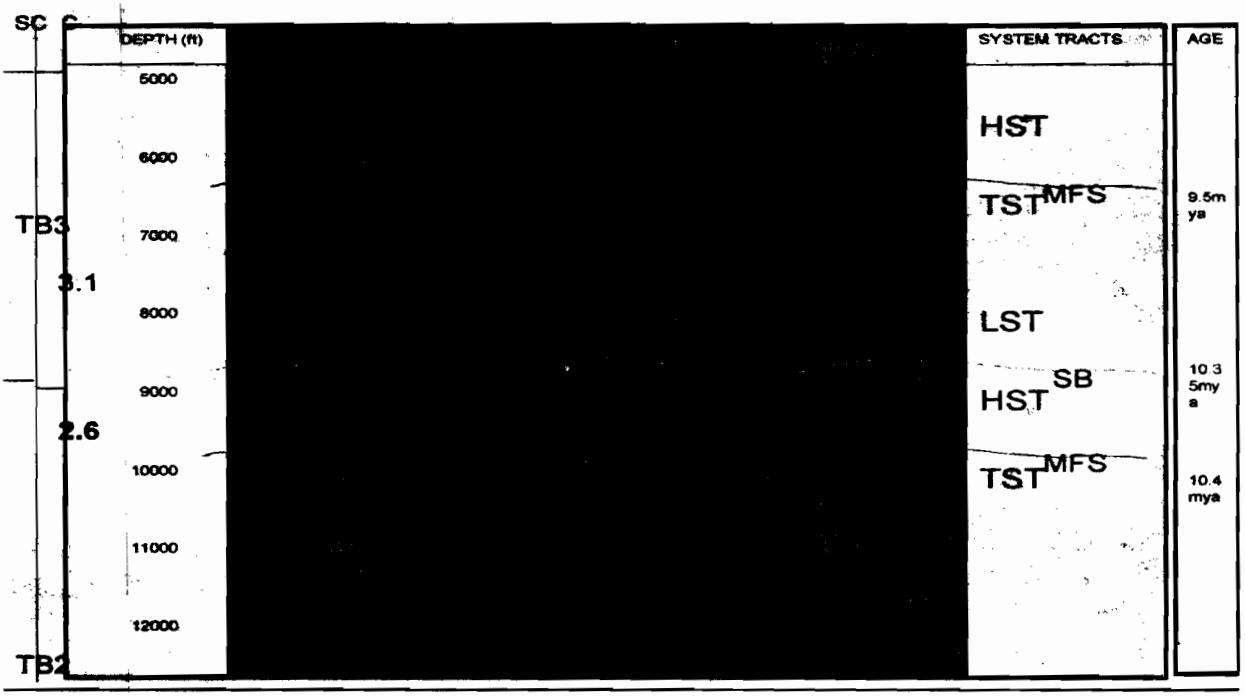

Fig. 7: Stratigraphic correlation along dip

CONCLUSION

The depositional model of 'AB' Field based on the identified system tracts conforms to the Type 1 sequence of Vail (1987). Integrated results of well log and biofacies interpretations revealed that these strata were deposited by interaction of subsidence, eustatic changes in sea level and varying sediment supply during the late Miocene to middle Miocene. The dominant multiplicity of biofacies suggests the heterogenic depositional environment of 'AB' Field which ranges from coastal deltaic to deep marine. The chronostratigraphic framework consists of two depositional sequences related to depositional cycles 2.6 and 3.1, which were identified and delineated in the well. Two maximum flooding surfaces and a 3RD order sequence boundary were delineated across the field. Five system tracts were identified. Three parasequence stacking patterns; progradational, aggradational and retrogradational patterns were identified. Lateral/vertical continuity of facies depended on parasequence associations. Most reservoir units occur between the 10.4Ma MFS and the 10.35Ma SB. The morphology and importance of reservoirs and seals vary between systems tracts. The reservoir units include; Channel Sandstone, Channel Heterolith, Upper Shoreface Sandstone, Lower Shoreface Heterolith, and coastal Plain Sandstone. Seals include coastal plain shale and marine shales Stratigraphic traps include submarine fan and lowstand wedge. There is an observed overall shallowing upward log trend in 'AB' Field. The basin floor fan, the sand-rich prograding wedge, the transgressive sands and the highstand sands constitute good (potential) reservoirs. The distal shale toes of the prograding wedge as well as highstand shales and transgressive shales form seals for the (potential) stratigraphic traps formed in the study area. Possible migration pathways include carrier beds and faults.

The fundamental advantage of this study is that it provides a series of tools with which sedimentary architecture can be analysed and predicted in areas far away from well control. This study developed a sequence stratigraphic model for the Agbada Formation in the Niger Delta Basin based on integrated well log and biostratigraphic data from AB Field. The following conclusions are reached;

i. One sequence boundary (major erosion surface) divides the AB Field into two sequences, each formed during relative levels of eustacy.
ii. Sequence boundary appeared to have formed by lowstand fluvial incision (as commonly interpreted in other major deltaic successions).
iii. System tracts developed in response to sedimentation accommodation and eustacy.
iv. Complex deltaic sequences can be confined to time bound systems tracts within which the constituent sediment packages can be correlated in detail on well to well basis at the fourth order parasequence level.
v. Identifying and mapping of deeper water facies that would otherwise be overlooked in routine seismic mapping are revealed by sequence stratigraphy.
vi. The forecasting and identification of prospective plays in downdip portions of the Niger-Delta basin.

Table 3: Depth and age of major surfaces in AB Field

	MFS	TLPW	TSFS	TBFFS	SB	MFS
AB	DEPTH(FT)	DEPTH(FT)	DEPTH(FT)	DEPTH(FT)	DEPTH(FT)	DEPTH(FT)
1	6,500	6,900	7,110	7,340	7,720	9,850
2	6,080	6,980	7,230	7,500	7,950	9,960
3	6,640	6,920	7,130	7,330	7,690	9,770
5	6,530	7,290	7,860	8,240	8,500	9,720
6	6,400	7,100	7,670	8,000	8,500	9,720
7	6,350	7,140	7,300	7,500	7,960	9,860
AGE	9.5MYA				10.35MYA	10.4MYA

Table 4: Parasequence type and hydrocarbon distribution

P/SEQUENCE type	H/C	WELL 5	WELL 6	WELL 7	WELL 1	WELL 2	WELL 3
AGGRADING (LST)	DEPTH (ft)	8,960 - 9030	9,00 - 9100	7,490 – 7,580	8,200 – 8,280	6270 – 6320	8340 – 8360
AGGRADING (HST)	DEPTH (ft)	9,090 -9,120	9,310 - 9330	7,750 – 7,770	8,450 – 8,470	7350 - 7370	9030 – 9065
PROGRADING(HST)	DEPTH (ft)	9,150 – 9,165	9,370 – 9,440	7,780 – 7,820	9,210 – 9,230	7480 – 7490	9980 - 10500
RETROGRADING(TST)	DEPTH (ft)	9,300 – 9,415	9,590 – 9,650	8,260 – 8,290	9,260 – 9,280	8250 – 8300	
PROGRADING (LST)	DEPTH (ft)	9,970 – 9,990	10,100 – 10,140	9,350 – 9390	9,380 – 9,410	8610 - 8620	
	DEPTH (ft)	10,180 – 10,240	10,750 – 10,780	9,560 – 9,570	9,650 – 9,730		
	DEPTH (ft)		10,800 – 10,880	9,580 – 9,650	10,240 – 10,280		
	DEPTH (ft)				11,170 – 11,220		
	DEPTH (ft)				11,390 – 11,420		

REFERENCES

Avbovbo, A. A., 1978. Tertiary lithostratigraphy of Niger Delta. American Association of Petroleum Geologists Bulletin, 62: 295-300.

Burke, K., 1972. Longshore drift, submarine canyons, and submarine fans in development of Niger Delta. American Association of Petroleum Geologists, v. 56, p. 1975-1983.

Catuneanu, O., 2002. Sequence stratigraphy of clastic systems: concepts, merits, and pitfalls. Journal of African Earth Sciences, v. 35, p. 1-4

Doust, H., and Omatsola, E., 1990. Niger Delta, in, Edwards, J. D., and Santogrossi, P.A., eds., Divergent/passive Margin Basins, American Association of Petroleum Geologists, Memoir 48: 239 -248.

Embry, A., 2002. Tectonic and eustatic signals in the sequence stratigraphy of the Upper Devonian Canadaway Group, New York state: Discussion: American Association of Petroleum Geologists Bulletin, 86(4): 695.

Evamy, B.D, Haremboure, J., Kamerling, P; Knap, W A. Molloy, F. A and Rowlands, P.H., 1976. The hydrocarbon habitat of the Niger Delta Exploration Bulletin, 1976/1.

Fisher, W. L., and McGowen, J. H., 1967, Depositional systems in the Wilcox Group of Texas and their relationship to occurrence of oil and gas: Gulf Coast Association of Geological Societies Transactions, 27: 105-125.

Galloway, W. E., 1989, Genetic stratigraphic sequences in basin analysis. I. Architecture and genesis of flooding-surface bounded depositional units American Association of Petroleum Geologists Bulletin, 73. 125–142.

Henry W. P and George P. A, 1999, "Siliciclastic Sequence Stratigraphy - Concepts and Applications". Society of Economic Petrologists and Paleontologists. 216 pp.

Knox, G. J and Omatsola, E. M., 1989. Development of the cenozoic niger delta in terms of the 'escalator regression' model and impact on

hydrocarbon distribution. Proceedings KNGMG Symposium 'Coastal Lowlands' 1987: 181-202 Kluwer academic publishers, dordrecht.

Kulke, H., 1995. Nigeria, in, Kulke, H., ed., Regional Petroleum Geology of the World. Part II: Africa, America, Australia and Antarctica: Berlin, Gebrüder Borntraeger, p. 143-172.

Lehner, P., and De Ruiter, P. A. C., 1977. Structural history of Atlantic Margin of Africa: American Association of Petroleum Geologists Bulletin, v. 61: 961-981.

Middleton, G. V. 1973. Middleton , Johannes Walther's law of the correlation of facies. Bulletin of the Geological Society of America 84 (1973), p. 979–988

Mitchum Jr., R. M. and Vail, P. R., 1977. Seismic stratigraphy and global changes of sea-level. Part 7: stratigraphic interpretation of seismic reflection patterns in depositional sequences. In: Payton, C.E.(Ed.), Seismic Stratigraphy—Applications to Hydrocarbon Exploration, vol. 26. A.A.P.G. Memoir, p. 135 –144.

Short, K. C., and Staublee, A. J., 1965. Outline of geology of Niger Delta: American Association of Petroleum Geologists Bulletin, 51: 761-779.

Vail, P. R., R. G. Todd,and J. B. Sangree, 1977. Seismic Stratigraphy and Global Changes of Sea Level: Part 5. Chronostratigraphic Significance of Seismic Reflections: Section 2. Application of Seismic Reflection Configuration to Stratigraphic Interpretation Memoir 26: 99 – 116.

Van Wagoner, J. C., Mitchum, R.M., Campion, K. M., and Rahmanian, V. D., 1990. Siliciclastic Sequence Stratigraphy in Well Logs, Cores, and Outcrops. American Association of Petroleum Geologists, Tulsa, 55pp.

Weber, K. J., and Daukoru, E. M., 1975. Petroleum geology of the Niger Delta: Proceedings of the Ninth World Petroleum Congress, volume 2, Geology: London, Applied Science Publishers, Ltd., p. 210-221.

Wheeler, H. E., 1958. Time stratigraphy. American Association of Petroleum Geologists, Bulletin, v. 42: 1047-1063.

GLOBAL JOURNAL OF GEOLOGICAL SCIENCES VOL. 6 NO. 2 2008: 139 - 144
 ISSN 1696 – 6798

NSUGBE FORMATION (?): A CASE OF NON-COMPLIANCE WITH STRATIGRAPHIC NOMENCLATURAL PROCEDURES

B. N. NFOR

(Received 1 April, 2008; Revision Accepted 30 July, 2008)

ABSTRACT

The compliance level with the code of generally accepted stratigraphic nomenclature by authors who have introduced, used and disseminated the terminology "Nsugbe Formation" in both national and international geologic literature has been investigated using relevant articles of the American Commission on Stratigraphic Nomenclature (ACSN) and existing field observations/data on the lithologic unit. Results show that the said 'Nsugbe Formation (?) has never been officially proposed for consideration as a formal stratigraphic unit in any scientific journal (as required by the law) and should not be used as such. Results have further shown that this indiscriminate use of formal stratigraphic names without due diligence is not unconnected with the bizarre absence of neither any official Nigerian code on stratigraphic nomenclature nor any Compendia to record/guard Nigerian stratigraphic names. The case of the Nsugbe Formation (?) is not an isolated incident of non-compliance; it is believed to be one out of a multitude of non-compliant cases, if any stratigraphic watch dog committee were to beam its search light on existing stratigraphic units. The main objections to the acceptability of the formalization of the unit as 'Nsugbe Formation' (as has been introduced and used), borders on the non-compliance with legal stratigraphic nomenclatural requirements, viz; specifying a Type Section, Type Area, distinct lithologic characteristics, sedimentologic details and its mappability on scales of 1:25,000.

KEYWORDS: Nsugbe Formation, Anambra Basin, Type Section, International Code of Stratigraphic Nomenclature, Non-compliance.

INTRODUCTION

Between the years 1903 and 1904, Nigeria witnessed the inauguration of its pioneer geologic bodies – the Mineral Surveys of Southern and Northern Nigeria respectively. The two bodies were charged with the initial mineral survey/geological investigations of the country. The Geological Survey of Nigeria (GSN) was created in 1919, following the dissolution of the Mineral Survey units, and was charged with the responsibility of mapping the entire country. According to a Geological Survey of Nigeria (GSN) Report, (1987, p7.) the pioneer British expatriate geologists collected samples in Nigeria and took them to London for laboratory analyses/map production. It is thus logical to conclude that most important geologic works including the nation-wide geological survey and mapping that resulted in the drafting and production of all topographic and most geologic maps used in Nigeria today were guided by the British Geological Codes. Such codes including the Code on Stratigraphic Nomenclature, which possibly could have been either completely accepted (without amendments), or amended/adopted by Nigerian geologists is yet to be officially documented in the annals/archives of the GSN or any such related geological body, forty-seven years after Independence. The absence of such an important document is most probably responsible for the introduction and use (though not a common occurrence) of some stratigraphic names in the Nigerian stratigraphic record as though they had been formalized, as exemplified by the use of 'Nsugbe Formation'. If this scenario continues unabated, Nigerian stratigraphy could soon begin to witness a more chaotic state than that of the early European stratigraphy prior to its reorganization.

Well over thirty years ago, while investigating the sedimentologic and stratigraphic features of the Nanka Sands in Anambra State, Southeastern Nigeria, Nwajide, (1977) observed some remarkable lithologic changes extending from the northwestern part of Onitsha town to Nsugbe and environs. To him, the occurrence of a distinctly ferruginized and quite consolidated sandstone adjacent the Nanka Sand was a clear indication that he had reached the northwesterly boundary of the Nanka Sand. Nwajide, (1977) in his unpublished M.Phil Thesis, suggested 'Nsugbe Formation' status for the area. The extent of the formation according to Nwajide (1977) is presented in Figure 1. Such a binomial nomenclature in lithostratigraphic nomenclatural circles is indicative of a formally proposed, accepted and adopted lithostratigraphic unit whose geographic location (entity) is Nsugbe and its position in the lithostratigraphic ranking is of formational status. Since then, many authors including Umenweke (1996), Egboka (1993), Orajaka et al (1992) among others have embraced, taught and disseminated such literature in scientific journals (both local and international alike) and in classrooms.

The objectives of the present research are multiple; firstly, to investigate whether Nwajide (1977) or any other person had ever formally proposed 'Nsugbe Formation' for consideration as a formal stratigraphic unit, and secondly to find out whether due process was observed (as required by stratigraphic nomenclatural norms) in that event and if not to find out why the term

B. N. Nfor, Department of Geology, Anambra State University, Uli P.M.B. 02 Uli, Nigeria.

has continuously been and is still being used in current scientific publications.

METHODOLOGY

The methodology adopted for this work is an in-depth analysis of the relevant articles of the American Commission on Stratigraphic Nomenclature (ACSN) and the reappraisal of existing field data on the Nanka Sands and the 'Nsugbe Formation' as muted by Nwajide (1977) in his M.Phil Thesis. The articles of the ACSN, are a set of guidelines for naming/renaming of stratigraphic units. This is one of the most widely accepted and handy legal stratigraphic document, itself adapted from the documents of the International Commission on Stratigraphy (ICS). The ASCN document is adopted here in the absence of any such customized document in the annals of neither, the present Geological Survey Agency, the (GSA), nor the Nigerian Mining and Geoscience Society (NMGS).

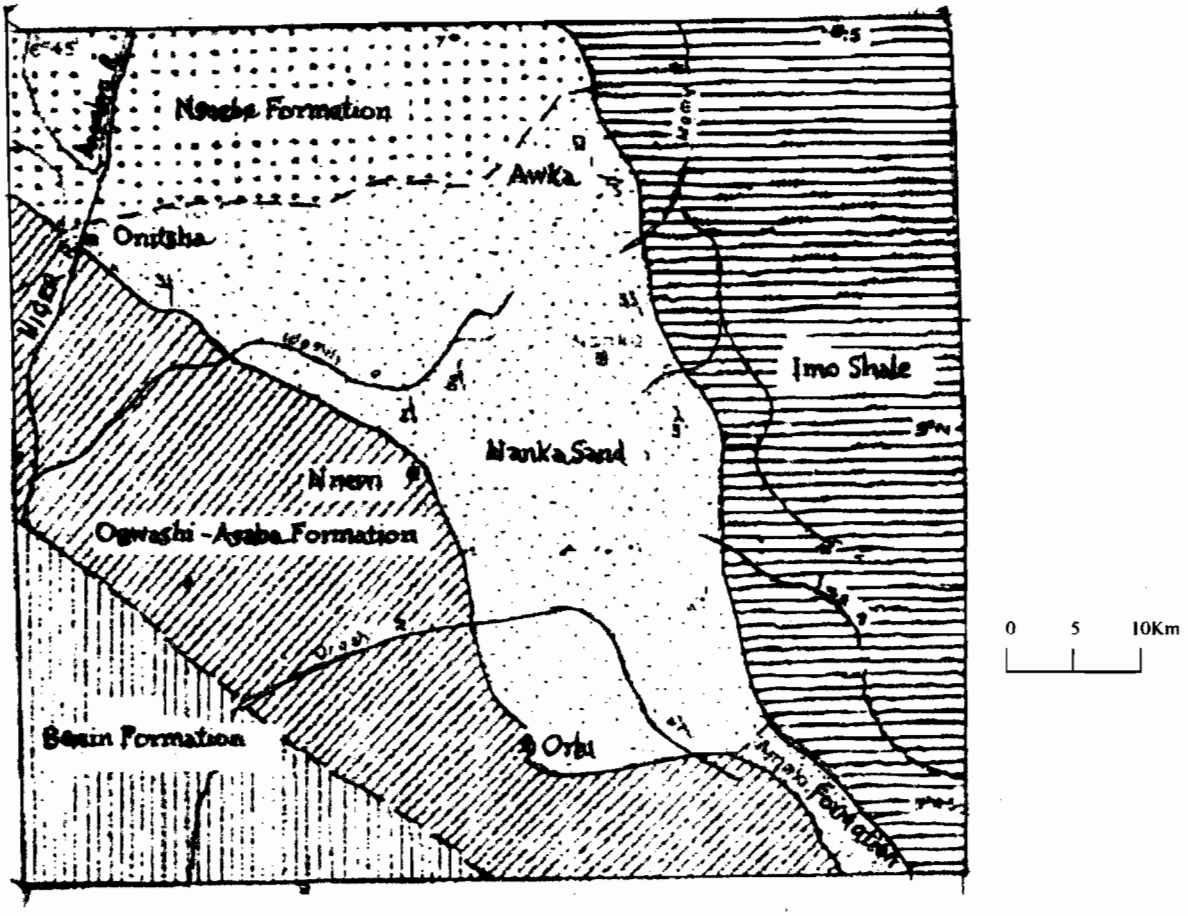

Fig. 1: The position of the Nsugbe Formation in Anambra State. (After Nwajide, 1977)

RESULTS

Outcrops of the Nsugbe Formation (?)

Egboka (1993) and Orajaka et al (1992) have identified and assigned some outcrops to the Nsugbe Formation, which include the outcrop located at Km 18, near Tempo Mill Factory, Umunya and that at the Onitsha Toll gate all along the Onitsha-Enugu express way; and the outcrop at Km 116 along the Onitsha – Adani-Nsukka road, near Nsugbe. The locations of these outcrops are presented in Figure 2.

The outcrop located at Km 18, Umunya is a focus of intense controversy since according to Nwajide and Reijers (1996) and Nwajide et al (2004), it is an outcrop of the Nanka Sand. In fact, Nwajide (personal communication) has even proposed the outcrop as a replacement to the original Nanka Sand Type Section because the original Type Section at Nanka is almost concealed and inaccessible due to unabated gully erosion activities. In order to give a fair and unbiased arbitration of two contrasting opinions about the Km 18 outcrop, this write-up briefly inspects the sedimentologic and stratigraphic variation between the Nanka Sand exemplified by its Type Section and those of the Nsugbe Formation. The Type Section of the Nanka Sand is presented in Figure 3.

The type locality of the Nanka Sand is a gully erosion site at Nanka (Reyment, 1965; Nwajide, 1977, Kogbe, 1989). At the type locality, the vertical lithologic section of the Nanka Sand is about 305m thick and is subdivided into seven subunits; I, III, V and VII. The sands are uncemented, loose, medium to coarse, often pebbly sandy beds, while units I and V consist of ferruginous sandstone bands. Subunits I, III and VII are

characterized by cross-beds, and occasionally flaser and burrowed beds or occasionally silt and clays/shales intercalations are observed, which are grey in colour and contain clots of carbonaceous matter as disseminated specks of pyrite, glauconite, gypsum nodules and muscovite flakes.

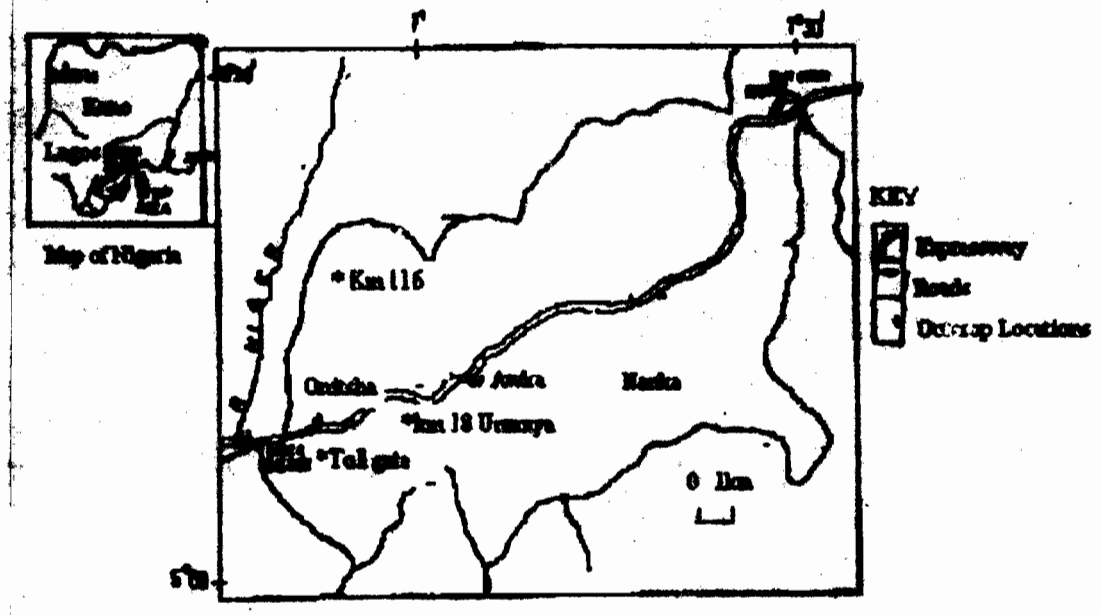

Fig. 2: Sketched road map showing outcrop locations ascribed to Nsugbe Formation (adapted from Egboka, 1993)

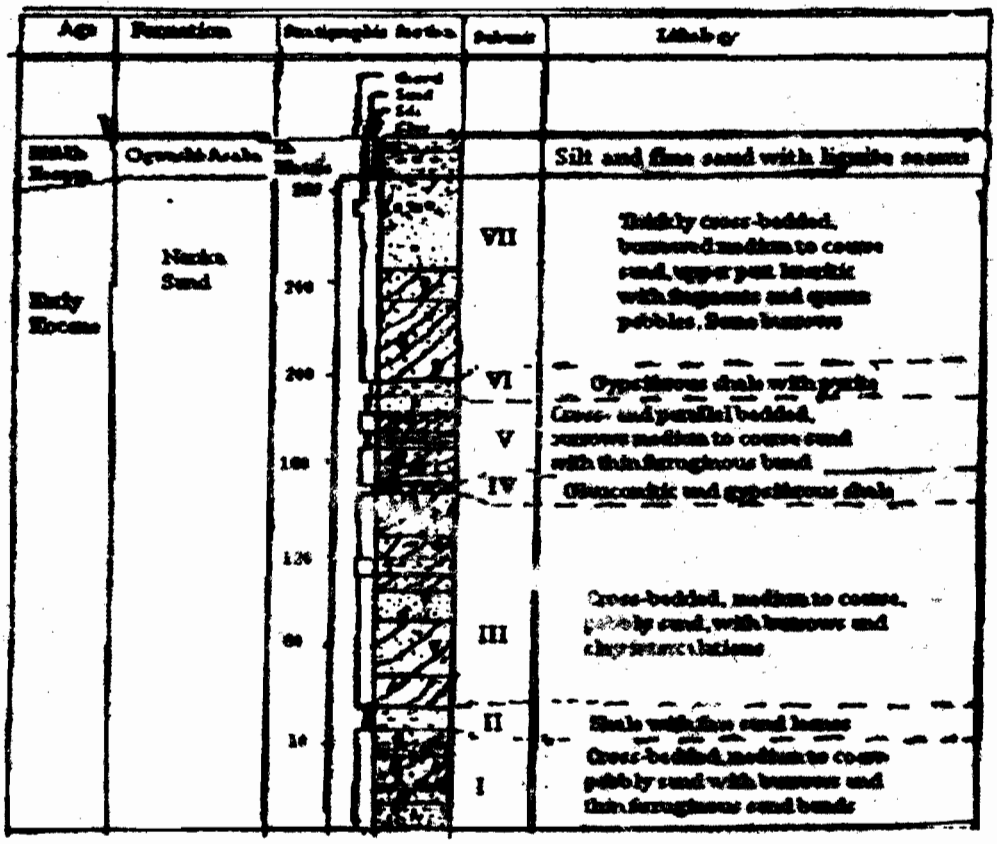

Fig. 3: Stratigraphic and lithologic summary of the Type Section of the Nanka Sand at Nanka Town (after Nwajide 1980)

At Km 18, the outcrop consists essentially of three subunits based on lithology and lithologic associations, gross appearance and parasequence stacking patterns; a lower unit of poorly sorted, medium grained, quartzose, friable sandstone with clay matrix; a mid-section consisting of laminated, slightly fissile mudrocks and sandstone and an upper section of regular alternation of decimeter-thick beds of fine, clayey, ripple laminated, sandstone and grey clays. The sandstone is predominantly cross-stratified, ripple laminated and contains horizontal burrows. This description seems to correlate more closely with the outcrop type section of the Nanka Sand shown in Figure 4 whose type locality has been interpreted as tidal deposits formed by neap-spring tidal cycles (Nwajide, 1996).

The description of the Nanka Sand here greatly contrast with an adjoining unit, which exhibits high level of ferruginization, coarse to pebbly cement and thus highly consolidated sands. The outcrops at Km 116 along the Onitsha – Adani – Nsukka road and at the Onitsha Toll gate were compared with those described above by Nwajide (1977). At these two locations, the outcrops sections consist of ferruginized, indurated coarse grained sandstone, grading into gravels. By virtue of their stronger resistance to erosion (in contrast to the friable and gully-prone areas underlain by the Nanka Sands), areas underlain by the Nsugbe Formation ? exhibit isolated rounded hills, which have been occasionally exposed at stream channels and by local miners who quarry the rocks into gravelly aggregates for construction works. Abandoned quarry sites would thus be the most ideal sites to study the Nsugbe Formation? and could constitute excellent sites for its type section.

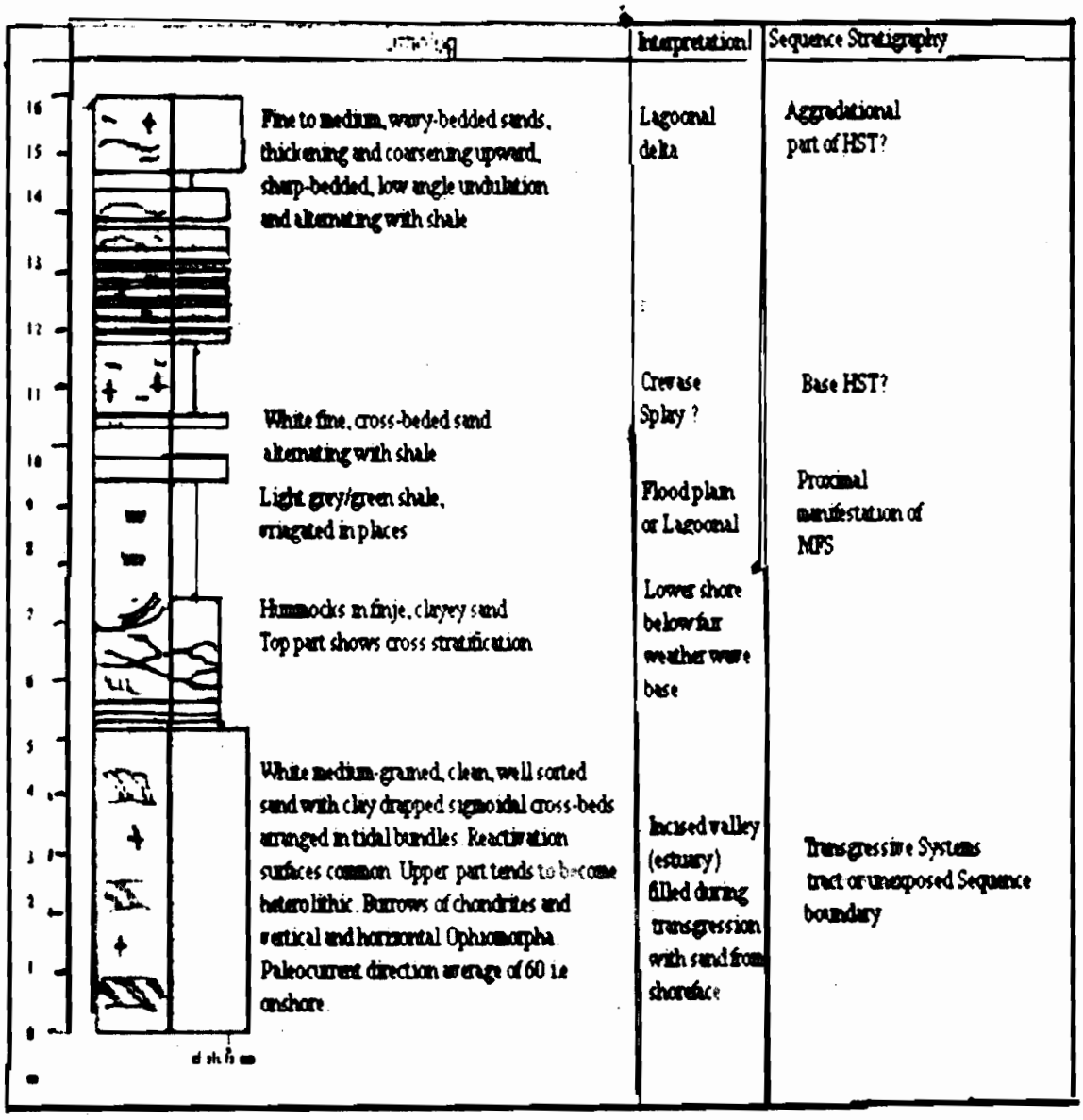

Fig. 4: Lithologic section of Nanka Sand at Umunya exposed at Km 18 Onitsha along the Enugu-Onitsha expressway

DISCUSSIONS

The articles of the American Commission on Stratigraphic Nomenclature.

The Preamble of the ACSN among other things states that "*The articles of this code are recommendations that cannot be generally mandatory, but geological organizations may adopt these articles as their rules of nomenclatural procedures...*" Article 3 of the ACSN dwells on *formal* and *informal* names and units. The article is a systematic collection of rules of formal stratigraphic classification and nomenclature. Articles 4 to 13 of the same ACSN dwell generally on lithostratigraphic units and more specifically on the nature of the nature of the rock-stratigraphic units. The salient points of Article 4 are as follows;

1. A rock stratigraphic unit is distinguished and delineated on the basis of the lithologic characteristics, recognized and defined by observable physical features, with boundaries placed at sharp contacts, or drawn arbitrarily within the zone of gradation.
2. For the purposes of nomenclatural stability, a type section should be designated, with a clear description of the lateral and vertical variations.

The highlights in article 3 of the ACSN are better appreciated when applied in consonance with article 13. Article 13 deals with the procedures for establishing *formal* stratigraphic units. According to article 3, a stratigraphic unit is formal if it has been proposed in publication in conformance with article 13, and has met other requirements specified in the code. On the other hand, a stratigraphic unit and its name are classified as *informal* if they have not been formally proposed. The connotation of the nomenclature "Nsugbe Formation" in stratigraphic circles is that, it is a formal lithostratigraphic unit of formational rank status, whose geographic location/entity is Nsugbe. The present research however has identified very serious legal stratigraphic flaws in the use of such a designation, in defiance of article 13 of the ACSN. Firstly, there has never been a statement of intention to designate the unit as formal. Furthermore, for such a proposal to be accepted (if it were ever made at all), the following vital requirements must be provided; specific type section, specific type locality, one or more of representative sections near the geographic feature and more especially, map of the section, whose practical mappability should be at scales of the order of 1:25,000. As far as this researcher is concerned the only information provided by Nwajide (1977) included a partial and provisional Nanka Sand/Nsugbe Formation ? boundary, lithology of the unit, its stratigraphic position relative to the Nanka Sand and its age – Eocene. When this information is weighted against the requirements for formalizing a lithostratigraphic unit, it becomes evident that it is too little to be accepted if proposed without providing further information as demanded by the code of the ACSN. Furthermore, such observations and suggestions by Nwajide (1977), were simply highlighted in his M.Phil Thesis and not in any *recognized scientific medium* as stipulated by article 13 of the ACSN. The phrase *recognized scientific medium* according to article 13 means '*a form of publication, available to the scientific public, regardless of size of edition or form of publication but it clearly excludes restricted media such as letters, company reports, theses, dissertations, newsletters and commercial/trade journals*'. Article 13 further emphasizes that "*...to be valid, a new name should be duly proposed as outlined above*'. The provisions of the last two paragraphs of Article 13 have provided very strong evidence against the continual use of the terminology 'Nsugbe Formation' since Nwajide's (1977) medium of communication was his M.Phil thesis.

CONCLUSIONS AND RECOMMENDATIONS

Based on available field data relating to the muted Nsugbe Formation (?)there exist some remarkable differences between it and an adjacent formation – Nanka Sand, which is its lateral equivalent. The data has further shown that, the major lithologic .differences between the two is the highly ferruginized nature of the Nsugbe Formation (?) in contrast to the friable, unconsolidated Nanka Sands. The only work in the unit was done by Nwajide (1977) and other existing minor reports have not provided enough evidence/data to enable it attain formal lithostratigraphic nomenclatural status, as required by the rules guiding lithostratigraphic nomenclature. It is thus logical that the terminology 'Nsugbe Formation' is unlawfully used since its introduction and use are not in compliance with the rules/procedures guiding stratigraphic nomenclature. It is also hereby advocated that relevant geological bodies like the Geological Survey Agency (GSA), Geological Survey of Nigeria (GSN), Council of Nigerian Mining Engineers and Geoscientists (COMEG) and the Nigerian Mining and Geosciences Society (NMGS) etc should establish a Compendia, maintained by a proposed Geologic/Stratigraphic Committee of Nigeria (in the likes of ACSN), where names and nomenclatural procedures and history of formal units will be recorded and preserved. These, it is believed will go a long way in enthroning high compliance levels with stratigraphic norms and also easy referencing.

REFERENCES

Egboka, B.C.E. (ed). 1993. The Raging War: Erosion, Gullies, and Landslides, Ravage Anambra State. Publ. The Government of Anambra State, Nigeria. 223pp.

Kogbe, C. A., 1976. The Cretaceous and Paleocene Sediment of Southern Nigeria, In Geology of Nigeria. Elizabethan Publ. Co., Lagos, Nigeria. 215pp.

Krumbein, W. C. and Sloss, L.L., 1963. Stratigraphy and Sedimentology. 2nd Ed. W.H. Freeman and Company. San Francisco. 660pp.

Nehikhare, J.I. (ed) 1987. Mineral and Industry in Nigeria with notes on the history of the Geological Survey of Nigeria. Publ. Geological Survey of Nigeria. 60pp.

Nwajide, C..S., 1977. Sedimentology and Stratigraphy of the Nanka Sands. Unpublished M.Phil Thesis, Department of Geology, University of Nigeria, Nsukka. 114pp.

Nwajide, C.S. and Reijers, T. J. A., 1996. Field Guide In Selected Chapters on Geology. Shell Petroleum Development Company Nigeria. 97pp.

Nwajide, C.S. and Nwaozor, L.A.U., 2004. Guide for Geological Field Trip to the Anambra Basin, Nigeria. The Shell Petroleum Development Company of Nigeria Limited. 37pp.

Orajaka, I.P., Egboka, B.C.E., Umenweke, M.O., and Obi, G.C., 1992. Report on the first phase of outcrop studies in Southereatern Nigeria. Unpublished Report sponsored by Shell Petroleum Development Company Nigeria. 48pp.

Reyment, R. A., 1965. Aspects of Geology of Nigeria. Ibadan University Press, Ibadan. 145pp.

Umenweke, M.O., 1996. Geotechnical and Hydrogeological Characteistics of an Eocene Multi-chambered Caves, S.E. Nigeria. Journal of the Sydney Speleological Society. 40(7): 107-114.

GLOBAL JOURNAL OF GEOLOGICAL SCIENCES VOL. 6 NO. 2 2008: 145 - 152
 ISSN 1596 – 6798

STRUCTURAL EVOLUTION OF PRECAMBRIAN BASEMENT ROCKS OF JEBBA AREA, S.W. NIGERIA

C. T. OKONKWO

(Received 1 February, 2006; Revision Accepted 7 April, 2006)

ABSTRACT

Geological studies show that the Jebba area, S.W. Nigeria is underlain by metasedimentary and metaigneous rocks including gneisses which have been intruded by Neo-Proterozoic (Pan-African) granitic rocks. The metamorphic rocks including migmatitic gneiss, quartzofeldspathic gneiss, metagreywacke, quartzite, quartz-mica schist and granitic gneiss have been subjected to polyphase deformation. Early, D_1, deformation gave rise to recumbent folds associated with axial planar foliation. Later, D_2 event produced asymmetrical folds and axial planar crenulation cleavages. The D_3 episode was associated with ductile thrusting at deeper crustal levels and D_4 with brittle thrusting at upper crustal levels, as well as tight to open folds with subhorizontal axial planes. D_5 involved strain localisation along steep, strike-slip faults.

KEYWORDS: Jebba area, polyphase deformation, foliations, folds, ductile thrusts, stretching lineations, brittle thrust faults, strike-slip faults

INTRODUCTION

The Nigerian basement complex forms part of the internal zone of the Pan-African orogenic belt east of the West African craton (Fig. 1) This basement complex comprises Archean and Proterozoic rocks which have been subjected to Liberian (ca 2700Ma), Eburnean (ca 2000 Ma) and Pan-African (ca 600 Ma) orogenic events (Grant 1970, Oversby 1975, van Breemen *et al* 1977, Fitches *et al* 1985, Rahaman 1988, Dada *et al* 1994). The existence of the Kibaran (ca 1100 Ma) event in Nigeria claimed by some workers (Ogezi 1977, Ekwueme 1987) on the basis of some Rb/Sr dates on metamorphic rocks is not generally accepted (Ajibade *et al*, 1987).

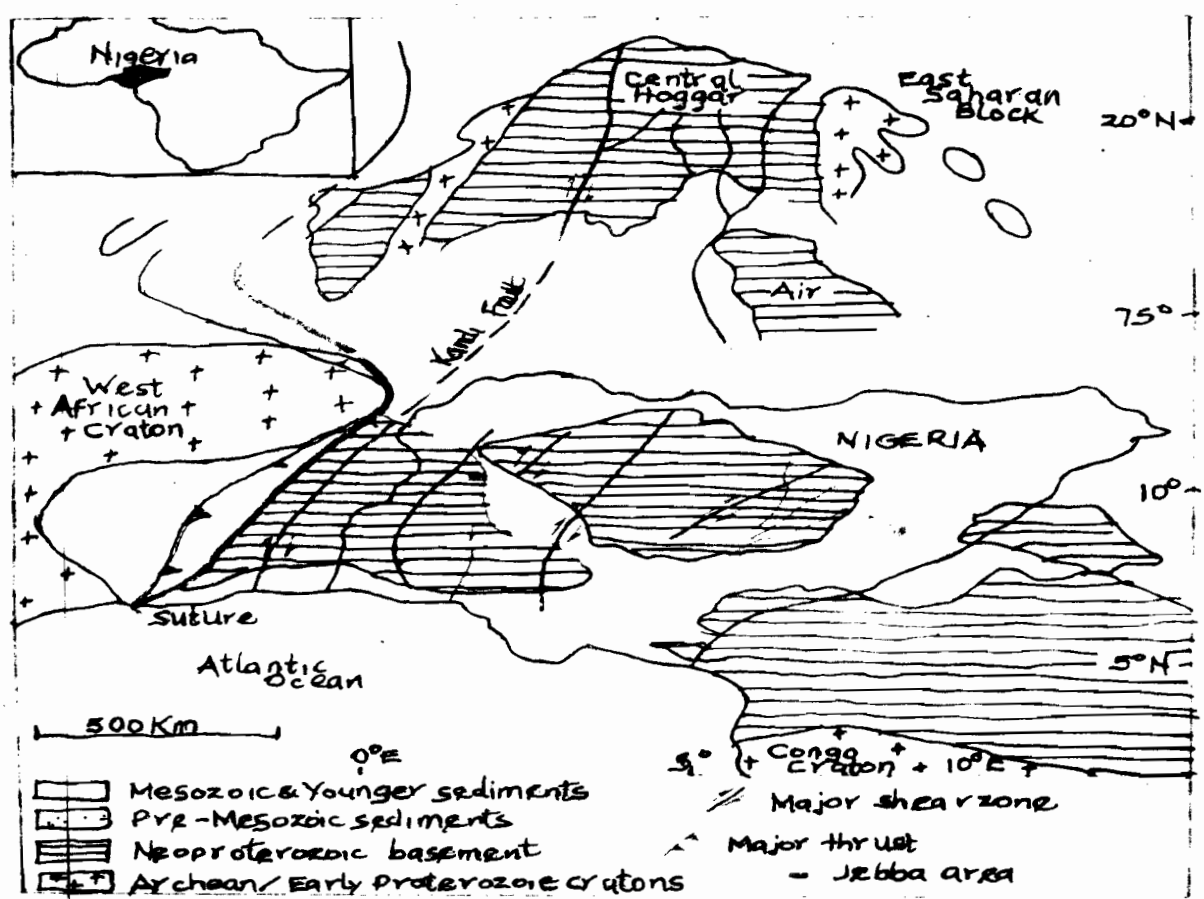

Fig. 1: Index map of the Trans-Saharan belt showing the location of Nigeria including Jebba area (after Ferre *et al* 2002)

C. T. Okonkwo, Department of Applied Geology, Federal University of Technology, Akure, Nigeria.

The polyphasal nature of the deformation of the Nigerian Precambrian basement rocks has been recognised by several workers eg Annor and Freeth (1985), Fitches et al (1985), Ajibade and Wright (1988), Odeyemi (1988), Rahaman (1988), Ekwueme (1987), and Ukaegbu and Oti (2005).

Since Okonkwo (1992) much more work has been done in the Jebba area; the field mapping has been extended to Aderan in the west, more data have been collected enabling a better understanding of the structural relationships and the structural development of the rocks in this area. This paper discusses the structural evolution of Jebba area in the light of these new developments.

LITHOSTRATIGRAPHY OF JEBBA AREA

The Jebba area is underlain by metasedimentary and metaigneous rocks which have been intruded by post-tectonic granitic rocks of probable Pan-African age (Fig. 2) A provisional lithostratigraphic classification of these rocks is presented here.

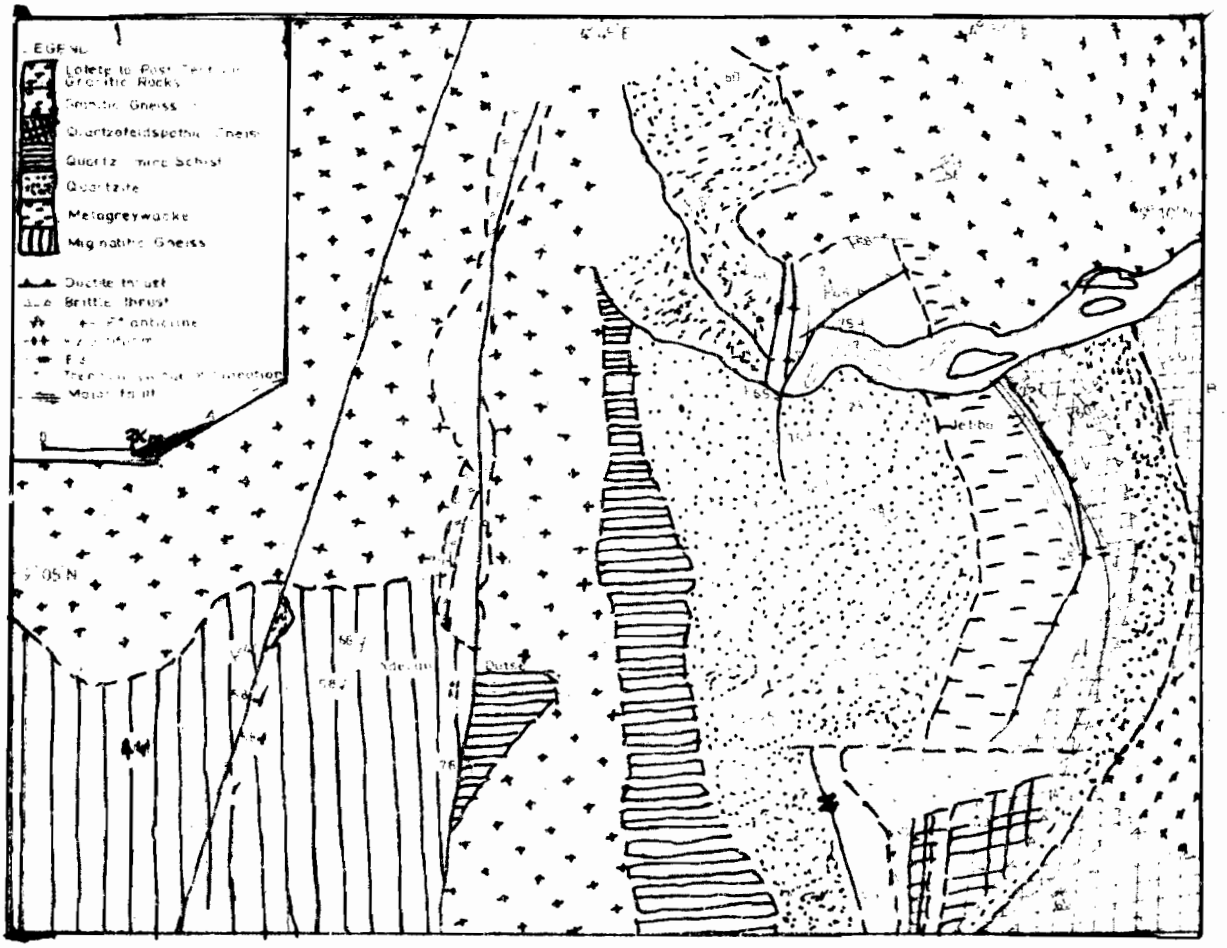

Fig. 2: Geological map of Jebba area

Migmatitic Gneiss

This unit outcrops in the western part of the study area and comprises a sequence of variably migmatised gneisses with concordant quartzo-felspathic segregations and bands. Locally it may also comprise augen gneiss components. The paleosome appears to be dominantly metaigneous and the migmatisation seems to be be the pro ducts of both metamorphic segregation and injection of granitoid material.

Quartzofeldspathic Gneiss

This unit outcrops in the eastern part of the area and comprises a sequence of grey, gneisses containing quartz, microcline, plagioclase and biotite which may locally contain thin concordant to subconcordant granitic veins.

Metagreywacke

A sequence of grey, quartz - plagioclase- and biotite-bearing psammitic rocks is exposed in the eastern part of Jebba area (Fig. 2). Occasionally, these rocks show relict grading with quartz-and feldspar- rich bases and biotite-rich tops. These petrographic characteristics suggest that these rocks were immature psammitic sediments similar to greywackes (Pettijohn 1975).

Thin, pale-coloured and discontinuous 0.5 to 5cm thick calc-silicate-rich bands containing epidote, plagioclase, biotite, actinolite and sphene occur sporadically within the metagreywacke. Concordant to discordant sheets of amphibolite containing hornblende, oligoclase, epidote, minor quartz, biotite and accessory sphene occur within the metagreywacke. The metamorphic assemblage in much of this unit indcates greenschist facies of metamorphism.

Quartzite

A sequence of quartzites which is locally micaceous is exposed in the N-S trending ridges extending from west of Jebba in the northwest to west of Biribiri village in the south-west (Fig. 2). Near the contact with the

metagreywacke, the sequence is marked by 3 to 5m thick lenses of pebbly quartzite containing pebbles of white vein quartz and smoky quartz as well as smaller grains of microcline in a matrix of finer quartz and muscovite grains interpreted as representing a matrix-supported conglomerate.

The quartzites locally show preserved cross-stratification and locally occur as thinly-bedded, flaggy units. Also locally, crystals of randomly-oriented tourmaline grains occur especially within foliation planes in the quartzites and 30 to 200m thick quartzite units occur as intercalations in the metagreywacke (Fig. 2).The eastern band of quartzite possess evidence of higher grade of metamorphism in the upper amphibolite facies which was probably acquired in deeper levels of the crust.

Quartz- Mica Schist

A sequence of quartz-biotite muscovite schists structurally overlies the quartzite in the west (Fig. 2). Locally the schists contain thin psammitic bands which are gradational with the schists probably reflecting original sedimentary grading. The schists range from dominantly muscovite-rich bands to more biotite-rich ones best exposed in Dutse village (Fig. 2).

Granitic Gneiss

This unit is exposed east of Jebba town (Fig. 2) where it occupies a N-S belt between the metagreywacke and quartzofeldspathic gneiss. The granitic gneiss is a pinkish, medium-grained rock containing quartz, K-feldspar, oligoclase, minor biotite and muscovite along with accessory ilmenite, epidote, sphene and chlorite. This unit is marked by heterogeneous strain producing rocks from weakly deformed granite to mylonitic granitic gneiss.

Late- to Post-tectonic Granitic Rocks

Several bodies of undeformed granitic intrusions occur within the metasedimentary rocks (Fig. 2). The rocks comprise mainly medium-grained granites and granodiorites which contain variable amounts of quartz, microcline, plagioclase, biotite and minor hornblende. A porphyritic variety occurs in the northern margin of the study area.

STRUCTURAL HISTORY

Five phases of deformation termed D_1, D_2, D_3, D_4 and D_5 have been recognised in the Jebba area.

D_1 Structures

Foliation

A penetrative foliation, S_1, is widely-developed in the various metamorphic rocks. The character of this foliation varies from a preferred orientation of micas and amphiboles in the metasedimentary rocks and amphibolites to gneissic banding in the gneisses. The attitude of the S_1 foliations is highly variable in the area as a result of their initial orientation and subsequent rotations during the D_2 and later events. The gross distribution of the S_1 planes define the geometries of the major fold structures in the area (Fig. 2).

S_1 is generally parallel to bedding, So, in the metasedimentary rocks except at the closures of the F_1 folds where it cuts the bedding at high angles (Fig.3).

Fig. 3: F_1 (D_1) folds in quartzite with axial planar S_1 foliations

Folds

The earliest recognised minor folds (F_1) deform the bedding as defined by lithological banding and possess an axial planar foliation, S_1 (Fig. 3). They are generally tight to isoclinal, locally, recumbent structures. Minor F_1 fold axes and other lineations show some scatter on stereographic plots (Fig. 4) probably as a result of their variable rotation by later deformation events (Ramsay 1967).

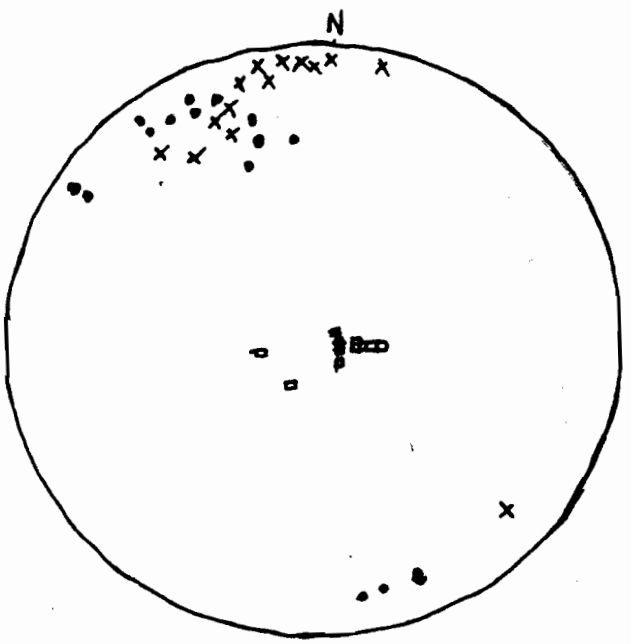

Fig. 4: Equal area stereographic plot of minor F_1 fold axes (crosses), ductile shear zone lineations (filled circles), poles to brittle thrust planes (open squares)

Major Fold

Rock exposures in the northwestern part of the area show a belt of subhorizontal S_1 foliations which are approximately perpendicular to the almost vertical bedding in the quartzite (Fig. 5). This belt is also marked by F_1 minor recumbent folds with axial planar cleavage. The relationships of these structural elements here indicate the closure of a major F_1 recumbent fold (Fig.

6). The fold axial surface is locally steepened in the east by later F_3 folding and late thrusting.

Fig. 5: Subhorizontal S_1 foliations perpendicular to the bedding in quartzite at major fold closure

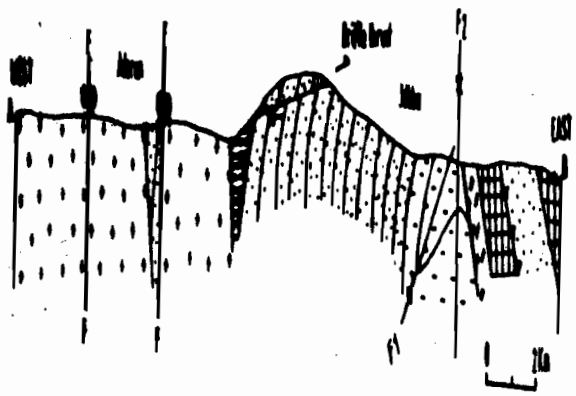

Fig. 6:. Structural (E-W) cross-section showing the major structures across the area (symbols as in Fig. 2)

Fig. 7: Tight, asymmetrical F_2 folds in quartzite

Fig. 8: F_1 and F_2 fold interference producing a type 3 (hook-type) pattern

D_2 Structures

Foliation

A younger set of crenulation cleavages, S_2, locally deform the S_1 foliations and are axial planar to later generation of folds. They are best developed in more micaceous lithologies.

Folds

A group of tight, asymmetric folds (Fig. 7) commonly deform the rocks. These structures fold D_1 structural elements and are locally associated with a crenulation cleavage. Locally, as in NW and NE sectors, they, the F_2 folds, occur as open to close recumbent folds which have caused the steepening of the earlier structures. They are related to a major antiformal fold structure, the Jebba Antiform, (Figs. 2 & 6). Interference between F_2 m inor folds and F_1 minor folds gave rise to coaxial, hook-type patterns (Fig. 8) similar to type 3 of Ramsay (1967) and Ramsay and Huber (1987).

Major Fold

A major fold associated with this event in the area is the Jebba antiform (Fig. 6) which has refolded the D1 recumbent major fold.

D_3 Structures

Ductile Thrust

A major N-S trending shear zone lies at the contact between the the metagreywacke and the granitic gneiss (Fig. 2). The granitic gneiss has been strongly sheared and the original mineral grains have been subjected to a very high degree of grain size reduction. The shear zone fabric, S_3, is also locally marked by the tectonic interbanding of granitic bands with those of the metagreywacke to produce a banded gneiss. The granitic bands were boudinaged and drawn into asymmetric augens (Fig. 9) with increase in the strain intensity indicating a top to the SSE sense of shear Stretching lineations in the shear zone trend NNW-SSE and plunge very shallowly (Fig. 4).

Fig. 9: Asymmetric augens of granitic gneiss in the shear zone indicating top to the SSE transport

D_4 Structures

Thrust Faults

Flat- lying to gently - dipping thrust faults occur at several horizons in the Jebba area. These thrust faults are especially well - exposed in the quartzites in the northwestern part of the area. They cut the limbs and other parts of early, D_1, tight to isoclinal folds in quartzite (Fig. 10). The thrusts therefore appear to have formed after the development of these early folds. They are mainly westerly dipping imbricate fans (Fig. 11) which are locally, densely developed in the quartzite with tectonic transport to the east. The total displacement on each fault cannot be ascertained because of lack of appropriate markers. It is known that imbricate thrusts are very efficient means of shortening and thickening a sequence (Boyer and Elliot 1982) so although the displacement on each fault may be small the aggregate displacement on the series of faults may be considerable. Locally, there are also easterly-dipping backthrusts which intersect the forethrusts producing pop-up structures.

Fig. 10: Shallowly-dipping thrust fault truncating early, F_1 fold in quartzite

Fig. 11: Shallowly-dipping imbricate thrust faults in the quartzite

Folds

There are tight to open, asymmetrical minor folds with generally subhorizontal axial planes which deform the shear zone fabric (Fig. 12) as well as the dominant foliation n, S_1. These folds are responsible for the steepening of the foliations, locally within the zones of imbricate thrust faults and ductile thrusts.

Fig. 12: Late SE-verging asymmetrical folds with subhorizontal axial planes which deform the shear zone fabric

Extensional Faults

Locally, minor, brittle, extensional faults occur in the quartzites. These are late structures and may be a reflection of a phase of gravitational spreading associated with late-orogenic uplift (Platt and Lister 1985).

D_5 Structures

Major Strike-slip Faults

Two major subparallel approximately N-S-trending and steeply-dipping faults have been mapped in the Aderan area (Fig. 2) These faults are defined by cataclasites

and mylonites developed in the truncated rocks especially the quartzites (Fig. 13) and the granites. Stretching lineations in the mylonitic granitic gneisses are sub-horizontal. Since these faults cut both the older metamorphic rocks and the presumably Pan-African granites the faulting is interpreted to be late Pan-African (Late Proterozoic) in age.

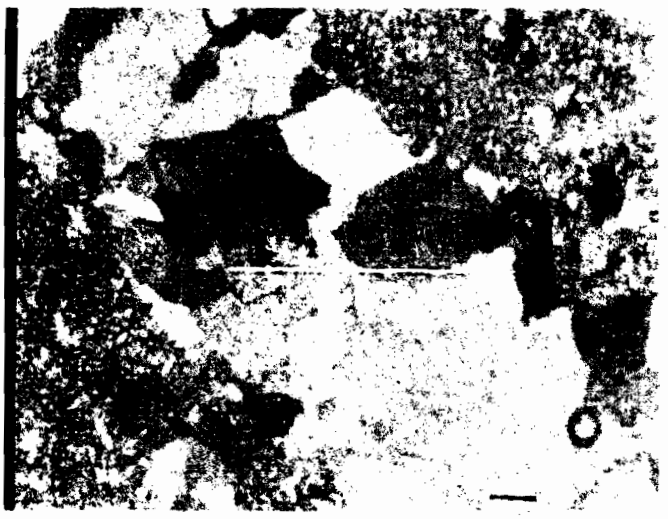

Fig. 13: Photomicrograph of cataclastic, very fine-grained quartzite which has been cut by a late quartz vein in a fault, NW of the study area. (Scale bar represents 0.32 mm)

DISCUSSION AND REGIONAL CORRELATIONS

Deformation of the Precambrian basement rocks of Jebba area was polyphase; the early phases involved contractional structures which were associated with the Pan-African orogenic convergence. These structures including major recumbent folding and ductile thrusting at deeper (lower) structural levels have SE-directed transport. This early phase of crustal shortening was followed by late folding which caused local steepening of the earlier structures.

A later phase of brittle thrusting cross-cut the earlier folds and structures reflecting a SE-verging shear and an out of sequence deformation of previously folded and deformed sequences in a break-back sequence (Butler 1992).

Several, major , approximately, N-S-trending fault zones have been recognised in Nigeria eg Kalangai Fault (Truswell and Cope 1963), Zungeru (Ajibade 1982), Ifewara (Caby and Boesse 2001). Although these faults have been mostly recognised as showing strike-slip displacement there are indications of oblique-slip and even earlier thrust displacements on them. In the Central Hoggar Belt to the north of the Nigerian Basement Complex (Caby 1989) had recognised similar shear zones in the Trans-Saharan Belt of the Tuareg Shield.

In Jebba area the D_1 recumbent folding and the ductile thrusting predated the brittle thrusting in the quartzite. Boesse *et al* (1989) also recognised the nappes of Ife- Ilesha area as D_1 structures. Caby (1989) and Caby and Boesse (2001) have argued that the D_1 thrusting and nappe formation in SW Nigeria is of Pan-African age and is similar to that observed in central Hoggar (Lapique *et al*. 1986) with ages bracketed between 629 and 618 Ma (U-Pb on zircons - Bertrand *et al*, 1986).

In the Nigerian basement complex, there is a general lack of appropriate radiometric dates to constrain the timing of these deformational events. However, since the brittle and ductile shear zones also affected some Pan-African granitic rocks, it appears that these structures in Jebba area are also Late Proterozoic (Pan-African) in age..

These structures (nappes, ductile shear zones, thrusts and strike slip faults) in the Jebba area are similar to those described from the Ife region of SW Nigeria by Caby (1989), Caby and Boesse (2001), and in Lokoja area by Ajibade and Wright (1989). Ferre *et al* (2002) have also described nappe tectonics and strike-slip movements in Pambegua-Bauchi area associated with granite emplacement. All these indicate a regime of horizontal tectonics associated with Pan-African continental convergence was of widespread occurrence in this sector of the Pan-African mobile belt.

Some of these structures are also geometrically similar to metamorphosed thrusts and nappes described from the Scottish and Scandinavian Caledonides (Butler 1984, Barr *et al* 1986, Holdsworth 1989, and Gee 1975) and also the Appalachians (Hatcher 1978) and the Hoggar (Caby *et al* 1981). The thrust faults are very similar to those described by Booth and Shone (1999, 2002) from the Cape Fold Belt, South Africa.

CONCLUSIONS

1. Early deformation associated with Pan-African orogenic convergence involved major recumbent folding and ductile thrusting.
2. These early structures were refolded by coaxial F_2 and later F_3 folds which along with late brittle thrusting led to local steepening of these structures. Late north- westward-directed back-thrusting also truncated the earlier structures..
3. Late- orogenic crustal uplift and gravitational spreading associated with strain localisation were marked by brittle faulting, including extensional faults and conjugate transcurrent faults.

ACKNOWLEDGEMENTS

I acknowledge the generous hospitality and assistance of Engr. L.C. Ewurum and other staff of the Jebba HydroPower business Unit and useful comments by some colleagues.

This research was supported by grants from the Senate Research Fund of the University of Ilorin.

REFERENCES

Affaton, P., Sougy, J. and Trompette, R., 1980. The tectonostratigraphic relationships between the upper Precambrian and lower Paleozoic Volta basin and the Pan-African Dahomey orogenic belt (West Africa) *American Journal of Science*, 280: 224 - 248.

Ajibade, A.C., 1982. The cataclastic rocks of the Zungeru region and their tectonic significance. *Journal Mining and Geology* 18: 29 – 41.

Ajibade, A.C., Woakes, M. and Rahaman, M. A., 1987. Proterozoic crustal development in the Pan-African regime of Nigeria. In: Proterozoic crustal evolution. (Edited by A. Kroner). *American Geophysical Union Geodynamic Series*, 17: 259-271.

Ajibade, A.C. and Wright, J. B., 1988. Structural relationships in the schist belts of Northwestern Nigeria. In: *Precambrian Geology of Nigeria* (Edited by Oluyide, P.O.,Mbonu, W.C., Ogezi, A.E., Egbuniwe, I.G., Ajibade, A.C. and Umeji, A.C.), Geological Survey of Nigeria, pp 103 - 109.

Ajibade, A.C. and Wright, J. B., 1989. The Togo-Benin-Nigeria shield: evidence of crustal aggregation in the Pan-African belt. *Tectonophysics* 165: 125-129.

Annor, A.E. and Freeth, S. J., 1985. Thermo-tectonic evolution of the basement complex around Okene, Nigeria, with special reference to deformation mechanism. *Precambrian Research* 28: 269-281.

Barr,D., Holdsworth, R. E. and Roberts, A. M., 1986. Caledonian ductile thrusting in a Precambrian metamorphic complex: the Moine of NW Scotland *Geological Society of America Bulletin,* 97: 754 - 764.

Bertrand, J. M. L., Michard, A. Boullier, A. M. and Dautel, D., 1986. Structure and U-Pb geochronology, tectonic implications for the Hoggar shield. *Precambrian Research*, 7: 349 - 376.

Boesse, J. M., Ocan, O.O. and Rahaman. M. A., 1989. Lithology and the structure of the Ife - Ilesha area. *Abstracts* - the 25th Annual Conference Nigerian Mining Geosciences Society, 6 - 7.

Booth, P. W. K. and Shone, R. W., 1999. Complex Thrusting at Uniondale, eastern sector of the Cape Fold Belt, Republic of South Africa: structural evidence for the need to revise the lithostratigraphy. *Journal of African Earth Sciences* 29: 125 – 133.

Booth, P. W. K. and Shone, R. W., 2002. Areview of thrust faulting in the Eastern Cape Fold Belt, South Africa, and the implications for current lithostratigraphic interpretation of the Cape Supergroup. *Journal of African Earth Sciences* 31: 179-190.

Boyer, S. E. and Elliot, D., 1982. Thrust systems. *Bulletin American Association of Petroleum Geologists* 66: 1196 - 1230.

Butler, R. W. H., 1982. The terminology of structures in thrust belts. *Journal of Structural Geology* 4: 239 - 245.

Butler, R.W.H. 1984. Structural evolution of the Moine thrust belt between Loch More and Glendhu, Sutherland. *Scottish Journal of Geology* 20: 161 – 179.

Caby, R., 1989. Precambrian terranes of Benin - Nigeria and northeast Brazil and the Late Proterozoic South Atlantic fit. *Geological Society of America Special Paper* 230: 145 - 158.

Caby, R., Bertrand, J. M. L. and Black, R. 1981. Pan-African closure and continental collision in the Hoggar-Iforas segment, Central Sahara. In: *Precambrian Plate Tectonics* (Edited by Kroner, A.) pp. 407 - 434. Elsevier, Amsterdam.

Caby,R. and Boesse, J.M. 2001. Pan-African nappe system in southwest Nigeria: the Ife-Ilesha schist belt. *Journal of African Earth Sciences.* 33: 211 – 225.

Dada, S. S., Dupre, B., Brique, L. and Rahaman, M.A. 1994. Geochemical characteristics of reworked Archean Gneiss complex of North-central Nigeria. *Abstracts* - 30th Annual Conference Nigerian Mining Geosciences Society, pp. 65.

Ekwueme, B. N., 1987. Structural orientation and Precambrian deformational episodes of Uwet area, Oban Massif, S.E. Nigeria *Precambrian Research* 34: 269 - 289.

Ferre, E., Gleizes, G. and Caby, R. 2002. Obliquely convergent tectonics and granite emplacement in the Trans-Saharan belt of Eastern Nigeria: a synthesis. *Precambrian Reasearch* 114: 199 – 219.

Fitches, W. R., Ajibade, A. C., Egbuniwe, I. G., Holt, R. W. and Wright, J. B., 1985. Late Proterozoic schist belts and plutonism in NW Nigeria. *Journal Geological Society of London* 142: 319 - 337.

Gee, D. G., 1975. A tectonic model for the central part of the Scandinavian Caledonides. *American Journal of Science* 275: 468 - 515.

Grant, N.K. 1970. Geochronology of Precambrian basement rocks from Ibadan, South Western Nigeria. *Earth and Planetary Science Letters* 10: 29 - 38.

Hatcher, R. D., 1978. Tectonics of the western Piedmont and Blue Ridge, Southern Appalachians: review and speculation. *American Journal of Science,* 278: 276 - 304.

Holdsworth, R. E., 1979. The geology and structural evolution of a Caledonian fold and ductile thrust zone, Kyle of Tongue region, Sutherland, Scotland. *Journal Geological Society of London* 146: 809 - 823.

Lapique, F., Bertrand, J. M. and Meriem, D., 1986. A major Pan-African crustal decoupling zone in the Timgaouine area (Western Hoggar, Algeria). *Journal of Africa Earth Sciences* 5: 617 - 625.

Odeyemi, I. B., 1988. Lithostratigraphy and structural relationships of the Upper Precambrian Metasediments in Igarra area, southwestern Nigeria. In: *Precambrian Geology of Nigeria* (Edited by Oluyide, P.O., Mbonu, W.C., Ogezi, A.E., Egbuniwe,I.G., Ajibade, A.C. and Umeji, A.C.), Geological Survey of Nigeria, pp. 111-125.

Ogezi. A. E. O., 1988. Origin and Evolutin of the Basement complex of Northwestern Nigeria in the light of new Geochemical and Geochronological data. In: *Precambrian Geology of Nigeria* (Edited by Oluyide, P.O., Mbonu, W.C., Ogezi, A.E., Egbuniwe, I.G., Ajibade, A.C. and Umeji, A.C.), Geological Survey of Nigeria, pp. 301-312.

Okonkwo, C.T. 1992. Structural geology of basement rocks of Jebba area, Nigeria. *Journal Mining of Geology* 28, 203 - 209.

Oversby, V.M. 1975. Lead isotope study of aplites from the Precambrian rocks near Ibadan, South western Nigeria. *Earth Planetary Science Letters* 27: 177 - 180.

Pettijohn, F.I. 1975. *Sedimentary Rocks*, 628p. Harper & Row, New York.

Platt, J. P. and Lister, G.S. 1985. Structural evolution of a nappe complex, southern Vanoise massif, French Penninic Alps. *Journal of Structural Geology*, 7: 145-160.

Rahaman, M.A. 1988. Recent advances in the study of the basement complex of Nigeria. In: *Precambrian Geology of Nigeria* (Edited by Oluyide, P.O., Mbonu, W.C., Ogezi, A.E., Egbuniwe, I.G., Ajibade, A.C. and Umeji, A.C.). Geological Survey Nigeria, pp. 11 - 41..

Ramsay, J. G., 1967. *Folding and Fracturing of Rocks*, 568p. McGraw Hill, New York.

Ramsay, J. G. and Huber, M.I. 1987. *Techniques of modern structural Geology*, 700p. Academic Press, London.

Talbot, C. J. 1974. Fold nappes as asymmetric mantled gneiss domes and ensialic orogeny. *Tectonophysics* 24: 259 - 276.

Truswell, J.F. and Cope, R.N. 1963. The geology of parts of Niger and Zaria provinces, Northern Nigeria. *Bulletin Geological Survey* Nigeria, 29.

Ukaegbu, V.U. and Oti, M.N. 2005. Structural elements of the Pan-African orogeny and their geodynamic implications in Obudu Plateau, southeastern Nigeria. *Journal of Mining and Geology* 41: 41-49.

Van Breemen, O., Pidgeon, R. and Bowden, P. 1977. Age and isotopic studies of Pan-African granites from north central Nigeria. *Precambrian Research* 4: 301 - 319.

GLOBAL JOURNAL OF GEOLOGICAL SCIENCES VOL. 6 NO. 2 2008: 153 - 156
 ISSN 1596 – 6798

GROUNDWATER PROTECTION AS VIABLE OPTION FOR SUSTAINABLE WATER SUPPLY IN NIGERIA

H. O. NWANKWOALA AND G. J. UDOM

(Received 18 March, 2008. Revision Accepted 29 September, 2008)

ABSTRACT

The threat of contamination of groundwater due to indiscriminate refuse disposal, bad management of sewage and septic tanks, industrial effluent discharges, leakage of underground fuel pipes and storage tanks and non-point pollution sources in major urban and semi- urban locations across the country are real. The argument to start planning for groundwater protection before there is serious contamination is clear and powerful. Such preventive action is the essence of groundwater protection. The logic of preventing groundwater contamination is clear but our problem or concern is in remediation of groundwater contamination. Although there are many well documented examples of groundwater remediation and good sources of information on how to clean up contaminated aquifers, the need to protect our groundwater supplies cannot be over emphasized. The age long aphorism " *prevention is better than cure*" applies here. This is because, once polluted, groundwater supplies are difficult and expensive to purify and the aquifer requires a long time to "heal" naturally. It then constitutes a health hazard to the consumers. This paper therefore addresses the question of how we can protect groundwater from becoming polluted. The paper not only concentrates on the problems of protecting groundwater from toxic chemicals but also discusses ways of protecting groundwater from conventional pollutants.

KEYWORDS: Groundwater protection, contamination, pollution, sustainable water supply, Nigeria.

INTRODUCTION

The overwhelming number of activities concerning groundwater has been involved with remediating contamination rather than protecting groundwater from becoming contaminated. This results from the necessity to protect the public from the potential health threat of existing contamination. Many contaminants that reach our potable water are harmful at even trace concentrations. Small quantities of these toxic chemicals can contaminate many thousands of gallons of groundwater. Once in groundwater, they may be protected from the unusual environmental degradation processes. Their movement in the aquifer may be difficult to predict. Remediation efforts are usually extremely expensive. Because of these factors, it is now time to look beyond immediate crises and develop programs that will prevent future groundwater contamination.

On a national scale, the extent of groundwater contamination is thought to be small. Indeed, the pollution of our national water resources seems to be a gradual process that tends to render the resources irredeemable. And the rate of pollution tends to be on the increase owing to increases in the emerging industries and lack of effective monitoring of these industries and commercial establishments in keeping with the national environmental protection acts or legislations (FEPA,1991).

A country where solid wastes are dumped in burrow pits and most times in abandoned shallow wells with no regard to groundwater contamination, surely must inherit serious water resources management problems.

The true extent of contamination is unknown in Nigeria because no comprehensive national database or monitoring system exists. Groundwater contamination is of national concern because it is often found where the concentrations of human population are dependent on groundwater sources for their drinking water.

There are many sources from which toxic chemicals may reach groundwater. These sources are widely dispersed. Industrial solvents are found in our urban industrial centres, but are also widely distributed because of the decentralization of our industrial base and also because of disposal practices. Pesticides and herbicides are problems in many agricultural areas. The problems also extend to suburban areas because of manufacture, storage, and transportation accidents. Leaking storage tanks are problems everywhere. Hazardous waste disposal sites, abandoned dumpsites, and the disposal of small quantities of toxic wastes by commercial establishments and private households all have the potential of causing serious groundwater contamination.

Groundwater Resource Protection and Water Policy Imperatives

Unlike most environmental problems, Nigeria has not passed comprehensive legislations to protect groundwater. Perhaps the possible reason for this *laissez faire* attitude over groundwater protection is the belief that Nigeria is blessed with an abundance of groundwater, which is ubiquitous in every geological setting, ranging from crystalline rock terrains to regions that are underlain by sedimentary rocks and in most cases, groundwater may be used without prior treatment. Given these scenarios groundwater resource supply should not constitute a problem. This is of course, not the case.

H. O. Nwankwoala, Department of Geology, University of Port Harcourt, Nigeria.
G. J. Udom, Department of Geology, University of Port Harcourt, Nigeria.

Groundwater source protection is extremely important because when the resource is no longer available at source either in terms of quantity and/or quality, there is scarcely any substitute for the overwhelming population which depends on groundwater.
There is a dire need for a policy. This is imperative because as pollution increases, the amount of useable water decreases and whatever remains is endangered.

A detailed study of the decree for water resources management (Decree 101 of 1993) by several workers (Akpoborie, 1999; Nwaogazie, personal communication) showed it drew heavily on the Riparian law concept without detailed distinction of groundwater concepts and their significance, thus resulting in a great bias to mainly surface water development and management. It is this bias of Decree 101 of 1993 towards surface water that underscores the built-in neglect of groundwater resource development in Nigeria. This has created a lacuna in the control and practice of groundwater resources development

Offodile (2000) lamented seriously on the inability of the government to "deliberately and intensively integrate regional groundwater exploration and exploitation programs in the overall National Water Resources Development Programmes. Groundwater is exploited rather haphazardly and indiscriminately by government, private institutions and individuals without any control, management or organization" even in open breach of Decree 101 (of 1993). It is in this context that Nwaogazie (2006) concluded that *"the Nigerian people are in desperate need for industrial waste disposal acts to protect the resources for the future"*. He further stated that without the strict implementation of such acts, our national water resources will be grossly polluted in the shortest possible time and thus water for all will become a dream. Akpoborie (1997) articulated the modalities for the establishment of a consistent and goal oriented national policy on water quality in order to give added fillip to work being undertaken by academia.
It is to be noted that the science of hydrogeology was born and evolved from the necessity to search for and procure water for various uses. It is worth-emphasizing as Linsky (2003) argues, *"Good science cannot be left out of policy making"*.
It is absolutely important that the groundwater resource be handled and protected in a sustainable manner so as to align the Nigerian nation with the UN-driven Millennium Development Goal (MDG). To achieve this objective and to avoid future crises, policy makers need to update groundwater policies and take steps to:

- ★ Understand the situation – recognizing the importance of groundwater and the value of protecting it and understanding the trends and drivers behind groundwater use;
- ★ Use resource analysis – to identify hot-spots of unsustainable groundwater use and prioritize these for action;
- ★ Actively manage groundwater-even in the early stages of the groundwater socio-ecology, shifting from 'resource- development' to ' resources – management' policies.

Policy makers must as a matter of urgency, rise to the challenge of finding ways to manage groundwater and sustain same. It is, after all, the most 'democratic' source of water available for improving livelihoods and household food security, and reducing poverty in the country. Amendment of Decree 101 or outright separate policy on groundwater protection should be considered without delay to ensure a regulated and well-controlled groundwater development and management programme in Nigeria.

Groundwater Protection Techniques
In this section, specific techniques that are thought to be useful for groundwater protection are discussed:

The reduction, recycling, and treatment of waste products
Reduction of the volume of waste products, including recycling, and treatment of waste products to make them less damaging to the environment are approaches that facilitate the protection of groundwater from contamination.

Ambient Groundwater Standards
Ambient groundwater standards for contaminant concentrations in groundwater can be an important component of groundwater protection efforts. Their basic role is to provide benchmarks on groundwater quality that are available to identify when potential problems exist that require intervention. A monitoring system that collects and analyses data on groundwater quality to ensure that standards are met is also required. When standards are exceeded, intervention is required. Intervention may be taken an action to remediate contamination or it may be new controls or adjustment of existing controls on sources of contamination. In fact, there is need for the establishment of numerical groundwater standards. Standards based on scientific risk assessments, analogous to the uniform national standards for contaminants in surface water, would be an important contribution to groundwater protection.

Effective Enforcement Provisions for Groundwater Protection Regulations
These are needed to ensure compliance with groundwater protection requirements. Enforcement provisions may range from administrative orders to civil and criminal penalties. Enforcement provisions at the federal, state, and local government levels must be available to force violators to comply with groundwater protection regulations.

Control of groundwater withdrawals
Control of groundwater withdrawals is necessary in order to manage groundwater resources to avoid contamination. Issues of groundwater quantity and quality are integrally related and must be managed in a coordinated fashion. Management to ensure that optimum yield (maximum stable basin yield) is not exceeded can prevent many groundwater problems including contamination. Some form of a groundwater withdrawal permit system will provide control if and when it is needed. This is important, especially for the coastal towns where the use of large capacity pumps cause salt water up-conning through excessive withdrawal from a well.

An Inventory of Potential Sources of Groundwater Contamination

This is needed for groundwater protection planning, especially at the local level. The inventory may be accomplished at the aquifer, regional, municipal, or the wellhead level. All potential sources of contaminants in the study area should be inventorized. The potential sources should include sites where potential pollutants are produced, stored, used, transported, and disposed of. The toxic chemicals which are of great concern in groundwater should receive the most attention because even small quantities can contaminate large volumes of groundwater for long periods of time. Potential sources of conventional pollutants should also be included in the inventory. The inventory should identify the potential sources, the potential pollutants at each source, and estimates of volumes. Planning to mitigate the anticipated problems should then be directed to the targets indicated in the inventory.

Effective Controls on all Potential Sources of Groundwater Contamination

These are needed to prevent contamination. These controls take many forms. The controls may be granting licence or permit for the construction of facilities or the discharge of potential pollutants. The license or permit may be required of new or existing facilities that are source(s) of potential groundwater contaminants. The license or permit is usually conditional upon compliance with design specifications, performance standards for the operation of the facility, and discharge limits established to protect groundwater.

The license or permit requires application, inspection, and renewal that allow the regulating unit to assess compliance. Permits may be required for all activities that have a potential adverse impact on groundwater. Activities that require permits may range from constructing new wells or septic systems to constructing waste disposal facilities.

Inventory of Aquifers, their Characteristics and Classification

Inventory of aquifers and their characteristics is an important activity for the protection of groundwater. In order to effectively protect our groundwater resources, it is essential to know about them. We need to know their boundaries, their hydrogeologic characteristics, and their chemical characteristics. Knowledge of aquifer recharge areas and hydrological connection to other aquifers are essential information if we are to develop and implement programs designed to protect and sustain groundwater quality. Details of the investigations needed may vary tremendously. In areas where there is no contamination and known sources of potential contamination, the inventory of aquifers and their characteristics may consist of no more than collecting existing knowledge about the aquifer. In areas where many people depend on groundwater for their drinking water supplies and where many potential sources of contamination exist, extensive hydrogeological investigations may be appropriate (Page, 1989; Nwankwoala and Odigi,2008). Also, a classification of aquifer is necessary to determine which aquifer should receive the highest attention in developing aquifer protection plans. When constrained by limited resources, the aquifers that are most important and most threatened should receive the most immediate attention.

Land use Controls

Land use controls are among the most important techniques for protecting groundwater. Controlling the uses of the land that overlies an aquifer can be an effective way of controlling what substances might reach and contaminate the aquifer. Land use controls are most effective if they are site- specific and are used to restrict activities on aquifer recharge areas or other sensitive land. A wide variety of techniques are available for controlling the uses of land. The most useful of these land use planning tools for groundwater protection include: Zoning, siting, development and construction regulations, conservation easements, and transfer of development rights programs, among others.

CONCLUSIONS

It is possible to protect our groundwater resources from conventional and toxic contaminants. Mechanisms to accomplish groundwater protection exist. No single mechanism or technique can be entirely effective, but combination of the options discussed above can be coordinated in a comprehensive groundwater protection plan that will greatly enhance the probability that groundwater resources will remain free of serious contamination.

Protecting groundwater is not an easy task. Even with broad political support to use all of the techniques available, there are many uncertainties that may hinder with success. This is obvious as our knowledge of aquifer characteristics hidden below the surface of the earth is limited. Aquifers are rarely composed of homogenous material, and it is not very possible to know all of the locations and the extent of the non-homogenous material that can affect the quality and movement of groundwater. Heterogeneities in aquifers produce many uncertainties that affect our ability to understand groundwater systems and our ability to plan for groundwater protection.

There are substantial gaps in our knowledge of what contaminants are present in our groundwater, how to predict their movement, how long they will remain, how they will affect human health, the contribution of contaminants in drinking water relative to other health risks, and the effectiveness of our efforts to develop and implement a groundwater protection plan. The entire process of planning for groundwater protection may be, on the whole, much more important than the set of groundwater protection techniques that have been used at any given time and place. Because of the uncertainties involved, it is important that groundwater protection plans be continually reassessed. The process of collecting information needed to get the groundwater protection process started should be continued to keep inventories of potential contaminant sources current and to evaluate if each protection option and/or technique is having its intended effect. It is the process of studying, developing, implementing, and monitoring groundwater protection plans that may lead to the understanding that will finally enable us protect our groundwater.

REFERENCES

Akpoborie,I. A., 1997. A framework for developing a groundwater quality management policy for Nigeria. Paper presented at the 10th Annual Conference of the Nigeria Association of Hydrogeologists, Enugu, Nov. 22-25.

Akpoborie, I.A., 1999. Implications of Decree 101 for water resources development and management in Nigeria. *Water Resources Journal*, Nigeria Assoc. Hydrogeol. 10: 19 – 25.

FEPA, 1991. Guidelines and Standards for Environmental Pollution Control in Nigeria,Federal Environmental Protection Agency, The Presidency, Lagos.

Linsky, R. B., 2003. Is there a Paradox in Translating Science and Technology into the Decision – Making Process? Water Resources Update, Issue 123: 49-554.

Nwankwoala, H. O. and Odigi, M. I., 2008. Hydrogeological Problems caused by Mining,Quarrying and Petroleum Exploration in Nigeria (In Press)

Nwaogazie, I. L, 2006. Water supply for all: who cares. University of Port Harcourt Inaugural Lecture Series No. 52.

Offodile, M. E., 2000. The development and management of groundwater for water supply in Nigeria. Paper Presented at the 2nd Fellows workshop of the Nigeria Mining and Geosciences Society 6th May, 2000.

Page, G. W., 1989. Groundwater Protection, Water Resource Systems, Encyclopedia Article, Encyclopedia of Physical Science and Technology, 1989 Yearbook. pp 312 – 316.

GLOBAL JOURNAL OF GEOLOGICAL SCIENCES VOL. 6 NO. 2 2008: 157 - 174
 ISSN 1596 – 6798

MINERAL ASSOCIATIONS IN THE BOUSSOUMA POST BIRIMIAN MAFIC DYKE AND THEIR PETROGENETIC SIGNIFICANCE (BURKINA FASO, WEST-AFRICAN CRATON)

URBAIN WENMENGA AND JEAN LUC DEVIDAL

(Received 20 May, 2008; Revision Accepted 16 September, 2008)

ABSTRACT

A systematic electron microprobe analysis, was carried out on constituent mineral phases (olivine, pyroxene, amphibole, plagioclase, micas, opaques) in dolerite, gabbro and pegmatitic suite associated with a mafic dyke of the Boussouma area in Burkina Faso, in order to characterize the magmatic and tectonic affinity of this intrusion. The compositions and microtextures of minerals and their paragenesis led the re- examination of the magmatic origin of this dyke. The mineralogical sequence made up of ferriferous olivine, calcic- plagioclase, orthopyroxene, augite, quartz/ micropegmatite and titano-magnetite, indicates a tholeiitic composition of the parent magma of the dyke. The composition of clinopyroxenes is in agreement with tholeiitic character of this mafic dyke and typical of rocks formed by anorogenic processes in a crustal distension zone. Enrichment in quartz/ micropegmatite and in ferro- titanic oxides from the edge to the centre of the dyke and the corresponding impoverishment of olivine, are compatible with a magmatic fractionation process. The temperature of the magma during crystallization using coexistent augite and orthopyroxene geothermometry, is estimated between 1000 and 1150°C and it progressively decreased to about 600 to 800°C, during the late crystallization stages as revealed by biotite thermometry. The post magmatic evolution of the dyke is marked by the neoformation hydrothermal minerals of dominantly low temperature hydrous phases.

KEYWORDS: Dolerite, micro-analysis, minerals, tholeiite, distension, geothermometry.

INTRODUCTION

Little attention has been given to the systematic micro-characterization of mineralogical paragenesis of post Birimian mafic intrusions, which form a vast swarm in the Baoule Mossi shield within the West- African craton. Geological investigations carried out both local and regional scales on dolerite/gabbro dykes particularly, in Burkina Faso where Gamsonré (1975), P.44, Sawadogo (1983), P.42, Somda (1995), P.27 highlighted various mineral associations, but however these authors could not address to a reasonable extent, their petrogenesis, magmatic affinity and geotectonic setting. The detailed mineralogical study of Boussouma mafic dyke (Fig. A-B-C) has enabled the reconstitution of the magmatic history of this intrusion. The dyke is free of penetrative deformation or regional metamorphism, which are the major features of the Birimian hosted rocks emplaced during Eburnean orogeny (2200-2000Ma) (Castaing et al., 2003, P.24).

Geological setting

The Birimian belt of Boussouma area (Fig.1) in the Palaeoproterozoic Baoule Mossi shield (2200-2000 Ma) is cut by a basic dyke swarm among which is that of Boussouma area (Fig.1B-C), detected due to its clear aeromagnetic characteristics and geological interpretations (Paterson et al., 1985). This belt consists of dominantly greenschist volcano- sedimentary facies comprising of chemical and clastic sediments, basic and acid flows and pyroclastics. Early to late Eburnean gabbro and granite intrusions induced in these series, low grade contact metamorphism

Urbain WENMENGA, University of Ouagadougou, UFR-SVT, Department of Earth Sciences, 03 B P. 7021 Ouagadougou 03, Burkina Faso
Jean Luc DEVIDAL, Blaise PASCAL University, Laboratory "Magmas et Volcans" 5, rue Kessler, 63038 Clermont Ferrand, France.

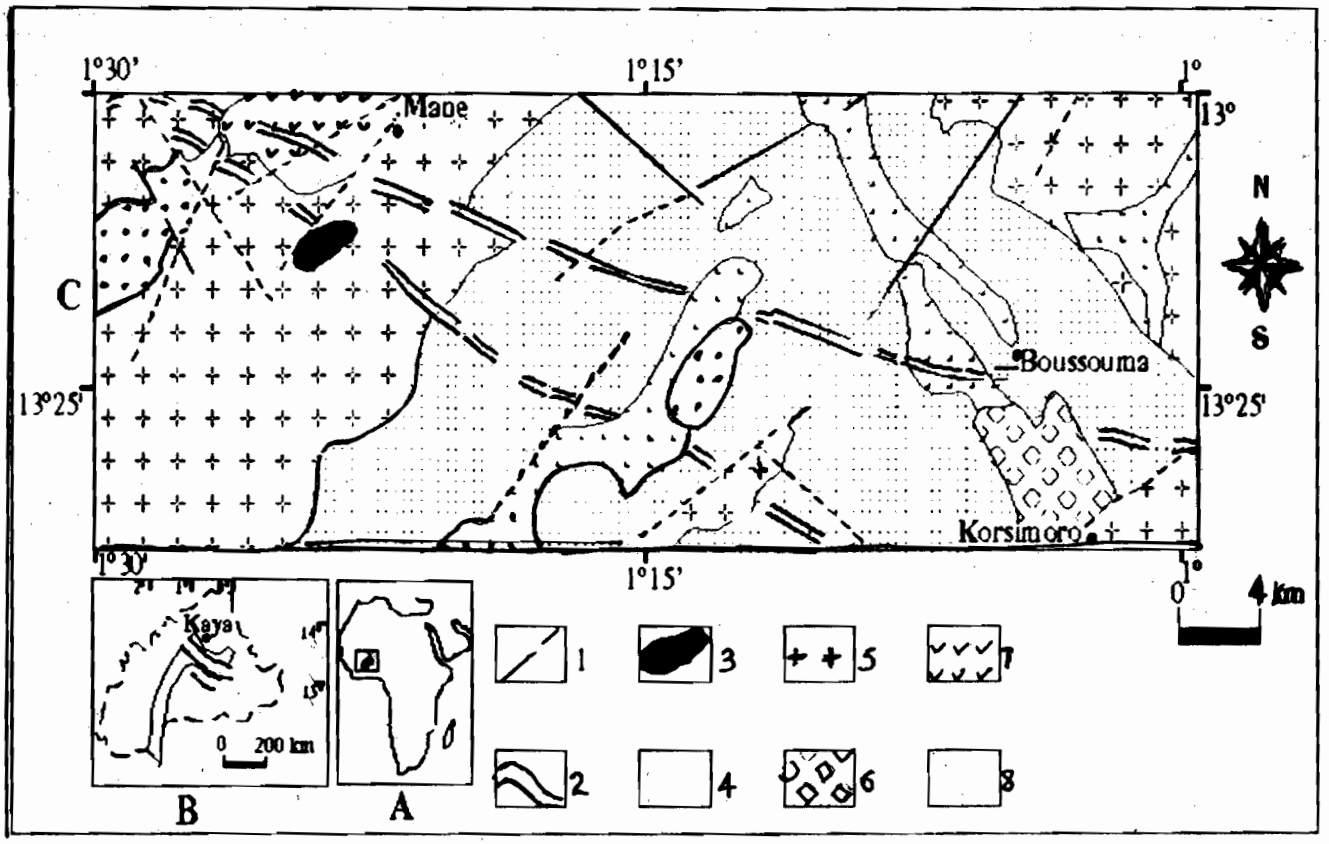

Fig. 1. A- B- C: Location (A-B) and geological map interpretation of aeromagnetic survey of Kaya- Boussouma study area (C) at 1/400.000 scale (Paterson et al.,1985)
1. Aeromagnetic fracture ; 2. Dolerite dyke ; 3. Undifferentiated basic rocks ; 4.Late gabbro intrusion ; 5. Granite ; 6. Metagabbro ; 7 Metabasalt ; 8. Birimian volcano- sedimentary series.

Analytical methods

A micro-analysis of minerals with electron microprobe Cameca SX100, was carried out in the " Magmas et Volcans " Laboratory, Blaise PASCAL University at Clermont Ferrand, France. Eight samples representing the main facies of Boussouma dyke, such as chilled (B21), fine grained (B17) and medium grained dolerite (B1, B19), coarse grained gabbro (B17", B17"') and pegmatite (B"3, B'1) were analyzed. Major and minor elements were determined on the predominant anhydrous mineral phases of which, include olivine (Table 1), pyroxenes (Tables 2, 3, 4), plagioclases (Tables 5,6,7); on the hydrous phases such as amphiboles (Tables 8,9,10), micas (Table 11) and on accessory opaque minerals (Table 12). More than one hundred analyses were performed.

Table 1: Representative chemical composition (%) of olivines from electron microprobe analysis

N° Sample	B21		B1			
N° Analysis	66	69	23	24	27	35
SiO_2	35.38	35.65	36.28	36.85	37.50	36.83
Al_2O_3	0.00	0.00	0.04	0.00	0.03	0.01
FeO	37.47	36.93	35.10	32.55	29.64	31.10
MgO	26.57	27.45	29.66	31.61	33.41	32.21
CaO	0.14	0.09	0.24	0.19	0.20	0.21
Na_2O	0.04	0.00	0.01	0.00	0.00	0.00
K_2O	0.06	0.00	0.02	0.00	0.03	0.00
TiO_2	0.06	0.17	0.11	0.00	0.00	0.05
MnO	0.45	0.50	0.45	0.40	0.37	0.50
Cr_2O_3	0.06	0.06	0.00	0.00	0.00	0.02
Total	100.24	100.84	101.92	101.60	101.19	100.94
Si	.993	.990	.987	.992	.998	.992
Al	.000	.000	.001	.000	.001	.000
Fe	.879	.858	.798	.732	.660	.700
Mg	1.112	1.136	1.202	1.268	1.326	1.293
Ca	.004	.002	.007	.005	.005	.006
Na	.002	.000	.000	.000	.000	.000
K	.002	.000	.000	.000	.001	.000
Ti	.001	.003	.002	.000	.000	.001
Mn	.010	.011	.010	.009	.008	.011
Cr	.001	.001	.000	.000	.000	.000
Total	3.006	3.004	3.010	3.007	3.001	3.006
FM	.444	.433	.402	.396	.335	.355
FO	55.53	56.65	59.78	63.09	66.49	64.50
FA	44.47	43.35	40.22	36.91	33.51	35.50

Table 2: Representative chemical composition (%) of pyroxenes from electron microprobe analysis

N° Sample	B21											B19		
N° Analysis	43	44	59	60	78	79	81	86	90	93	96	116	118	120
SiO_2	52.67	51.36	51.11	51.68	51.99	50.48	51.51	50.67	51.74	52.00	51.87	52.32	51.39	52.52
Al_2O_3	2.96	3.76	1.36	0.64	2.06	4.22	1.25	2.65	2.05	2.82	1.24	1.14	3.18	2.05
FeO	8.18	7.82	14.15	28.64	8.18	8.26	23.00	14.51	14.26	11.08	19.52	20.84	9.68	10.65
MgO	14.94	15.82	11.92	17.58	14.57	16.77	10.63	12.82	15.35	18.47	9.70	21.74	16.88	18.16
CaO	21.24	18.89	19.71	1.61	21.21	18.38	12.22	17.39	15.73	13.91	16.08	2.19	17.02	15.04
Na_2O	0.13	0.37	0.22	0.06	0.27	0.31	0.34	0.24	0.23	0.12	0.33	0.00	0.19	0.18
K_2O	0.02	0.01	0.01	0.00	0.00	0.03	0.02	0.00	0.00	0.00	0.04	0.03	0.01	0.00
TiO_2	0.40	0.53	0.37	0.19	0.46	0.47	0.32	0.92	0.56	0.39	0.18	0.44	0.46	0.28
MnO	0.23	0.19	0.41	0.53	0.19	0.22	0.60	0.38	0.44	0.29	0.56	0.44	0.29	0.29
Cr_2O_3	0.07	0.43	0.00	0.04	0.33	0.20	0.00	0.06	0.05	0.21	0.00	0.00	0.24	0.07
Total	100.85	99.18	99.26	100.97	99.26	99.35	99.88	99.63	100.42	99.29	99.52	99.15	99.34	99.24
Si	1.933	1.907	1.959	1.972	1.944	1.875	1.997	1.925	1.937	1.927	2.007	1.963	1.911	1.949
Al	0.128	0.164	0.061	0.028	0.090	184	.057	118	.904	123	.056	.050	139	.899
Fe	0.251	0.242	0.453	0.914	0.255	256	.745	461	.446	.343	631	.653	.301	.330
Mg	0.817	0.876	0.681	1.000	0.812	928	.614	725	.856	1.020	.559	1.215	.935	1.004
Ca	0.835	0.751	0.809	0.065	0.850	731	507	707	631	552	666	088	678	597
Na	0.009	0.026	0.016	0.004	0.019	.022	.025	.017	.016	.008	.024	.000	.013	013
K	0.000	0.000	0.000	0.000	0.000	.001	.000	.000	.000	.000	.002	.001	.000	000
Ti	0.001	0.014	0.010	0.005	0.013	.013	.009	.026	.015	.010	.005	.012	.012	.007
Mn	0.007	0.005	0.013	0.017	0.006	.007	.019	.012	.014	.009	.018	.013	.009	.009
Cr	0.001	0.012	0.000	0.001	0.009	.005	.000	.001	.001	.006	.000	.000	.007	.002
Total	3.995	4.002	4.006	4.009	4.001	4.027	3.977	3.996	4.009	4.001	3.972	3.999	4009	4.003
FM	0.240	0.221	0.406	0.482	0.243	.221	.554	.394	.349	.256	.537	.354	.249	.252
WO	43.71	40.06	41.36	3.29	44.18	38.07	26.90	37.12	32.39	28.69	35.54	4.47	35.25	30.79
EN	42.78	46.68	34.78	50.08	42.21	48.27	32.54	38.06	43.97	53.00	29.81	61.66	48.63	51.72
FS	13.51	13.25	23.86	46.62	13.61	13.71	40.55	24.82	23.64	18.31	34.65	33.87	16.12	17.49

Table 3. Representative chemical composition (%) of pyroxenes (continuous)

N° Sample	B19					B1							B17'''	
N° Analysis	128	129	131	136	140	20	25	26	28	30	38	102	103	104
SiO_2	53.12	51.27	52.60	51.47	53.37	50.58	52.62	52.56	51.70	52.38	50.79	50.63	51.14	51.99
Al_2O_3	0.60	2.29	1.88	3.06	1.93	0.98	1.99	2.29	1.58	2.59	2.60	2.30	2.62	2.39
FeO	23.18	14.72	13.30	11.86	19.67	30.23	14.11	11.13	22.98	14.17	13.67	15.10	13.79	10.77
MgO	20.73	15.55	17.94	15.51	23.14	15.70	19.83	17.98	21.35	20.53	14.34	14.22	13.70	15.44
CaO	1.96	14.58	13.38	17.55	1.54	1.98	10.19	15.46	1.84	9.22	16.67	16.59	17.81	19.77
Na_2O	0.02	0.25	0.15	0.21	0.00	0.04	0.25	0.25	0.01	0.10	0.23	0.20	0.16	0.44
K_2O	0.07	0.00	0.06	0.00	0.02	0.01	0.50	0.00	0.02	0.00	0.00	0.00	0.02	0.02
TiO_2	0.42	0.38	0.29	0.59	0.23	0.32	0.46	0.31	0.39	0.36	0.73	0.58	0.68	0.62
MnO	0.52	0.37	0.44	0.27	0.40	0.70	0.31	0.35	0.44	0.34	0.38	0.30	0.33	0.33
Cr_2O_3	0.02	0.08	0.00	0.11	0.01	0.01	0.06	0.08	0.00	0.13	0.00	0.00	0.00	0.07
Total	100.64	99.50	100.04	100.64	100.3	100.55	99.86	100.40	100.31	99.82	99.41	99.93	100.24	101.83
Si	1.981	1.935	1.951	1.910	1.959	1.960	1.944	1.935	1.936	1.930	1.922	1.919	1.924	1.912
Al	.026	102	.082	134	083	044	.086	.099	.069	112	115	102	116	.103
Fe	.723	464	.412	.368	.603	979	.436	.342	.720	436	432	478	434	.331
Mg	1.152	875	992	857	1.266	907	1.092	986	1.191	1.[illegible]	809	803	768	846
Ca	.078	589	531	.697	.060	.082	.403	.610	.073	[illegible]	.676	.674	718	.779
Na	.001	018	011	015	.000	002	017	.017	000	[illegible]	.017	014	.012	031
K	.003	000	002	000	.000	.000	.002	.000	000	[illegible]	.000	.000	000	000
Ti	.011	010	008	.016	.006	009	012	.008	011	[illegible]	.020	.016	019	.017
Mn	.016	.011	.013	.008	.012	.022	.009	.010	013	[illegible]	.012	.009	.010	.010
Cr	.000	.002	.000	.003	.000	000	001	002	000	[illegible]	.000	.000	.000	002
Total	3.995	4.010	4.005	4.011	3.992	4.009	4.008	4.013	4.018	4.004	4.006	4.019	4.003	4.033
FM	.390	.352	.300	.305	.327	.525	.289	.263	.381	.284	.354	.378	.366	.287
WO	3.97	30.37	27.27	36.11	3.11	4.12	20.78	31.28	3.69	18.78	35.02	34.29	37.19	39.61
EN	58.49	45.08	50.86	44.39	65.16	45.54	56.26	50.59	59.60	58.16	41.92	40.87	39.79	43.02
FS	37.54	24.55	21.87	19.50	31.72	50.34	22.96	18.13	36.70	23.06	23.05	24.85	23.02	17.36

Table 4: Representative chemical composition (%) of pyroxenes (continuous)

N° Sample	B17''17					B''3	
N° Analysis	105	106	108	112	115	27	29
SiO_2	50.91	51.17	51.05	50.47	50.54	50.89	51.17
Al_2O_3	3.35	2.78	1.95	1.79	2.37	0.21	0.05
FeO	10.08	10.29	16.55	16.64	15.30	18.31	17.06
MgO	14.02	14.33	12.89	11.99	14.40	8.35	9.11
CaO	19.94	19.60	16.84	16.80	15.26	20.66	21.49
Na_2O	0.25	0.19	0.28	0.25	0.27	0.18	0.49
K_2O	0.03	0.00	0.00	0.00	0.02	0.07	0.03
TiO_2	0.71	0.57	0.63	0.65	0.67	0.10	0.11
MnO	0.13	0.30	0.52	0.41	0.37	0.47	0.65
Cr_2O_3	0.07	0.06	0.08	0.11	0.01	0.00	0.05

Total	99.49	99.27	100.19	99.10	99.20	99.24	100.21
Si	1.909	1.924	1.933	1.946	1.925	1.998	1.986
Al	.148	.123	.087	.081	.106	.009	.002
Fe	.316	.323	.524	.536	.487	.601	.553
Mg	.783	.803	.727	.689	.818	.488	.526
Ca	.801	.789	.683	.694	.622	.869	.893
Na	.018	.013	.020	.018	.020	.013	.036
K	.001	.000	.000	.000	.000	.003	.001
Ti	.020	.016	.017	.018	.019	.002	.003
Mn	.004	.009	.016	.013	.011	.015	.021
Cr	.002	.001	.002	.003	.000	.000	.001
Total	4.004	4.004	4.013	4.001	4.012	4.002	4.027
FM	.290	.293	.426	.443	.379	.557	.521
WO	42.05	41.01	35.02	35.90	32.10	44.03	44.78
EN	41.13	41.71	37.28	35.65	42.16	24.75	26.40
FS	16.82	17.29	27.70	28.45	25.73	31.22	28.82

Table 5: Representative chemical composition (%) of plagioclases from electron microprobe analysis

N° Sample	B21										
N° Analysis	58	70	50	51	61	65	55	56	57	63	67
SiO_2	54.05	52.70	53.43	53.25	49.78	52.19	49.83	51.07	49.14	49.66	50.12
Al_2O_3	28.44	29.21	28.36	28.60	30.70	29.54	31.08	30.36	30.87	31.15	30.81
FeO	0.64	0.79	0.87	0.61	0.81	0.58	0.46	0.55	1.39	0.81	0.63
MgO	0.06	0.09	0.06	0.08	0.22	0.05	0.05	0.11	0.60	0.11	0.17
CaO	11.28	11.59	11.36	11.68	14.58	12.76	14.52	13.70	14.47	14.64	14.39
Na_2O	4.87	4.46	4.81	4.56	2.84	3.91	2.93	3.29	2.49	3.03	2.84
K_2O	0.18	0.11	0.24	0.10	0.02	0.15	0.07	0.08	0.07	0.03	0.02
TiO_2	0.04	0.00	0.05	0.04	0.01	0.03	0.00	0.10	0.03	0.00	0.06
MnO	0.00	0.03	0.04	0.06	0.03	0.11	0.00	0.05	0.04	0.00	0.01
Cr_2O_3	0.03	0.00	0.03	0.02	0.00	0.00	0.05	0.02	0.07	0.02	0.02
Total	99.59	99.09	99.25	99.00	99.00	99.32	99.00	99.34	99.17	99.44	99.06
Si	2.456	2.411	2.443	2.436	2.298	2.387	2.296	2.340	2.271	2.284	2.307
Al	1.523	1.575	1.528	1.542	1.670	1.592	1.688	1.639	1.681	1.689	1.671
Fe	.024	.030	.033	.023	.031	.022	.017	.021	.053	.031	.024
Mg	.003	.005	.004	.005	.014	.003	.003	.007	.041	.007	.011
Ca	.549	.573	.556	.572	.721	.625	.717	.672	.716	.721	.709
Na	.429	.396	.426	.404	.254	.346	.261	.292	.223	.269	.253
K	.010	.006	.013	.005	.001	.009	.004	.004	.003	.001	.001
Ti	.001	.000	.001	.001	.000	.000	.000	.003	.001	.000	.001
Mn	.000	.001	001	.002	.001	.004	.000	.002	.001	.000	.000
Cr	.001	.000	.001	.000	.000	.000	.001	.000	.002	.000	.000
Total	4.999	5.001	5.010	4.995	4.993	4.992	4.990	4.984	4.998	5.005	4.981
FM	.862	.841	.888	.829	.689	.878	.839	.753	.574	.808	.681
AB	43.41	40.57	42.75	41.17	26.02	35.34	26.62	30.14	23.66	27.17	26.29
OR	1.08	0.67	1.40	0.57	0.13	0.91	0.40	0.46	0.41	0.18	0.10
AN	55.51	58.75	55.85	58.26	73.86	63.75	72.97	69.40	75.93	72.65	73.61

Table 6: Representative chemical composition (%) of plagioclases (continuous)

N° Sample	B17	B19							B1				
N° Analysis	88	91	121	132	133	122	123	135	13	14	15	18	29
SiO_2	53.76	53.18	49.31	50.31	50.22	53.61	51.73	51.20	54.50	49.94	51.41	51.08	51.21
Al_2O_3	28.65	28.01	31.51	30.76	31.16	28.55	29.39	30.29	28.33	31.00	29.93	30.44	29.60
FeO	0.78	0.78	0.54	0.66	0.58	0.75	0.80	0.47	1.26	0.42	0.85	0.40	0.77
MgO	0.10	0.14	0.05	0.14	0.09	0.10	0.14	0.06	0.06	0.00	0.08	0.06	0.10
CaO	11.82	12.41	15.52	14.35	15.00	12.19	13.10	13.40	11.27	14.35	13.63	13.47	13.84
Na_2O	4.47	4.54	2.73	3.07	3.17	4.32	3.85	3.64	5.05	3.19	3.78	3.64	3.52
K_2O	0.10	0.08	0.03	0.00	0.00	0.05	0.06	0.00	0.13	0.09	0.09	0.04	0.05
TiO_2	0.07	0.09	0.16	0.07	0.00	0.00	0.00	0.09	0.01	0.16	0.10	0.00	0.09
MnO	0.00	0.06	0.01	0.00	0.03	6.02	0.03	0.03	0.01	0.01	0.03	0.09	0.00
Cr_2O_3	0.00	0.03	0.02	0.00	0.08	0.00	0.01	0.02	0.02	0.11	0.14	0.00	0.06
Total	99.75	99.34	99.88	99.37	100.33	99.59	99.11	99.21	100.65	99.28	100.04	99.23	99.25
Si	2.441	2.434	2.261	2.310	2.290	2.439	2.376	2.346	2.458	2.296	2.346	2.342	2.354
Al	1.533	1.511	1.703	1.664	1.674	1.531	1.591	1.636	1.506	1.680	1.610	1.645	1.603
Fe	.029	.029	.020	.025	.022	.028	.030	.018	.047	.016	.032	.003	.029
Mg	.006	.009	.003	.009	.006	.006	.009	.004	.004	.000	.005	.004	.007
Ca	.575	.608	.762	.706	.732	.594	.644	.657	.544	.707	.666	.661	.681
Na	.393	.403	.243	.272	.279	.381	.342	.323	.441	.284	.334	.323	.314
K	.005	.004	.001	.000	.000	.002	.003	.000	.007	.005	.005	.002	.003
Ti	.002	.003	.005	.002	.000	.000	.000	.003	.000	.005	.003	.000	.002
Mn	.000	.002	.000	.000	.001	.001	.001	.001	.000	.000	.001	.003	.000
Cr	.000	.001	.000	.000	.003	.000	.000	.000	.000	.004	.005	.000	.002
Total	4.988	5.009	5.003	4.991	5.010	4.986	5.000	4.992	5.011	5.000	5.011	4.997	4.998
FM	.820	.765	.859	.727	.790	.816	.765	.822	.923	.999	.862	.816	.809
AB	40.38	39.65	24.13	27.87	27.64	38.99	34.60	32.97	44.45	28.52	33.21	32.73	31.43
OR	0.58	0.46	0.18	0.00	0.00	0.28	0.36	0.00	0.73	0.55	0.55	0.26	0.32
AN	59.04	59.89	75.70	72.13	72.36	60.74	65.05	67.03	54.83	70.93	66.25	67.01	68.25

Table 7: Representative chemical composition (%) of plagioclases (continuous)

N° Sample	B17''						B''3		B'1		
N° Analysis	109	110	98	99	100	101	114	22	29	30	38
SiO_2	53.24	55.37	50.82	53.14	51.79	52.27	53.60	53.22	55.22	55.19	54.84
Al_2O_3	29.92	28.48	30.54	29.41	29.84	29.76	28.66	28.32	27.35	27.83	27.59
FeO	0.61	0.48	0.64	0.53	0.64	0.55	0.83	0.59	0.65	0.53	0.51
MgO	0.09	0.05	0.11	0.11	0.11	0.07	0.08	0.06	0.07	0.04	0.07
CaO	13.12	11.28	14.30	12.38	13.48	12.79	11.62	11.89	10.36	10.97	10.68
Na_2O	4.07	5.13	3.54	4.25	3.72	4.01	4.18	4.68	5.42	5.13	5.17
K_2O	0.07	0.10	0.00	0.08	0.02	0.11	0.09	0.02	0.09	0.09	0.09
TiO_2	0.02	0.00	0.07	0.04	0.05	0.01	0.04	0.06	0.03	0.10	0.09
MnO	0.03	0.03	0.06	0.00	0.00	0.00	0.05	0.10	0.00	0.00	0.00
Cr_2O_3	0.00	0.00	0.00	0.00	0.00	0.00	0.01	0.00	0.05	0.00	0.00
Total	101.18	100.92	100.09	99.94	99.66	99.58	99.17	99.03	99.25	99.88	99.05
Si	2.391	2.478	2.319	2.410	2.365	2.383	2.445	2.440	2.510	2.494	2.497
Al	1.583	1.502	1.643	1.572	1.606	1.599	1.541	1.527	1.465	1.482	1.480
Fe	023	.018	.024	.020	.024	.021	.031	.022	.024	.020	.019
Mg	005	.003	.007	.007	.007	.004	.005	.004	.004	.002	.004
Ca	.631	.540	.699	.601	.659	.625	.568	.583	.504	.531	.521
Na	.354	.445	.313	.374	.329	.354	.370	41.54	.478	.449	.456
K	.004	.005	.000	.004	.001	.006	.005	0.13	.005	.005	.005
Ti	.000	.000	.002	.001	.001	.000	.001	0.19	.000	.003	.003
Mn	.001	.001	.002	.000	.000	.000	.002	0.39	.000	.000	.000
Cr	.000	.000	.000	.000	.000	.000	.000	0.00	.001	.000	.000
Total	4.995	4.995	5.012	4.991	4.994	4.996	4.970	5.001	4.996	4.988	4.989
FM	.806	.859	.776	.726	.764	.811	.855	.866	.834	.889	.798
AB	35.82	44.89	30.94	38.17	33.24	35.96	39.23	41.54	48.38	45.57	46.46
OR	0.41	0.57	0.00	0.45	0.12	0.67	0.54	0.13	0.54	0.54	0.54
AN	63.77	54.55	69.06	61.38	66.63	63.36	60.23	58.33	51.08	53.90	52.99

Table 8: Representative chemical composition (%) of amphiboles from electron microprobe analysis

N° Sample	B21							B17					B19
N° Analysis	40	41	42	46	73	77	80	82	84	85	87	92	95	127
SiO_2	47.89	51.82	51.65	44.65	44.92	51.30	50.30	51.77	49.15	50.15	49.46	50.72	51.12	45.85
Al_2O_3	7.12	2.86	2.68	8.51	8.39	1.60	2.59	1.84	3.17	2.23	1.04	1.95	2.88	6.36
FeO	7.21	7.30	8.61	18.81	18.18	17.01	22.79	23.42	13.40	14.82	31.51	22.76	25.05	28.35
MgO	15.21	15.19	16.80	10.82	11.27	16.91	9.72	7.95	13.28	12.46	4.03	8.49	10.10	5.80
CaO	17.14	20.40	17.96	10.77	10.80	9.78	10.74	12.59	18.03	17.89	9.06	12.61	5.88	9.18
Na_2O	0.95	0.18	0.19	1.71	1.69	0.16	0.48	0.49	0.32	0.27	1.30	0.5	1.32	1.52
K_2O	0.04	0.00	0.00	0.38	0.34	0.01	0.04	0.05	0.03	0.00	0.20	0.06	0.05	0.36
TiO_2	1.00	0.39	0.38	1.77	1.99	0.30	0.20	0.12	0.98	0.57	0.16	0.17	0.12	1.20
MnO	0.05	0.18	0.37	0.19	0.25	0.45	0.47	0.40	0.30	0.32	1.01	0.54	0.58	0.47
Cr_2O_3	0.85	0.10	0.08	0.05	0.05	0.07	0.09	0.00	0.00	0.02	0.02	0.00	.000	0.06
OH	2.07	2.09	2.09	1.99	2.00	2.04	1.97	1.99	2.04	2.03	1.89	1.97	1.98	1.94
Total	99.54	100.51	100.80	99.66	99.89	99.63	99.40	100.61	100.70	100.89	99.68	99.78	99.09	101.11
Si	6.929	7.432	7.392	6.732	6.735	7.543	7.634	7.795	7.232	7.411	7.826	7.707	7.753	7.071
Al	1.213	.483	.452	1.511	1.483	.276	463	326	.550	.387	.193	.349	.515	1.155
Fe	.872	.875	1.030	2.372	2.279	2.091	2.893	2.949	1.648	1.826	4.169	2.893	3.177	3.656
Mg	3.281	3.248	3.584	2.432	2.518	3.705	2.198	1.783	2.913	2.737	.949	1.922	2.283	1.333
Ca	2.657	3.134	2.754	1.729	1.735	1.541	1.746	2.030	2.842	2.824	1.536	2.053	.956	1.517
Na	.266	.051	.052	.500	.491	.045	.141	.142	.091	076	398	.148	387	455
K	.007	.000	.000	.073	.065	.002	.008	009	.005	.000	040	012	009	070
Ti	.108	.041	.040	.200	.224	.033	.022	.013	.108	.062	.019	019	013	.139
Mn	.006	.022	.045	.024	.031	.055	.060	.051	.037	.039	.135	069	.075	.061
Cr	.097	.011	.008	.006	.006	.007	.011	.000	.000	.022	003	000	.000	.007
OH	1.000	1.000	1.000	1.000	1.000	1.000	1.000	1.000	1.000	1.000	1.000	1.000	1.000	1.000
Total	16.441	16.301	16.360	16.593	16.572	16.303	16.179	16.102	16.430	16.368	16.273	16.176	16.172	16.469
FM	.211	.216	.230	.496	.478	.366	.573	.627	.366	.405	.819	.606	587	.736

Table 9: Representative chemical composition (%) of amphiboles (continuous)

N° Sample	B1				B17			B13					
N° Analysis	2	19	22	33	36	107	17	18	20	21	26	28	31
SiO_2	50.57	46.83	50.90	51.05	51.96	44.45	44.95	47.28	47.05	44.84	50.92	52.43	48.69
Al_2O_3	3.30	5.76	2.47	2.30	2.24	7.49	6.48	4.30	4.06	7.00	1.42	0.59	2.86
FeO	21.66	21.45	14.72	11.42	11.03	28.01	28.76	29.73	28.53	28.75	22.33	23.33	35.05
MgO	11.31	9.68	14.19	16.23	17.22	5.71	5.26	5.66	5.62	4.90	10.44	9.59	5.19
CaO	9.56	10.28	17.78	16.11	15.04	9.50	9.51	9.67	9.21	9.86	11.70	9.77	4.67
Na_2O	0.80	1.45	0.31	0.15	0.20	1.32	1.95	1.19	1.18	1.70	0.34	0.15	0.46
K_2O	0.27	0.24	0.11	0.05	0.00	0.39	0.37	0.41	0.42	0.55	0.06	0.10	0.07
TiO_2	0.25	1.14	0.46	0.49	0.38	0.82	1.39	0.51	0.58	0.81	0.21	0.13	0.13
MnO	0.53	0.35	0.20	0.34	0.48	0.15	0.49	0.31	0.47	0.36	0.42	0.99	0.76
Cr_2O_3	0.11	0.03	0.12	0.07	0.02	0.00	0.03	0.02	0.09	0.04	0.00	0.04	0.05
OH	2.01	1.96	2.04	2.06	2.09	1.92	1.93	1.93	1.90	1.92	1.98	1.97	1.90
Total	100.36	99.18	100.30	100.27	100.66	99.76	101.12	101.02	99.10	100.73	99.83	99.09	99.84
Si	7.547	7.141	7.463	7.409	7.464	6.945	6.979	7.332	7.403	6.989	7.696	7.960	7.675
Al	.580	1.034	.426	.393	.379	1.379	1.186	.786	.753	1.286	.253	.105	.531
Fe	2.703	2.734	1.805	1.386	1.325	3.660	3.735	3.855	3.754	3.748	2.822	2.962	4.620
Mg	2.515	2.199	3.102	3.511	3.687	1.330	1.217	1.307	1.318	1.139	2.351	2.171	1.220
Ca	1.529	1.678	2.322	2.505	2.315	1.591	1.582	1.606	1.552	1.646	1.894	1.589	.788
Na	.230	.429	.880	.042	.056	.400	.587	.357	.360	.512	.099	.043	.141
K	.052	.046	.020	.008	.000	.078	.073	.081	.083	.109	.011	.019	.014
Ti	0.27	.131	.050	.053	.040	.096	.162	.050	.068	.094	.024	.015	.015
Mn	.066	.045	.024	0.41	.058	.020	.064	.041	.062	.047	.053	.127	.101
Cr	.013	.003	.014	.007	.002	.000	.004	.003	.010	.005	.000	.048	.006
OH	1.000	1.000	1.000	1.000	1.000	1.000	1.000	1.000	1.000	1.000	1.000	1.000	1.000
Total	16.267	16.445	16.317	16.360	16.330	16.504	16.592	16.431	16.366	16.579	16.206	15.999	16.116
FM	.524	.559	.371	.289	.273	.734	.757	.748	.743	.769	.550	.587	.794

Table 10: Representative chemical composition (%) of amphiboles (continuous)

N° Sample	B1							
N° Analysis	21	22	25	27	31	32	33	36
SiO_2	51.17	44.28	44.07	50.88	48.30	48.91	51.92	44.05
Al_2O_3	2.02	7.15	7.15	2.50	6.51	6.67	1.23	6.23
FeO	27.35	28.10	27.41	27.12	15.02	14.49	8.62	28.67
MgO	8.88	5.44	5.64	9.24	13.79	13.95	13.92	5.56
CaO	6.37	9.56	9.34	7.39	10.77	10.68	22.54	9.20
Na_2O	0.37	1.78	2.03	0.39	1.19	1.05	0.09	1.63
K_2O	0.06	0.18	0.18	0.07	0.26	0.20	0.01	0.31
TiO_2	0.29	1.79	1.69	0.31	1.20	0.77	0.35	1.47
MnO	0.56	0.52	0.30	0.57	0.21	0.33	0.29	0.35
Cr_2O	0.01	000	0.03	0.08	0.08	0.03	0.00	0.02
OH	1.96	1.93	1.91	1.98	2.03	2.04	2.07	1.90
Total	99.05	100.72	99.75	100.51	99.36	99.11	101.04	99.39
Si	7.836	6.880	6.893	7.698	7.113	7.183	7.510	6.961
Al	364	1.309	1.319	445	1.129	1.155	210	1.160
Fe	3.502	3.651	3.586	3.431	1.850	1.780	1.042	3.789
Mg	2.027	1.259	1.314	2.083	3.026	3.055	3.001	1.308
Ca	1.045	1.590	1.564	1.197	1.699	1.680	3.494	1.557
Na	.110	535	614	113	340	297	025	497
K	011	034	036	012	048	038	002	063
Ti	033	208	198	035	132	084	037	174
Mn	073	067	039	072	026	040	035	047
Cr	001	000	004	009	009	003	000	002
OH	1.000	1.000	1.000	1.000	1.000	1.000	1.000	1.000
Total	16.006	16.539	16.570	16.100	16.377	16.319	16.358	16.561
FM	638	747	734	627	382	373	264	745

Table 11: Representative chemical composition (%) of micas from electron microprobe analysis

Mineral	Chlorite				Biotite	
N° Sample	B1		B19		B1	B1
N° Analysis	34	35	125	126	41	37
SiO_2	27.10	27.50	33.66	35.33	35.12	33.51
Al_2O_3	17.44	17.73	13.92	13.13	12.69	13.53
FeO	33.99	31.63	32.13	31.81	31.22	31.63
MgO	9.00	11.60	3.60	4.67	4.61	6.16
CaO	0.19	0.21	0.03	0.24	0.22	0.29
Na_2O	0.02	0.00	0.21	0.57	0.24	0.12
K_2O	0.05	0.00	8.96	8.08	8.12	5.40
TiO_2	0.07	0.12	4.02	3.48	3.56	4.34
MnO	0.24	0.15	0.16	0.16	0.20	0.11
Cr_2O_3	0.05	0.03	0.00	0.06	0.01	0.00

OH	10.91	11.18	3.71	3.78	3.73	3.73
Total	99.07	100.16	100.40	101.31	99.71	98.83
Si	5.951	5.893	5.432	5.598	5.645	5.378
Al	4.514	4.478	2.648	2.452	2.405	2.558
Fe	6.241	5.667	4.336	4.215	4.197	4.245
Mg	2.946	3.703	.867	1.102	1.105	1.473
Ca	.044	.048	.006	.041	.037	.050
Na	.009	.000	.065	.173	.073	.036
K	.014	.000	1.843	1.632	1.666	1.106
Ti	.010	.019	.487	.414	.430	.524
Mn	.044	.027	.022	.020	.026	.014
Cr	.008	.005	.000	.007	.001	.000
OH	8.000	8.000	2.000	2.000	2.000	2.000
Total	27.786	27.843	17.709	17.659	17.589	17.388
FM	.680	.605	.834	.793	.792	.743

Table 12: Representative chemical composition (%) of oxides from electron microprobe analysis

N° Sample	B19	B'1
N° Analysis	138	39
SiO_2	0.02	0.00
Al_2O_3	0.05	0.00
FeO	42.46	42.72
Fe_2O_3	6.56	4.52
MgO	0.13	0.02
CaO	0.06	0.06
Na_2O	0.07	0.06
K_2O	0.00	0.04
TiO_2	49.04	50.36
MnO	1.43	2.50
Cr_2O_3	0.00	0.00
Total	99.82	100.28
Si	.001	.000
Al	.003	.000
Fe	1.800	1.803
Fe	.250	.171
Mg	.009	.001
Ca	.003	.003
Na	.007	.006
K	.000	.002
Ti	1.869	1.911
Mn	.061	.106
Cr	.000	.000
Total	4.005	4.006
FM	.994	.999

Petrography

The dyke occurs as boulders of variable sizes and enclosing Birimian xenolith rocks. It also caused volcanic chilled margins at the contact with Eburnean granitic and volcano-sedimentary country rocks. From the margin to the centre of the dyke, appears a petrographic suite made up sequentially of chilled dolerite, dolerite (ss), gabbro, pegmatite and locally graphic micropegmatite. Within the group of dolerite and gabbro bodies which form the essential rocks of the dyke, there appears to be progressive and regular grain variations (fine, medium, coarse). Elsewhere, many authors (Ross, 1983, P.1120, Bertrand, 1987, P.118, Potdevin et al., 1994, P.251, Napon, 1988, P.36) have reported textural grain changes between the core and the margin of dolerite dykes. Under the microscope, the chilled dolerites are composed of pyroxene glomero-porphyritic or olivine and plagioclase with porphyritic texture, while in the group of dolerite/gabbro suite, coexist intergranular, ophitic and intersertal textures. In these major suites, the plagioclase phases are commonly embedded by interstitial pyroxenes and could be described as local adcumulate and orthocumulate microtextures in the gabbro as in the Neoproterozoic basic dykes of Igherm inlier (El Aouli et al., 2001, P.372). Their preferential orientation indicates fluidal or igneous lamination structures (Bickford, 1963, P.227, Rivers and Mengel, 1988, P.1630) frequent in layered intrusions (Pons, 1982, P.81). Similar petrographic differentiations were described in numerous mafic sills and dykes of various age throughout the world (Vicat et Pouclet, 1995, P.358, Hafid, 1992, P.112, Machairas, 1975, P.195, Cadman and Tarney, 1990, P.19). These observations are interpreted as the consequence of the variation of the cooling rate during magmatic emplacement (Machairas, 1975, P. 195, Vicat et Vellutini, 1987, P.62, Azambre et al., 1987, P.382, Sutcliffe, 1989, P.69). The optical features and the microtextural relationships in these rocks enable their categorization into three groups, (i) a primary anhydrous minerals group (olivine, pyroxene, plagioclase, quartz, opaques), (ii) a group of late magmatic hydrous phases (amphiboles, micas) related to local volatil enrichment (Rathna and al., 2000, P.405) and (iii) a group of secondary post magmatic phases (phyllites, carbonates, epidote, iron oxides).

Characterization of mineral associations

Primary anhydrous minerals

Olivine

In the fine or medium grained dolerites, olivine crystals are strongly corroded by plagioclase and pyroxene (Fig.2-1) or form globular inclusions in clinopyroxenes. The coexistence of quartz and olivine in some samples, may be due to a crustal contamination or hybridization of the parent magma (Botha and Hodgson, 1976). In the chilled dolerite, olivine forms euhedral or anhedral phenocrysts with etching pit filled by the mesostasis or gaps occupied by augite crystals. Coronas of magnetite and orthopyroxene spread out around these phenocrysts due to olivine and residual liquid reaction. For this purpose, the following reaction was proposed by Pons (1982, P.119).

$(Mg, Fe)_2 SiO_4 + SiO_2 = 2 [(Fe, Mg) SiO_3]$

olivine + liquid= orthopyroxene. In other dykes, olivine exhibits continuous clinopyroxene rim and is restricted to dolerite suite. The corona microtexture is interpreted as a consequence of slow cooling of the parent basic magma of the dyke (Rathna and al., 2000 P.406). The content of olivine decreases from 5% to 1% from chilled dolerites to interior gabbros and is absent in the pegmatites and micropegmatite suites. Olivine composition corresponds to a hyalosiderite (Fo: 55.3-66.49) (Table 1).

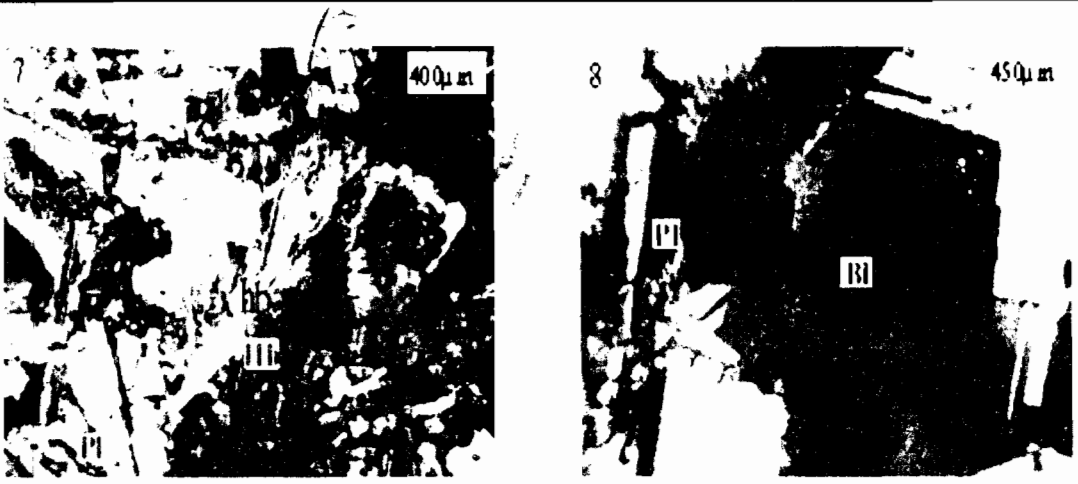

Fig. 2: Photomicrographs
1- Medium grained dolerite consisting of subhedral plagioclase (Pl), interstitial augite and strongly corroded anhedral olivine (Ol); 2. Ophitic and intergranular texture of coarse grained gabbro spaces between tabular crystals of plagioclase (Pl) are filled by poecilitic clinopyroxene (cpx). 3. Large crystal of clinopyroxene (augite) enclosing numerous plagioclase microlites in dolerite/ gabbro. 4. Aggregate of vermicular symplectite pyroxene crysts in the fine grained dolerite. 5. Photomicrograph illustrating accumulation of plagioclase microlites around poikilitic augite in chilled dolerite. 6. Cumulus phases of elongate plagioclase crystals displaying igneous lamination structure, in a medium grained dolerite. Ilmenite (dark crysts) is post cumulus phase. 7. Sheef- like texture of late fibrous greenish hornblende (Hb) in medium grained dolerite. 8. Large lamellar biotite (Bi) and iron oxide replacing uralites between spaces of plagioclase crystals.

Pyroxenes

Dominant clinopyroxenes and subordinate orthopyroxenes together with plagioclase, represent the most abundant phases of dolerite and gabbro constituting the dyke. The clinopyroxenes occur as irregular anhedral crystals, interstitial to plagioclase. (Fig.2-2). They are enclosed within the microlites of plagioclases (Fig.2-3) and constitute common prevalent species of all the suite. The orthopyroxenes generally form inclusions in clinopyroxenes or cluster of crystals with symplectite texture (Fig.2-4) developed at their contact with plagioclase or with the other types of pyroxene. This type of microtexture is interpreted as the product of exsolution reaction by atomic diffusion as the case of myrmekites (Mongkoltip and Ashworth, 1983, P.637). Frequent exsolution granules, discrete zoning and rare twins are associated with clinopyroxenes. The orthopyroxenes are of hypersthene composition, while clinopyroxenes display an important range of composition (Tables 2 to 4) evolving from calcic-subcalcic to ferriferous augites (Fig.3). Fe rich augites characterize the more differentiated suite of the dyke (Gabbro, pegmatite) and are attributable to magmatic fractionation (Reid, 1990, P.328). The absence of Ca-poor clinopyroxene such as pigeonite in this dyke, is due to the high water content in the magma (Pons, 1982, P.142).

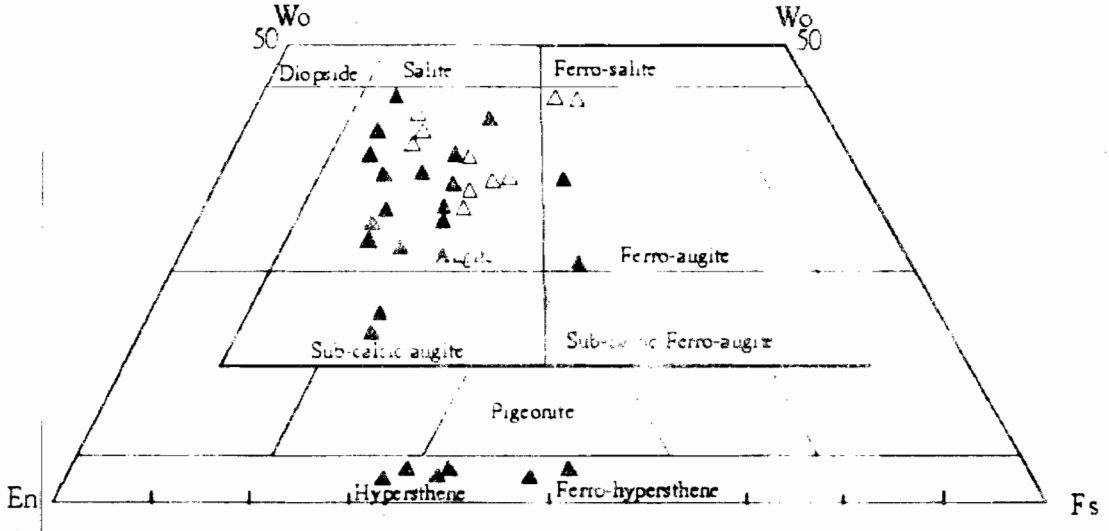

Fig. 3: Plot of pyroxene composition of representative rock samples of Boussouma dyke in Wo- En- Fs diagram (Poldervaart and Hess, 1951). Full triangle : pyroxene of dolerites ; empty triangle : pyroxene of gabbros and pegmatites.

Plagioclases

Plagioclases are the predominant minerals constituent (30 to 40%) of the various suite of the dyke and occur as tabular subhedral to euhedral crystals of increasing size from chilled dolerites to pegmatite or as laths ophitically inter- grow with pyroxenes (Fig 2-3). Plagioclase phenocrysts are confined to chilled dolerite displaying frequent gaps filled with augite crystals, but absent in

the core of the dyke. This observation is best explained by differentiation by a rapid quenchy magma rather than by flow differentiation (Ross, 1986, P.234). The accumulation of basic plagioclase microlites of mesostasis around mafic phenocrysts, suggests an emplacement in the country rocks of the magma still in molten stage (Fig.2-5). However, the massive accumulation of tabular or stubby crystals types in the medium or coarse- grained suites (Fig.2-6) rather suggests an earlier crystallization in the magmatic chamber. Plagioclase composition varies from labradorite to bytownite, irrespective of conditions of formation or that of host facies (Fig.4). These plagioclases contain high percentage of iron (0.40 to 1.39%) (Tables 5 to 7) relative to those of the Triassic "ophites" of Pyrenean field (Azambre et al., 1987, P.390).

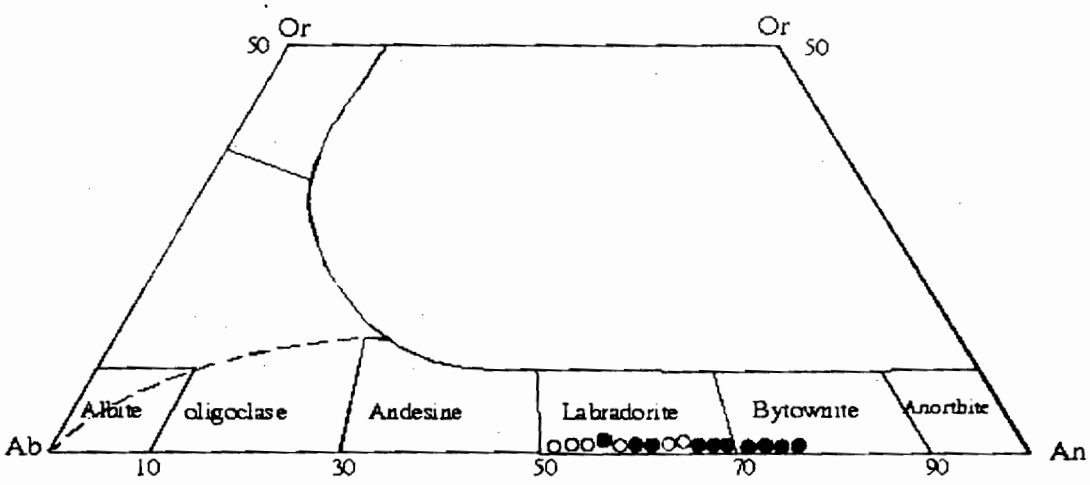

Figure 4. Labradorite to bytownite composition of feldspar in Or- Ab- An diagram Full circle : plagioclase of dolerites , empty circle : plagioclase of gabbros and pegmatites.

Quartz

The late crystallization of quartz is explained by its occurrence as interstitial and poecilitic minerals which must have crystallized after the opaque oxides. Its content is less than 5% in dolerite/gabbro, but increases within the pegmatite (10%) and the graphic micropegmatitic suite (60%), which could represent an eutectic crystallization products of the residual liquid (Somda, 1995, P.27, Gamsonre, 1975, P.70, Azambre et al., 1987, Hafid, 1992, P.116, Napon, 1988, P.37).

Opaque minerals

They are omnipresent minor components of all the suite of the dyke. Their proportion particularly increases (5 to 10%) in the gabbro and in the pegmatite bodies. They resemble inter-cumulus phases (Fig.2-6) of plagioclase, formed interstitial phases or as a result of symplectitic intergrowth with brownish hornblende. Some opaque oxides were developed as magmatic exsolution or oxidation products of mafic minerals. Their composition corresponds to ilmenites (Table 12) with relatively high ratio of MnO (1.43 to 2.5%) resulting from the major substitution of Fe-Mn in the lattice of the minerals (Reynolds, 1983, P.218). The development of biotite rim around opaques can be explained by the reaction between oxide phases and the residual liquid (Reynolds, 1983, P.218)

Accessory minerals

Zircon and sphene are rare in the dolerite body, while apatite forms euhedral prisms in the gabbros, pegmatites and micropegmatites bodies. The crystallization of this type of apatite described in some basic dykes, could result from a magma enriched in phosphorus, fluorine and probably chlorine (Hafid, 1992, P.137, Azambre et al., 1987, P.391) .

Late magmatic hydrous minerals

Amphibole

The abundance of amphiboles depends on the intensity of the transformation of clinopyroxene in the rock. Their color variation is used to distinguich two families of amphiboles in each body of the dyke; brownish amphiboles and the greenish amphiboles (Fig. 2-7). The first family may be magmatic, while the second could be derived from clinopyroxenes uralitization or from the successive alterations of uralites (Fig.2-7). The brownish amphiboles are distinguished from the other types by their enrichment in TiO_2 (1.14 to 1.99%) and in alkalis (1.45 to 2.32%) (Tables 8 to 10). They display a magnesio-hornblende composition similar to amphiboles of the Sirba valley dolerite dykes in Niger (Ama Salah, 1991, P.204) whereas the greenish amphiboles are related to actinolite and actinolitic hornblende (Fig.5) based on the classification of Leake, (1978). The amphibole composition has been reported in the Marocan Proterozoic dolerites (Hafid, 1992, P.120). Other types of classification suggest the brownish amphiboles formed ealier and is of ferro- edenite composition (Hafid, 1992, P.121) of pargasite (Pons, 1982, P.163, Pemberton and Offler, 1985, P 593) or of pargasitic hornblende (Fabries et al., 1984, P.731). The diagram Ti versus Si of Leake, (1965) (Fig.6) is not in conformity with the grouping of the amphibole into igneous brownish to the secondary or " metamorphic " greenish types. It seems that the color distinction of these two groups of amphiboles, reflects their chemical composition and the thermal condition of magmatic crystallization rather than a difference of metamorphic grade. All the amphiboles may be of magmatic to hydrothermal origin (Fonteilles et Muffat, 1970, P.557) The crystallization of two groups of amphiboles, implies

the presence in the residual liquids of abundant water (Pons, 1982, P.217) or deuteric fluids (Fonteilles et Muffat, 1970, P.557) permitting for continuous retrograde reactions. The distribution of Mg and Fe in these various types of amphiboles as manifested by the individual body, suggests a negative correlation between these elements (Fig.7). The behavior of these two elements in the amphiboles, is due to a ferro-magnesian substitution during magmatic cooling (Hafid, 1992, P.128).

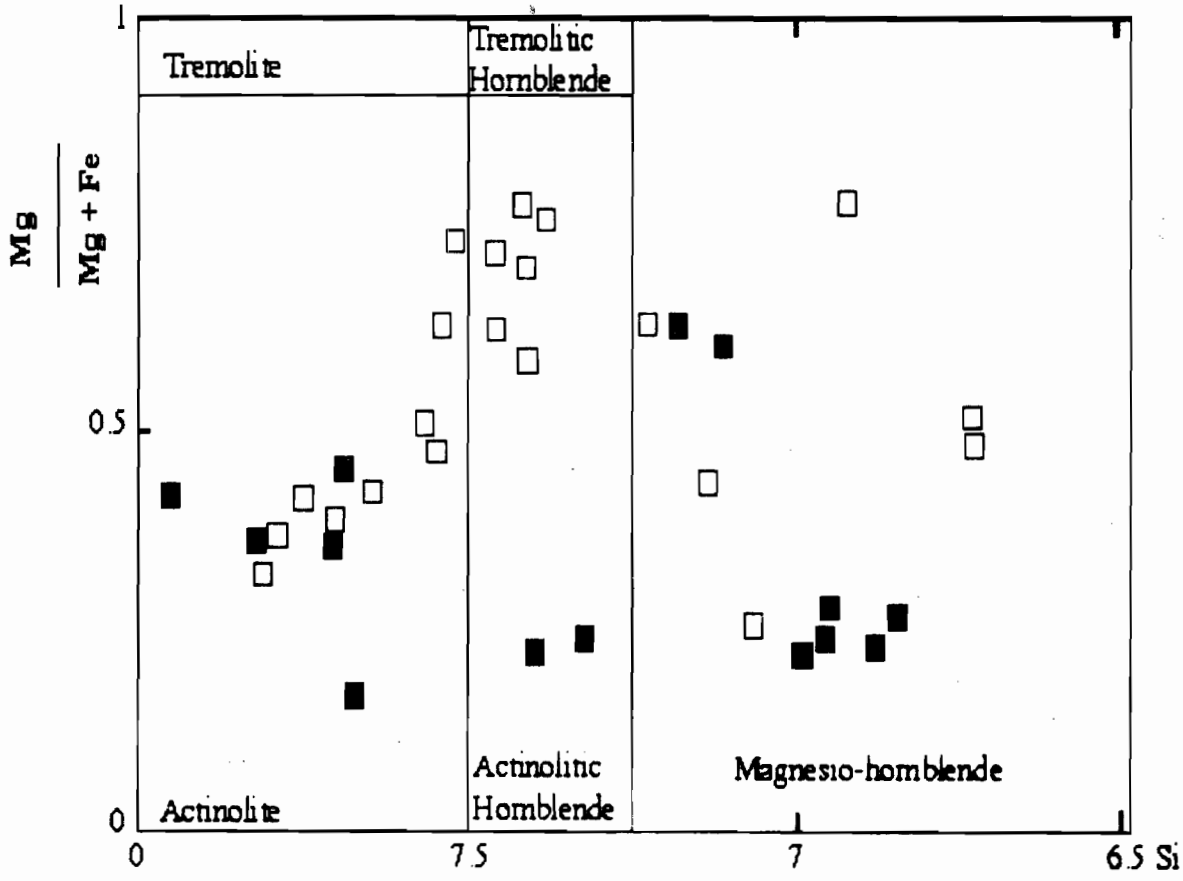

Figure 5. Classification diagram after Leake, (1978) showing various composition of amphiboles in the main facies of Boussouma dyke. Empty square : amphibole of dolerites., full square : amphibole of gabbros and pegmatites.

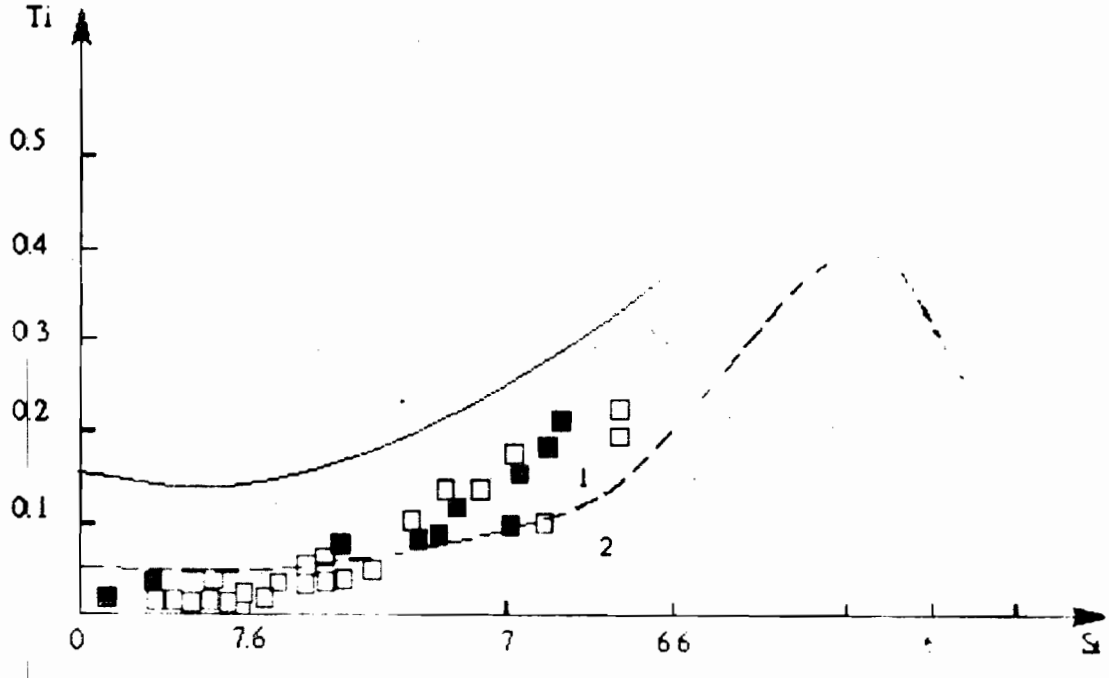

Figure 6: Plot in Ti- Si diagram (Leake, 1965) of amphiboles composition, pointing to igneous and metamorphic origin. 1. Magmatic amphiboles field ; 2. "Metamorphic amphibole" field. Same legend as figure 5.

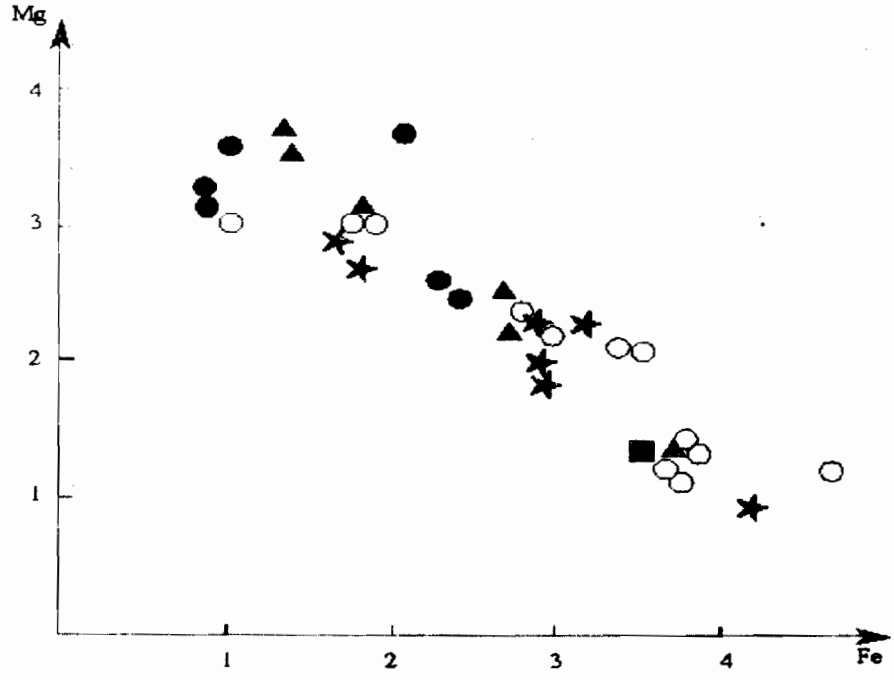

Figure 7: Chemical covariation of Mg versus Fe in amphibole minerals in the main facies of Boussouma dyke. Full circle : amphiboles of chilled dolerite ; full star : amphiboles of fine grained dolerite ; full triangle : amphiboles of medium- grained dolerite ; full square: amphiboles of gabbros ; empty circle : amphiboles of pegmatites.

Micas

Ti-rich biotite (3.5 to 4.5% TiO_2) (Table 11) in this dyke is a minor constituent showing lepidomelane composition (Fig.8). It partially replaces or pseudomorphoses with secondary iron oxide exsolution (Fig.2-8), actinolite or actinolitic hornblende minerals. Symplectitic intergrowth between biotite, opaques and amphiboles are frequent in the majority of the facies. In the sequence of retrograde transformation of the amphibole minerals, which is accompanied by systematic iron oxide exsoluion, biotite appears belatedly in the following mineral reactions: magnesio-hornblende → actinolitic- hornblende→ actinolite→ biotite→ chlorite. The cryptocrystalline chlorite which enhances intersertal texture of more altered gabbro and dolerite, is identified as brunsvigite (Hey, 1954) (Fig.9) (Table 11). The coexistence of lamellar brown biotite and brown amphibole suggests a late magmatic crystallization of these micas under moderately high temperature conditions and hydrostatic pressure (Ama Salah, 1991, PP.204-211, Azambre et al., 1987, P.392, Fabries and al., 1984, P.731, Cadman and al., 1990., P.18, Pemberton and Offler, 1985, P.596, Airo, 1999, PP.897-899).

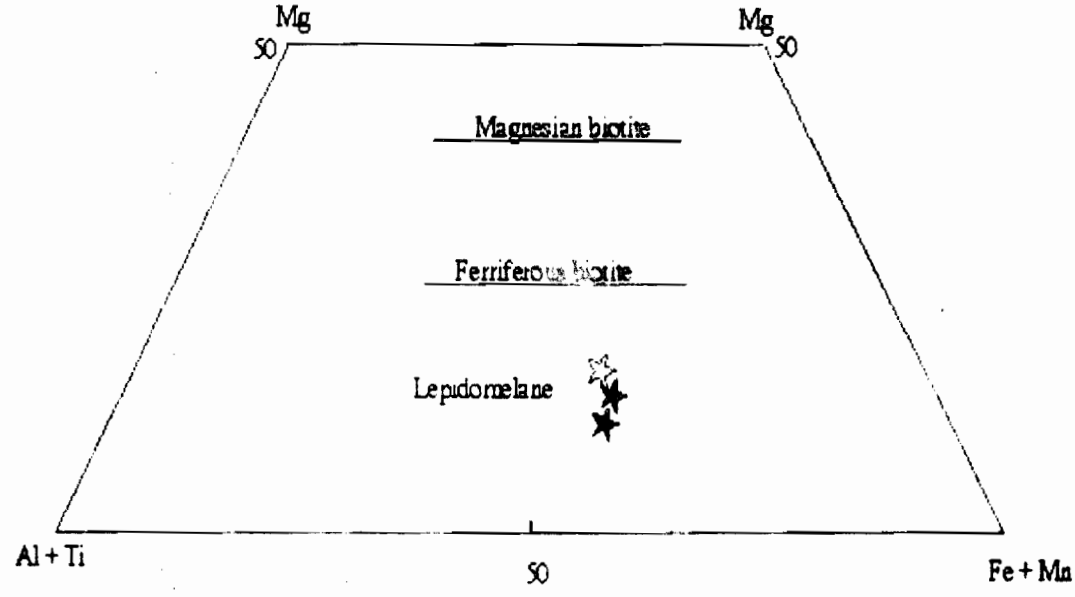

Figure 8: Lepidomelane composition of biotites plotted in Foster (1960) micas classification diagram. Full star : medium grained dolerite , empty star : pegmatites.

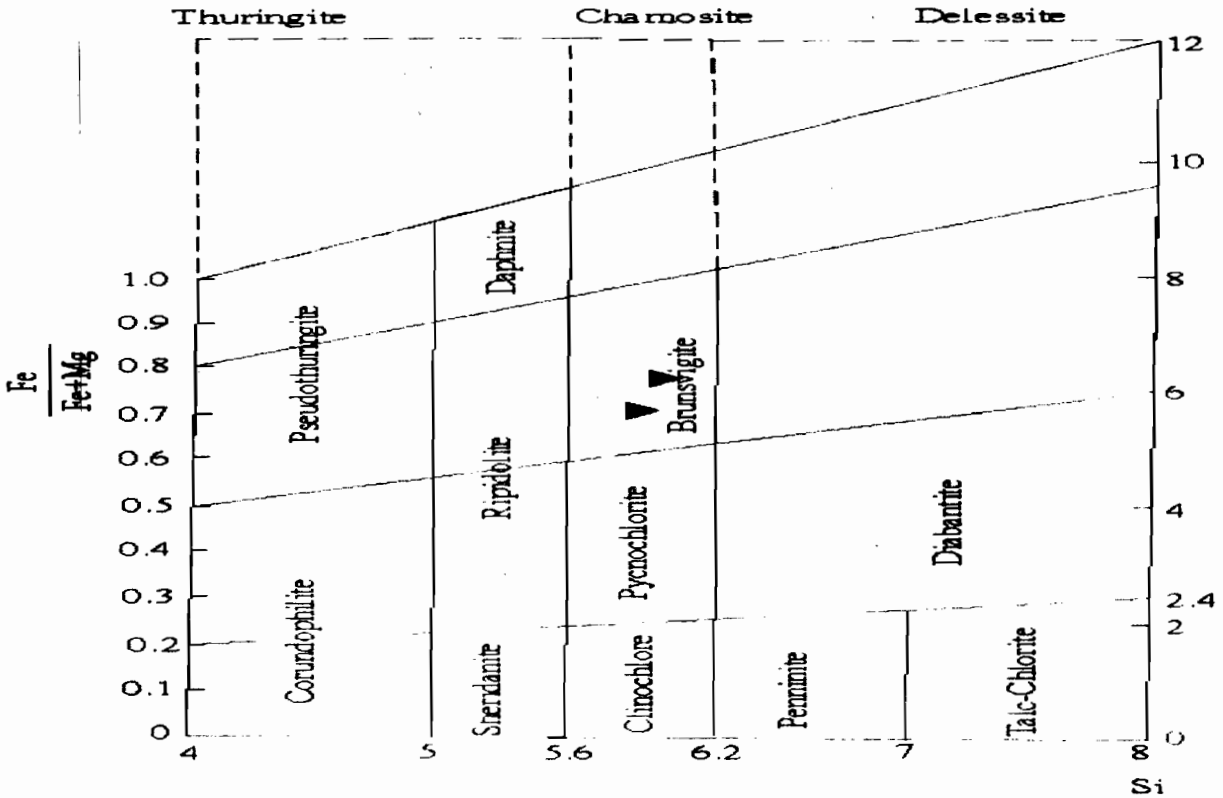

Figure 9: Brunsvigite composition of chlorites from pegmatite samples in the (Fe/Fe +Mg)-Si diagram (Hey, 1954).

Post magmatic hydrothermal minerals

The action of the hydrothermal fluids in the plastic strain rocks (undulating quartz, flexure of pyroxenes, mechanical twinnings of plagioclase) or the cracked or cataclastic bodies, consequently generates a neo-formation of a wide spectrum of dominant hydrous and subordinate anhydrous minerals. The cracks of primary minerals of some microfractured rocks serve as preferential drains for the circulation of fluids (Azambre et al., 1987, P.380). In the dyke, these bodies display perthitic and sericitic microtextures of plagioclase suggesting a formation during intense alteration; biotite flakes, epidote, carbonate, chlorite as filling the cracks of pyroxenes or amphiboles, actinolite in those of plagioclases are products of hydrothermal origin. Olivine is partially replaced by an aggregate of serpentine and chlorite or pseudomorphosed into serpentine and small brown hornblende. Talc is less frequent in the alteration products of tremolite/actinolite The skeletal or grid iron oxides are formed at the expense of leucoxene

Petrogenetic interpretation

The use of the composition of clinopyroxene phenocrysts to characterize the magmas affinities and the geotectonic settings of recent volcanic or paleovolcanic series, was introduced with previous works of Letterrier and al. (1982, P.140) and of Molard et al. (1983 P 903). Plots of the compositions of clinopyroxene extended from the dolerites and gabbros/pegmatites in Al versus Si diagram (Fig 10) show their non- alkaline affinity

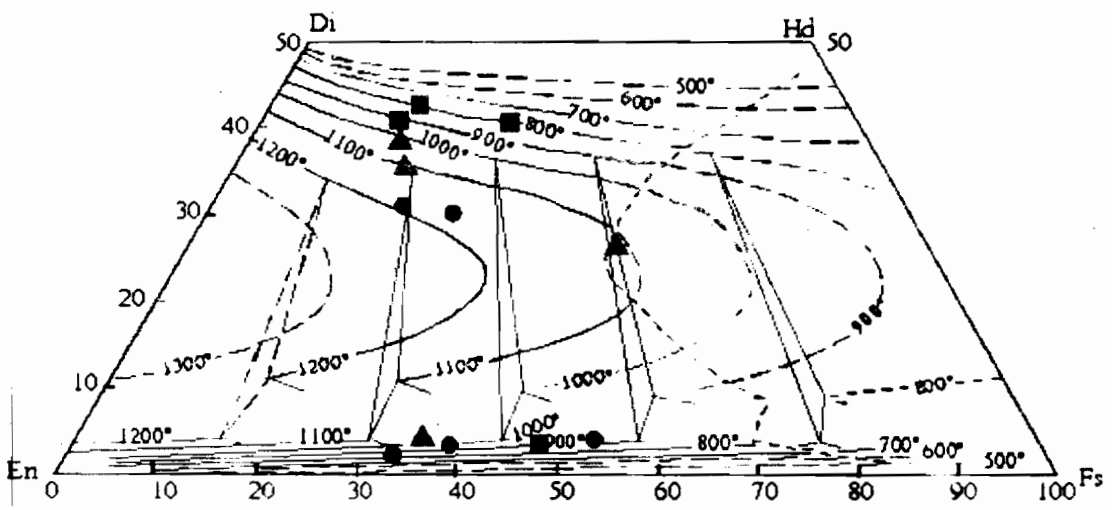

Figure 10: Alt versus Si diagram (Kushiro, 1960) showing non alkaline composition of clinopyroxene in the Boussouma dyke. Full triangle : dolerite; empty triangle : gabbros and pegmatites.

Those of dolerites are mainly tholeiitic basalt in composition (Fig.11), while clinopyroxenes of coarse - grained gabbro, plotted in calc- alkaline but remain nevertheless in the statistical overlap field of tholeiites. The over all mineralogical characteristics of the dyke attests to its tholeiitic affinity, especially due to the presence of ferriferous olivine (Ama Salah, 1991, P.195), augite, hypersthene, calcic- plagioclase, iron oxides, quartz and micropegmatite (Vicat et Pouclet, 1995, P.358, Fonteilles et Muffat, 1970, P.568, Ama Salah,1991, P.194, Fodor and al., 1972, Poidevin, 1977, P.1253). Geochemical data support the tholeiitic affinity of this dyke (Wenmenga, 1986, P.267) The coexistence of augite and orthopyroxene led to the application of Lindsley (1983, P.487) geothermometer under one atmosphere conditions in order to estimate the temperature of crystallization. This has been estimated between 1000 to 1150°C in the fine and medium grained dolerite and between 800 to 900°C in the rapid cooled chilled dolerites (Fig.12).

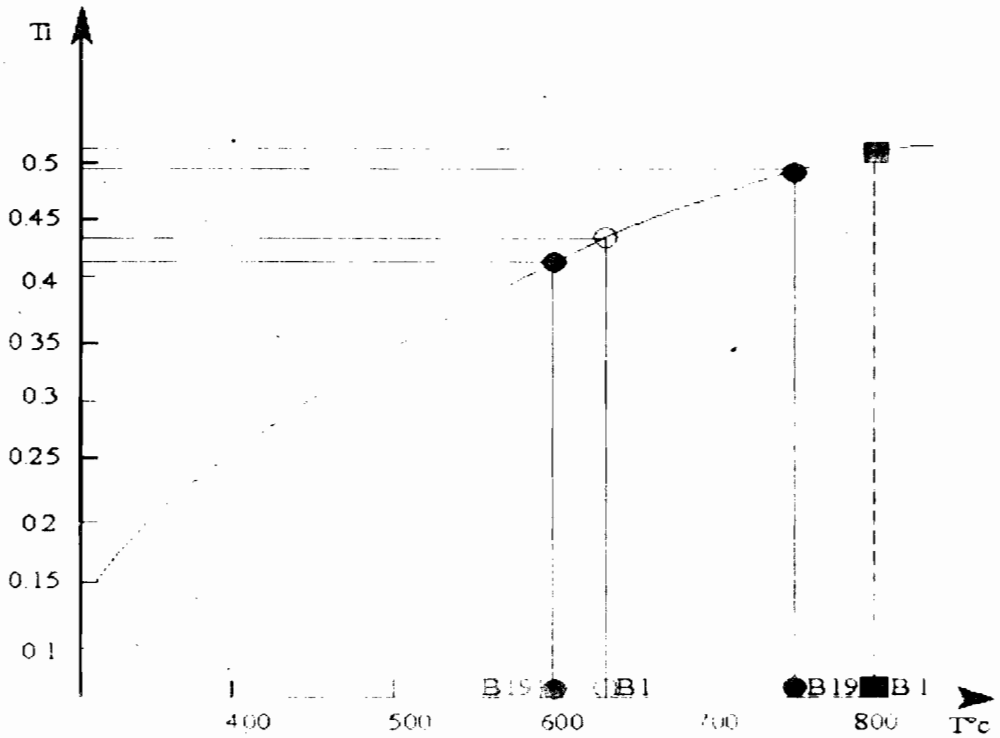

Figure 11: Discrimination diagram using Ti versus Alt composition of clinopyroxene (Leterrier and al 1982) showing dominant tholeiitic affinity of dolerites and calc-alkaline affinity of gabbros. Same legend as figure 10

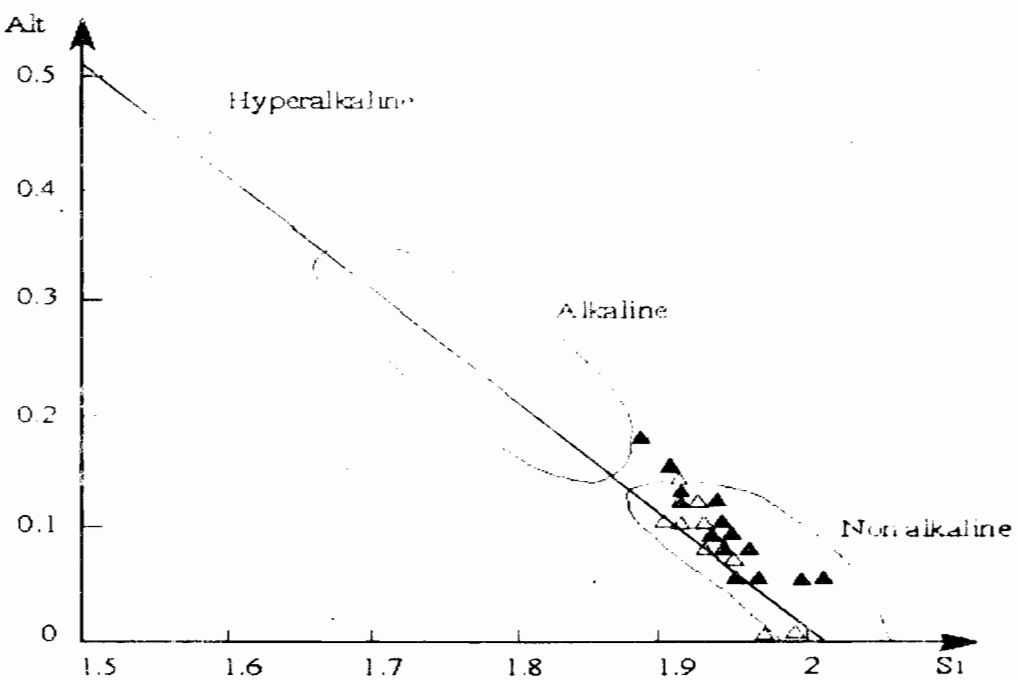

Figure 12: Coexisting augite- orthopyroxene thermometry using Di- En- Hd- Fs quadrilateral of Lindsley (1983) Full square : chilled dolerite ; full triangle and full circle : medium grained dolerite.

Similar results on the geothermometry of coexistent augite and pigeonite yielded similar temperatures between 1100° to 1150°C in Triassic dolerites (Azambre et al.,1987, P.388), 1100° to 1000°C in some Proterozoic dykes (Sutcliffe, 1989, P.71) and 900 to 1100°C in Tertiary dolerites of the south- west Greenland (Hall and al., 1988, P.705) and 900 to 1000° C in Paleozoic basaltic lavas (Pemberton and Offler, 1985, P.598). The crystallization temperature of biotite using Le Bell (1979) thermometry (Fig.13) is estimated between 600 and 750°C in the medium grained dolerites and approximately 800°C in the pegmatites. This range of temperature indicates a late magmatic crystallization of biotite. In the Sirba valley dolerite close to western Niger, Ama Salah, (1991, P.211) using the same geothermometer, obtained similar temperatures (580 to 780°C) from biotite and as well as ilmenite and titano-magnetite geothermometers. A large majority of clinopyroxenes composition representing the various bodies of the dyke, plotted in the anorogenic basalts field (Fig.14) related to crustal distension zones. The Boussouma dyke displays the same geotectonic setting as the Sirba dolerite dyke (Ama Salah, 1991, PP.204-218). Both could belong to the same distension and basic magmatic cycle, emplaced during Mesoproterozoic period (Ama Salah, 1991, P. 224) in west Africa.

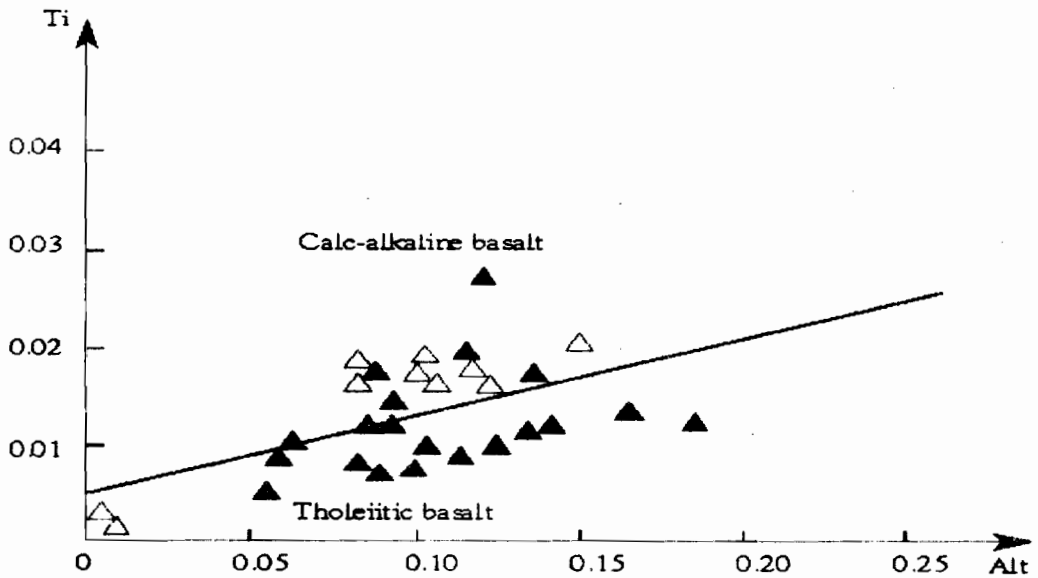

Figure 13 Crystallization temperature estimation of biotite in the basic rocks of the dyke after Le Bell, (1979). Full circle and empty circle : medium grained dolerite (B1, B19); full square : pegmatites (B'1).

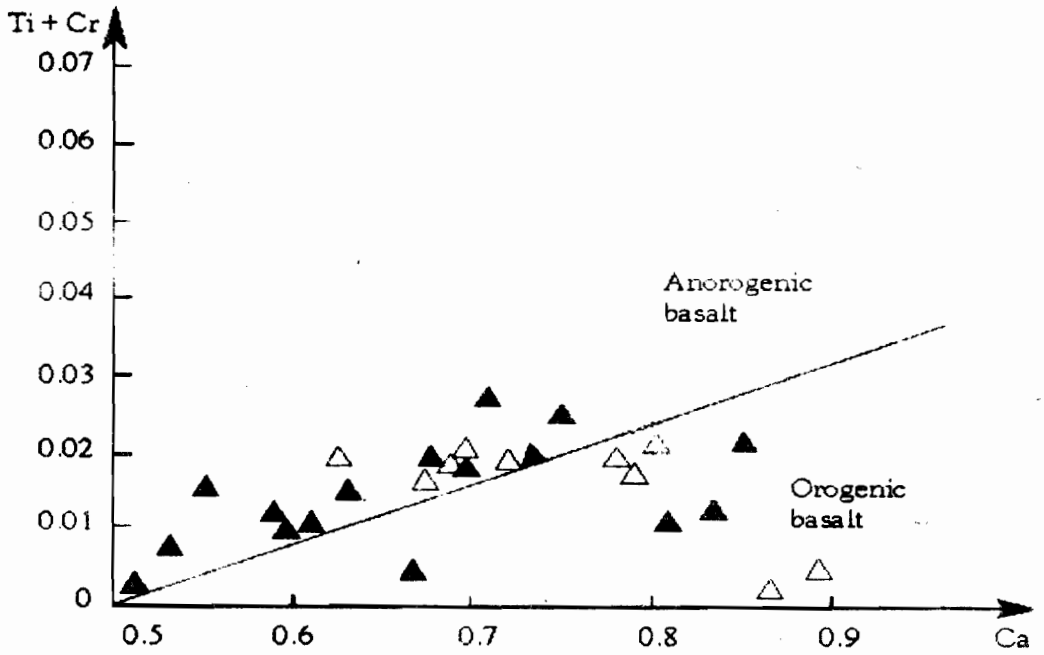

Figure 14: Clinopyroxene composition of representative rocks of Boussouma dyke, straddling the boundary between extensional and orogenic field (Leterrier and al., 1982) and showing nevertheless predominant anorogenic basalt affinity.

DISCUSSION

Boussouma dyke results from the crystallization of a tholeiitic magma saturated in water during the cooling process, which explains the constant coexistence of various anhydrous and hydrous minerals in the three main bodies of this intrusion. Silica saturation of the parental magma supports the persistence of quartz in all bodies even in olivine- bearing dolerite and gabbro. The increase in quartz content with the corresponding enrichment of Fe- clinopyroxenes and of Fe-Ti opaques from the margin to the centre of the dyke, are compatible with the process of magmatic fractionation. Major elements composition of pyroxenes is in support of the tholeiitic affinity and emplacement of the dyke in a non-orogenic setting along regional fractures. Crystallization temperatures of the melt using two pyroxenes geothermometer (1000-1150°C) corresponds to that of basaltic magmas. Temperatures provided by the biotite composition and geothermometer (750-600°C), could represent those of the final magmatic crystallization stage. Such thermal conditions of crystallization have been reported in Mesoproterozoic dolerites in Niger Republic, which are similar to Boussouma dyke in mineralogical and geochemical composition as well as in their geotectonic setting.

CONCLUSION

Field, macroscopic and microscopic observations supported by qualitative microprobe analysis have led to the identification of a petrographic suite with regular and continuous grain variation, from the margin to the core within the Boussouma dolerite dyke. This textural variation is interpreted as a result of various cooling rates and consequently to magmatic differentiation at the scale of the dyke. This cooling remained slow as expressed by the development of coronas texture in the chilled bodies. The increase of quartz and micropegmatite content and that of Fe-Ti oxides from the earlier phases (chilled dolerite, dolerite (ss), gabbro) to the evolved phases (Pegmatites), is attributed to a magmatic fractionation process. The Fe-rich composition of olivine and augite and the enrichment in ilmenite and quartz of the residual liquid are typical of tholeiitic magmas. The tholeiitic affinity related to the emplacement of the dyke in an anorogenic setting and crustal distension is further confirmed by major and minor elements composition of the clinopyroxenes and their hosted rocks. Enrichment influids of the residual liquid, generates important vapour pressure favourable to hydrated minerals crystallization as brownish to greenish hornblende and brown biotite. Two pyroxenes geothermometer indicates early temperature of magma crystallization ranging from 1000 to 1150°C and about 600 and 800°C during magmatic cooling as revealed by biotite thermometry. The excess hydrothermal fluids drawn by cracks within the magmatic mineral phases led to the formation of altered bodies in the dyke.

ACKNOWLEDGEMENTS

The authors are grateful to Michele VESCHAMBRE of the Laboratory " Magmas et Volcans " of Clermont Ferrand/France for providing graciously, microprobe analysis.

REFERENCES

Airo, M-L., 1999. Magnetic and compositional variations in Proterozoic mafic dykes in Finland, northern Fennoscandian shield. Canadian Journal of Earth Sciences, 36:891-903.

Ama Salah, I., 1991. Pétrographie et relation structurales des formations métavolcaniques et sédimentaires du Birimien du Niger occidental. Problème de l'accrétion crustale au Protérozoïque inférieur. Thèse, Université d'Orléans, Orléans, France 231 PP.

Azambre, B., Rossy, M. et Lago, M., 1987. Caractéristiques pétrologiques des dolérites tholéiitiques d'âge Triasique (ophites) du domaine pyrénéen. Bulletin de Minéralogie 110 : 379-396.

Bertrand, H., 1987. Le magmatisme tholeiitique continental de la marge ibérique, précurseur de l'ouverture de l'Atlantique central. Les dolérites du dyke de Messejana- Plasencia (Portugal-Espagne). Comptes Rendus Académiques des Sciences de Paris 304 (II, 6) : 215-220

Bickford, M.E., 1963. Petrology and structure of layered gabbro, Pleasant Bay, Maine. Journal of Geology 71 (2): 215-237.

Botha, B. J. V and Hodgson, F. D. I., 1976. Karoo dolerites in Northwestern Damaraland. Transactions Geological Society of South Africa 79: 186-190.

Cadman, A., Tarney, J and Park, R.G., 1990. Intrusion and crystallization features in Proterozoic dyke swarms In parker, Rickwood Tucker (Editors), Mafic dykes and emplacement mechanism. Balkema, Rotterdam PP.325-334.

Castaing, C., Billa, M , Milesi, J.P., Thieblemont, D., Le Metour, J., Egal, E., Donzeau, M., Guerrot, C., Cocherie, A., Chevremont, P , Tegyey, M., Itard, Y., Zida, B., Ouedraogo, I , Kote, S., Kabore, B.E., Ouedraogo, C., Ki, J.C et Zunino, C., 2003. Notice explicative de la carte géologique et minière du Burkina Faso à 1/1. 000.000. Projet "SYSMIN" n°7 ACP.BK 074UE, 3e édition, 134 PP.

El Aouli, E. H., Gasquet, D et Ikenne, M., 2001. Le magmatisme basique de la boutonnière d'Igherm (Anti- Atlas occidental Maroc) un jalon des distensions néoprotérozoiques sur la bordure nord du craton Ouest- Africain. Bulletin de la Société Géologique de France 172 (3) 309-317.

Fabries, J., Conquere, F and Arnaud, G., 1984. The mafic silicates in the Saint Quay- Portrieux gabbro-diorite intrusion crystallization conditions of a calc-alkaline pluton.. Bulletin de Minéralogie 107: 715-736

Fodor, R.V., Keil, K. and Bunch, T.E., 1975. Contribution to the mineral chemistry of Hawaiian rocks. Contribution to Mineralogy and Petrology 50: 173-195.

Fonteilles, M. et Muffat, S., 1970. Etude pétrographique de deux dolérites (ophites) à pigeonite et olivine des pyrenées occidentales. Bulletin de la Société Française de Minéralogie et de Cristallographie 93 : 555-570.

Foster, M.D., 1960. Interpretation of the composition of trioctahedral micas. Geological Survey Professional Paper 354B: 11-49.

Gamsonré, P.E., 1975. Contribution à l'étude géologique des formations précambriennes de la région de Ouahigouya (Haute Volta). Thèse, Doctorat es sciences, Université de Besançon, Besançon, France, 181 PP.

Hafid, M.A., 1992. Granites et dolérites protérozoïques de la boutonnière d'Irhem (Anti Atlas Occidental, Maroc) Pétrologie, géochimie et signification géodynamique. Thèse, Université Paris VI, Paris, France , 234 pp.

Hall, R.P.; Hughes, D.J.and Joyner, L., 1988. Complex pyroxene assemblages of Proterozoic dolerites, SE Greenland. Mineralogical Magazine 52: 703-705.

Hey, H., 1954. A new review of chlorites. Mineralogical Magazine 30: 277-292.

Kushiro, I., 1960. Si- Al relation in clinopyroxene from igneous rocks. American Journal of Sciences 258: 548-554.

Leake, B.E., 1965. The relation between tetrahedral aluminium and the maximum possible octahedral aluminium in natural calciferous amphiboles. American Mineralogists 50: 843-851.

Leake, B. E., 1978. Nomenclature of amphiboles. Canadian Mineralogist. 16: 501-520

Le Bell, L., 1979. Hydrothermal and magmatic micas within Cerrover de Santa Rosa, Perou Porphyry copper. Bulletin de Minéralogie 102: 35.41.

Leterrier, J., Maury, R.C., Thonon, P., Girard, D. and Marchal, M., 1982. Clinopyroxene composition as a method of identification of magmatic affinities of paleo- volcanic series. Earth and Planetary Sciences Letters 59: 139-154.

Lindsley, D.H., 1983. Pyroxene thermometry. American Mineralogist 68: 477-493.

Machairas, G., 1975. Le cuivre natif et les sulfures dans certaines dolérites. Bulletin de la Société française de Minéralogie et de Cristallographie 98 : 194-198

Molard, J. P., Maury, R. C., Leterrier, J. et Bourgeois, J., 1983. Teneurs en chrome et titane des clinopyroxènes calciques des basaltes: Application a l'identification des affinités magmatiques de roches paléovolcaniques. Comptes Rendus Académiques des Sciences de Paris 296 (II) : 903-908.

Mongkoltip, P. and Ashworth, J.R., 1983. Quantitative estimation of an open system symplectite forming reaction: Restricted diffusion of Al and Si in coronas around olivine. Journal of Petrology 54-(4): 635-661.

Napon, S., 1988. Le gisement d'amas sulfuré (Zn, Ag) de Perkoa dans la province du Sangyé/ Burkina Faso-Afrique de l'Ouest/ Cartographie- Etude Pétrographique, Géochimique et Métallogénique. Thèse, Université- Franche comté, Besançon, France, 275P.

Paterson, Grant et Watson Ltd., 1985. Interprétation du levé magnétique et du levé radiométrique du rayon Gamma, région d'Autorité du Liptako Gourma, Afrique Occidentale BUMIGE B Rapp. A.C.D.I (I) 377 pp.

Pemberton, J. W. and Offler, R., 1985. Significance of Clinopyroxene compositions from the Cudgegong volcanics and Toolamanang volcanics; Cudgegong- Mudgee district, NSW Australia. Mineralogical Magazine 49: 591-599.

Poidevin, J. L., 1977. Mise en évidence d'une série de tholeiites à pigeonite dans le Précambrien supérieur de la république centrafricaine. Relation avec la tectonique. Comptes Rendus Académiques des Sciences de Paris 284 : 1251-1254.

Poldervaart, A. and Hess, H.H., 1951. Pyroxenes in the crystallization of basaltic magma Journal of Geology 59: 472-489.

Pons, J., 1982. Un modèle d'évolution de complexes plutoniques: Gabbros et granitoïdes de la Sierra Morena occidentale (Espagne). Thèse, Doctorat es sciences, université Paul Sabatier, Toulouse, France, 451 PP.

Potdevin, J-L., Goffette, O. et Santallier, D., 1994. Les différences minéralogiques, chimiques et texturales entre cœur et bordures du filon de diabase de la Grande commune (Massif de Rocroi, Ardenne) des marqueurs d'un épisode d'infiltration par un fluide à CO_2 et H_2O lors d'un métamorphisme varisque synschisteux en faciès schiste vert. Bulletin de la Société géologique de France 165 (3) : 249-260

Rathna, K., Vijaya Kumar K and Ratnakar, J 2000 Petrology of the dykes of Ravipadu, Prakasam province, Andhra Pradesh, India Journal Geological Society of India 55 399-412

Reid, D.L., 1990. The Cape Peninsula dolerite dyke swarm, South Africa., In Parker, Rickwood and Tucker (Editors). Mafic dykes and emplacement mechanism, Balkema, Rotterdam.: pp. 325-334.

Reynolds, I. M., 1983. The iron- titanium oxide mineralogy of Karoo dolerite in the Eastern Cape and Southern Orange free state. Transactions Geological Society of South Africa 86: 211-220.

Rivers, T. and Mengel, F.C., 1988. Contrasting assemblages and petrogenetic evolution of corona and non corona gabbros in the Greenville province of Western Labrador. Canadian Journal of Earth Sciences 25: 1629-1648.

Ross, M. E., 1983. Chemical and mineralogic variations within four dikes of Columbia river basalt group, southeastern Columbia Plateau. Geological Society of America Bulletin 94: 1117-1126.

Ross, M. E., 1986. Flow differentiation, phenocryst alignement and compositional trends within a dolerite dike at rockport, Massachusetts. Geological Society of America Bulletin 97: 232-240.

Sawadogo, J., 1983.Etude géologique du sillon Birimien de Yalogo dans la région de Gangaol Nord de la Haute Volta. Thèse, 3e cycle, Université Franche Comté, France, 165 PP.

Somda, N.A., 1995. Etude pétrographique, géochimique et structurale des formations de Gose, au sein du Permis de recherche et d'exploitation minière d'Essakane (Sillon de Dori- Burkina Faso) Mémoire DGP, Université Blaise PASCAL, Clermont Ferrand, France, 95 PP.

Sutcliffe, R.H., 1989. Mineral variation in Proterozoic diabase sills and dykes at lake Nipigon, Ontario. Canadian Mineralogist. 27: 67-79.

Vicat, J.P. et Vellutini, P.J., 1987. Sur la nature et la signification des dolérites du Bassin Précambrien de Sembe- Ouesso (République du Congo). Precambrian Research 37 : 57-69.

Vicat, J.P. et Pouclet, A., 1995 : Nature du magmatisme lié à une extension pré- panafricaine. Les dolérites des bassins de Comba et de Sembe-Ouesso (Congo). Bulletin de la Société géologique de France 166, (4) : 355-364.

Wenmenga, U., 1986. Pétrologie des ensembles lithologiques du Protérozoïque Inférieur au Nord est de Ouagadougou (Burkina Faso, craton Ouest Africain). Etude pétrographique, géochimique et géochronologique. Thèse, Université Blaise PASCAL. Clermont Ferrand, France 275 P P.

GLOBAL JOURNAL OF GEOLOGICAL SCIENCES VOL. 6 NO. 2 2008: 175 - 183
 ISSN 1596 – 6798

BASINAL STRUCTURE OF YOLA ARM OF THE UPPER BENUE TROUGH NIGERIA; EVIDENCE FROM AEROMAGNETIC DATA

D. A. OBI, C. S. OKEREKE, U. E. EGEH, AND O. O. OLAGUNDOYE

(Received 12 May, 2008; Revision Accepted 29 September, 2008)

ABSTRACT

Aeromagnetic data interpretation of the Yola arm of the Upper Benue Trough has previously been carried out. However, no detail modeling of the Crustal Structures has been undertaken. Two composite reduced Aeromagnetic maps on a scale of 1:250,000 were digitized and processed using computer techniques. Analytical Signal, Power Spectrum and Upward Continuation methods were used prior to modeling of the subsurface structures. Forward and inverse modelings were done to determine the subsurface basin configuration. The result shows two sub-basins; the Lau and Yola sub-basins. The variations in sediment thickness within the Lau sub-basin is in the range of 2.0 – 4.5 km and in the Yola sub-basin 2.0 – 3.0 km respectively. The basin configurations from the modeled profiles depict that of horst and graben features resulting to variation in sediment thickness evident in Lau (Barwa to Yanga) subsector and Yola (Muleng) axis. The upward continuation revealed lineament trends in the NE-SW Yola (Muleng) axis and NW-SE Lau (Barwa to Yanga) subsector.

KEYWORDS: Upper Benue Trough, Basin configuration upward continuation, Analytical signal, power spectrum.

INTRODUCTION

The Yola Basin is located within the Upper Benue Trough and is part of the failed arm of a Cretaceous Triple Junction (Burke *and Dewey* 1973, Olade, 1975). The basin is closely associated with the separation of Africa from South America and the opening of the South Atlantic Ocean (Okereke and Ofoegbu, 1989, Wright, 1981).

The study area lies within latitudes 9° 00' – 10°00'N and longitudes 11°00' – 13°00'E and covers an area of about 260 sq km (Fig. 1). Earlier aeromagnetic study of the Yola Basin by previous workers such as Okereke and Ofoegbu 1989, Nur 2000 has been carried out for the mapping of lineament trends and depths to magnetic source. No detailed attempt on the modeling of the basin structure has been done.

Therefore, the main intent of this study is to use aeromagnetic data to model the structure of Yola Basin and estimate the sediment thickness overlying the basin floor. To accomplish this objective therefore, both qualitative and quantitative analysis were performed using 12 software programs in producing analytical signal, power spectrum and upward continuation subsurface maps (Ferdi and Santis 1977, Philips, 1987, Jacobsen 1987). The depth estimates obtained from the above methods aided the forward modeling of the subsurface basin configuration.

D. A. Obi, Department of Geology, University of Calabar, Cross River State, Nigeria.
C. S. Okereke, Department of Geology, University of Calabar, Cross River State, Nigeria.
U. E. Egeh, Department of Geology, University of Calabar, Cross River State, Nigeria.
O. O. Olagundoye, Total Exploration Energy, Nigerian Limited, Lagos Nigeria.

Fig. 1: Location map of the study area (modified from corridor, 2005)

GEOLOGY

The study area has mainly Upper Cretaceous Sediments that is overlying an ancient crystalline basement rocks (Fig. 2). The Cretaceous rocks cover about 90% of the study area and consist of the Bima formation which is Aptian-Albian in age. It is also the most widespread of all the formations, sitting directly on the magnetic basement rocks. Overlying the Bima Formation is the Yolde Formation, which consists of Calcareous beds interbeded with shalysandstones, found around Gatem and Gren areas. This bed is overlain by Dukul and Jessu Formation consisting of thick shales and sandstones.

The Numanha Formation is the topmost unit with massive deformation of shale deposits as a result of intense igneous activities (Granitoids) between Lau and Yola areas (Fig 2)

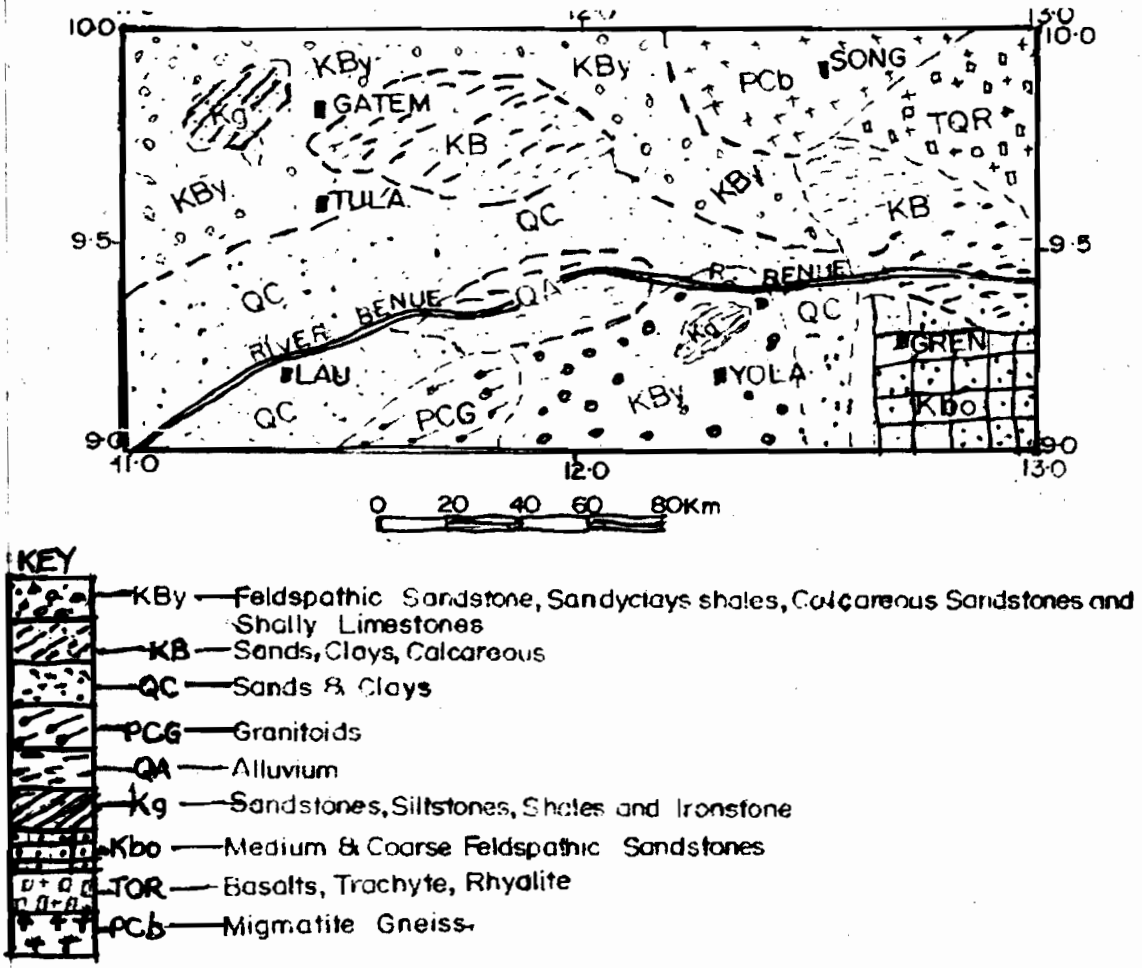

FIG. 2: Geologic Map of the study area. Modified from Geological Map of Nigeria. (1994).

DATA ANALYSIS

Two composite reduced one degree by one degree aeromagnetic total intensity field maps on a scale of 1:250,000 were acquired from the Geological Survey agency, Kaduna. The Survey was conducted along E-W profiles with a flight line spacing of 2.0 km and a tie line spacing of 20.0 km and a flight elevation of 0.5216km above sea level. The Geomagnetic gradient was removed using the International Geomagnetic Reference Field (I.G.R.F.) formula of first Janurary, 1974.

The first steps in the data analysis was to digitize the maps at 1.0 km interval to avoid the problem of frequency aliasing. This was followed by map merging directly without any continuation since both maps were flown at the same elevation above sea level. The following computer software programmes were used for this study P2GRD, MINC, Surfit, Addgrid, Jmerger, Contour, FFTFIL, Pdepth, Mfinite, Mf filter, Mf design and Saki. For a detail understanding of the applications of these programmes the interested reader should refer to United States Geological Services potential field version 2.2 software programmes.

The digitized data was gridded using the P2GRD and Minc programmes, the two grids were merged using Addgrid and Jmerger which does an arithmetic operation on point by point basis (Webring, 1985). The merged grided file is contoured to produce the total magnetic field intensity map of the study area (Fig. 3). Regional and Redidual anomaly separation was performed using the surfit software and the residual anomaly field used for further modeling of the subsurface structures (Fig 4). Upwards continuation was performed using the Fast Fourier Transformation software "FFTFIL" with a view to studying the subsurface deep fracture trends (Jacobsen 1987, Dobrin and Savit 1988, Naidu, 1970) (Fig. 5). Power Spectrum depth to the source determination from magnetic anomaly was performed using the software Mfinite; Mfdesign and Mffilter (Philips 1997, Hahn *et al.*, 1976, Nwogbo *et al.*, 1991), which by extension relates to the sediment thickness overlying the basin floor. The data was subjected to 0.25° by 0.25° grids at overlapping positions to generate over thirty five (35) depth points whose positions were digitized and contoured to show the sediment thickness variation within the study area (Fig. 6). The analytical signal technique was employed using the Pdepth software. This was done by taking four (4) profiles along prominent anomalous bodies seen on the residual map (Fig. 4), and the modeled profile digitized and contoured as analytical signal depth map (Fig 7). The result of the analytical signal computed depths was used to constrain the "Pdepth and Saki" forward and inverse modeling (Webring 1985, Nabighian 1972 and Shuey, 1972).

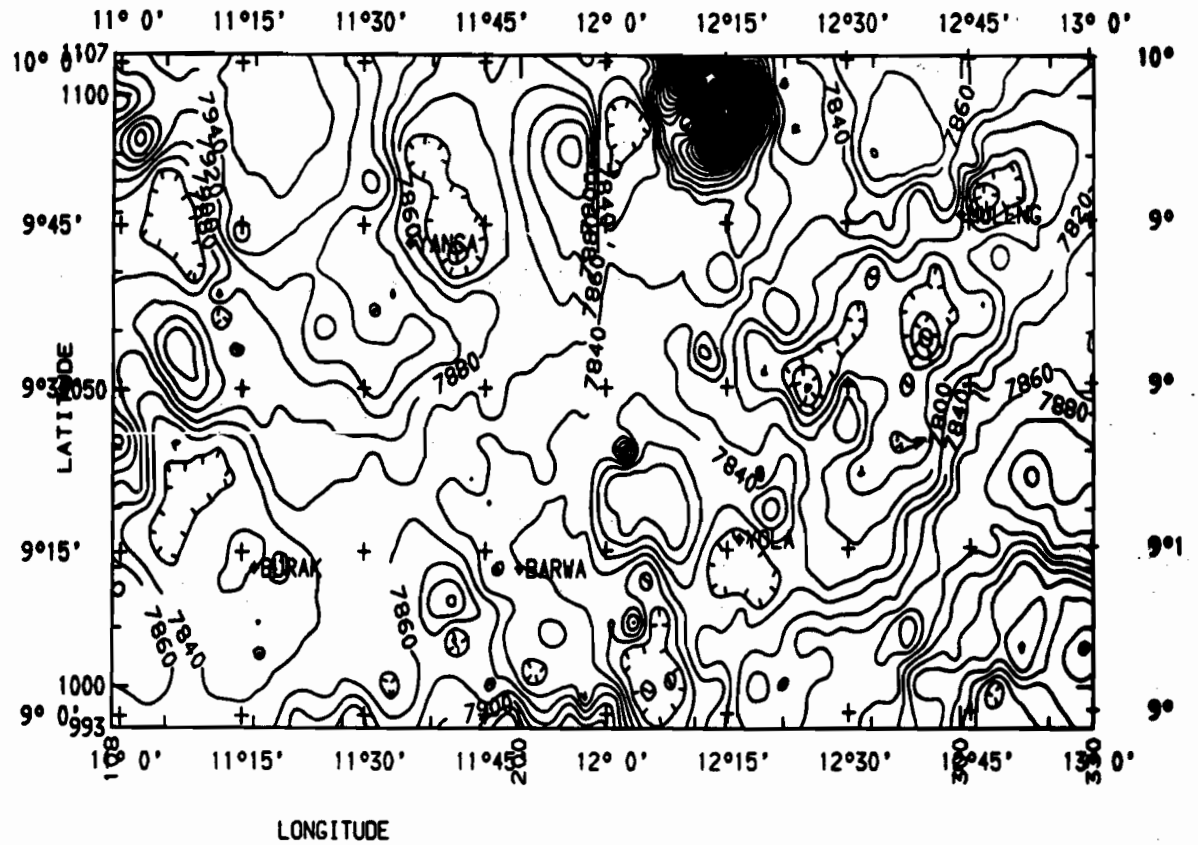

Fig. 3: Total Magnetic Field Intensity of Yola Basin (Contour Interval: 20nT).

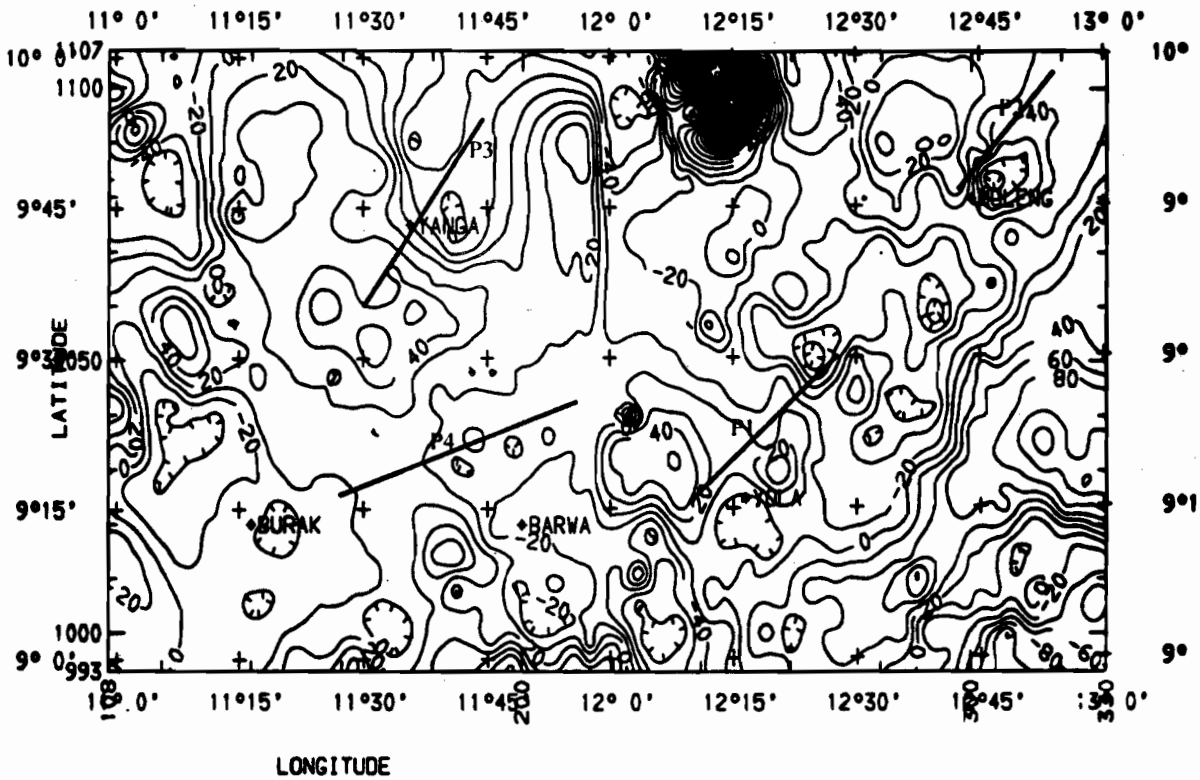

Fig. 4: Polynomial Residual Map of Yola Basin (Contour Interval: 20nT)

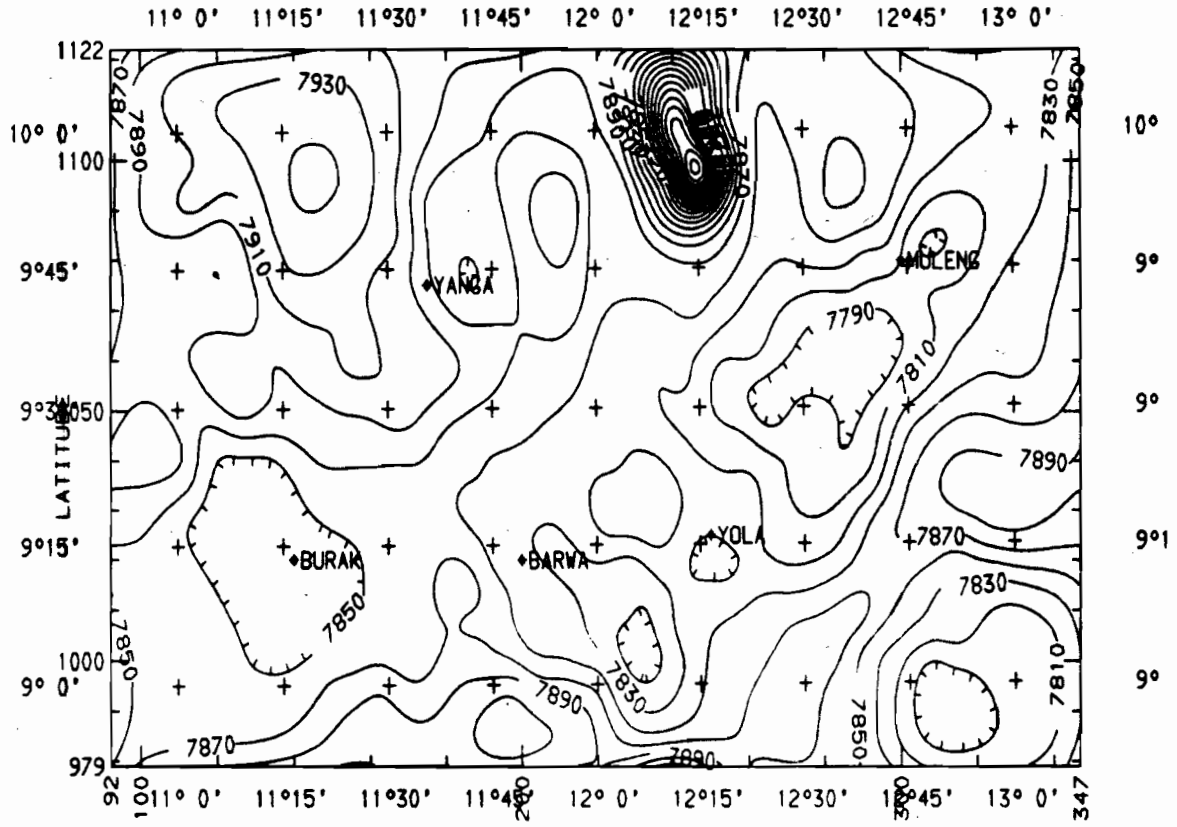

Fig. 5: Upward Continuation Map at 4 0km of Yola Basin Basin (Contour Interval: 20nT)

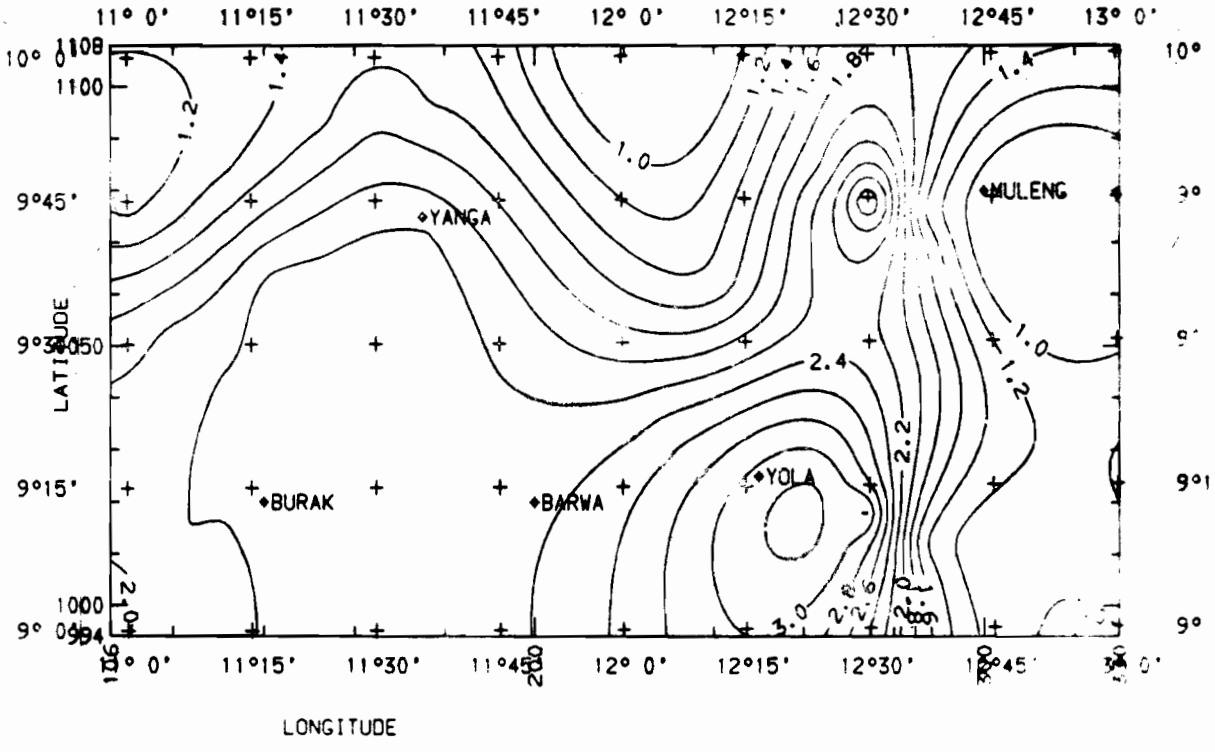

Fig. 6: Spectral Analysis Depth Map of Yola Basin Basin (Contour Interval: 1km)

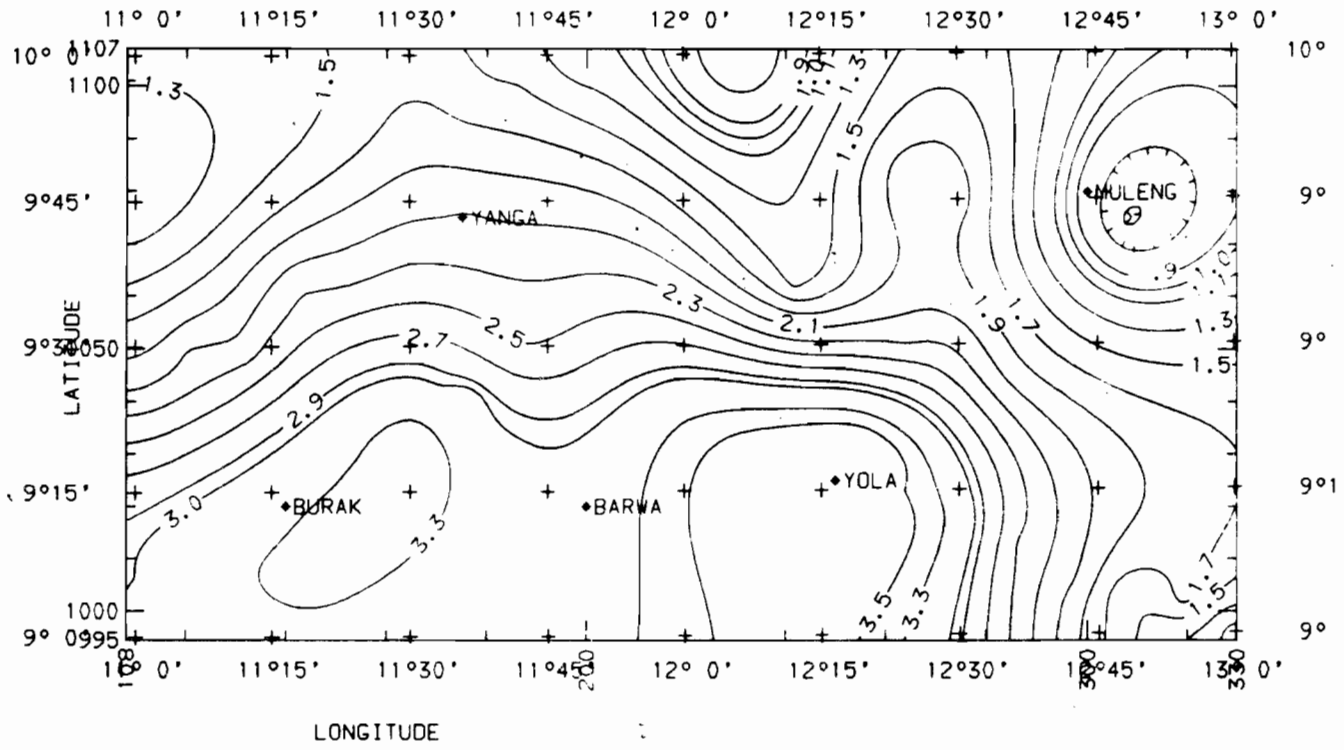

Fig. 7: Analytical Signal Depth Map of Yola Basin Basin (Contour Interval: 0.2km).

The modeled profiles (Fig. 8a-d) were generated using the software Pdepth, Saki and IGRFPT. The following modeling parameters as inclination = 4°, declination = 4°, and total field = 33541 60nT were generated using the IGRFPT software. While susceptibilities of intrusive = 0.012, sediments = 0.000005, and basement rocks = 0.001 – 0.0003 are basic S I units (Dobrin and Savit 1988). The above parameters gave a good fit between the calculated and the observed fields with low root mean square error of <1.0%

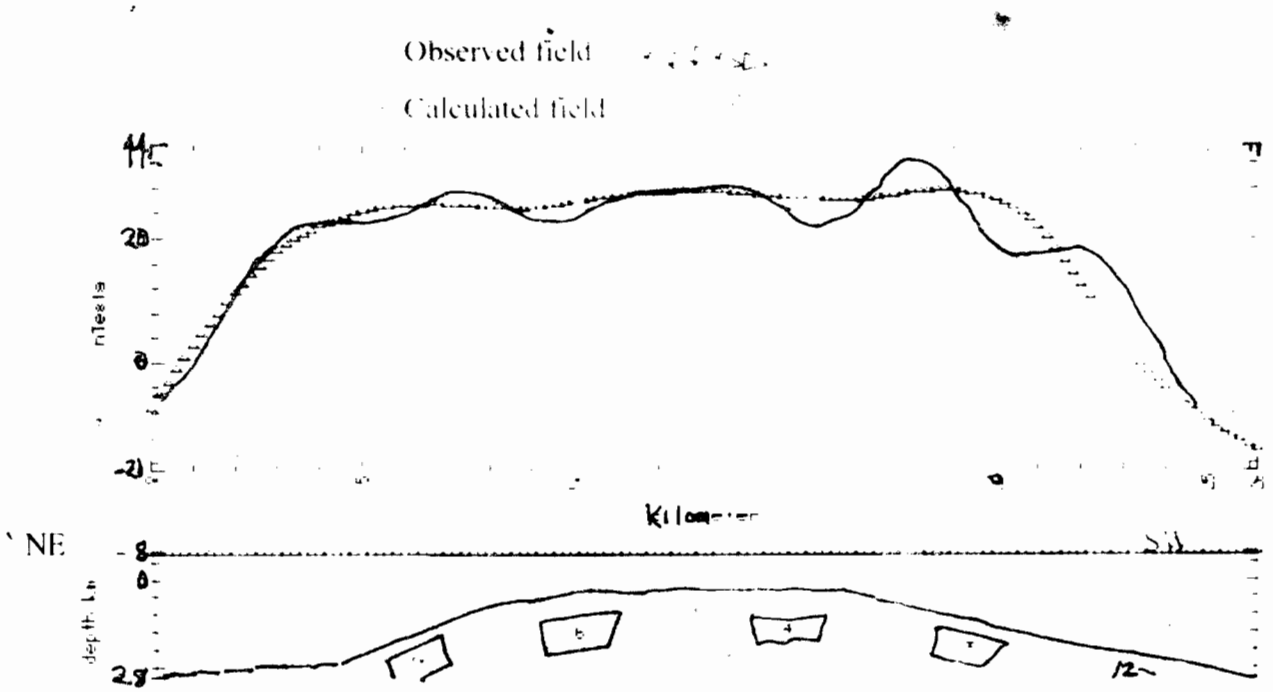

Fig 8a: Legend: 1 Sedimentary Rocks
2, 3, 6, 7 Basement rocks magnetics
4, 5 Intrabasement Intrusive

2.5D Modelled profile 1 along Yola Sub-sector

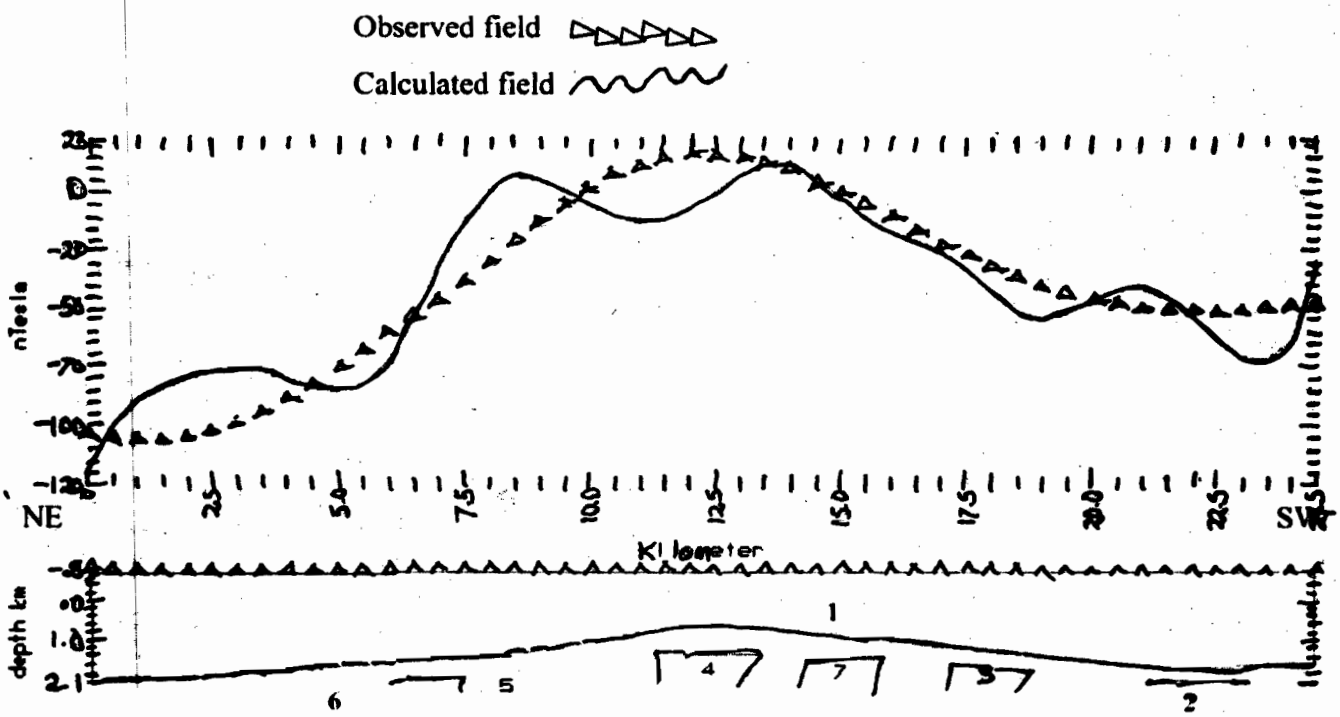

Fig 8b

Legend: 1= Sedimentary Rocks
2, 3, 5, 6, 8 = basement rocks magnetics
4, 7 = Intrabasement Intrusive

2.5D Modelled profile 2 along Yola (Muleng)

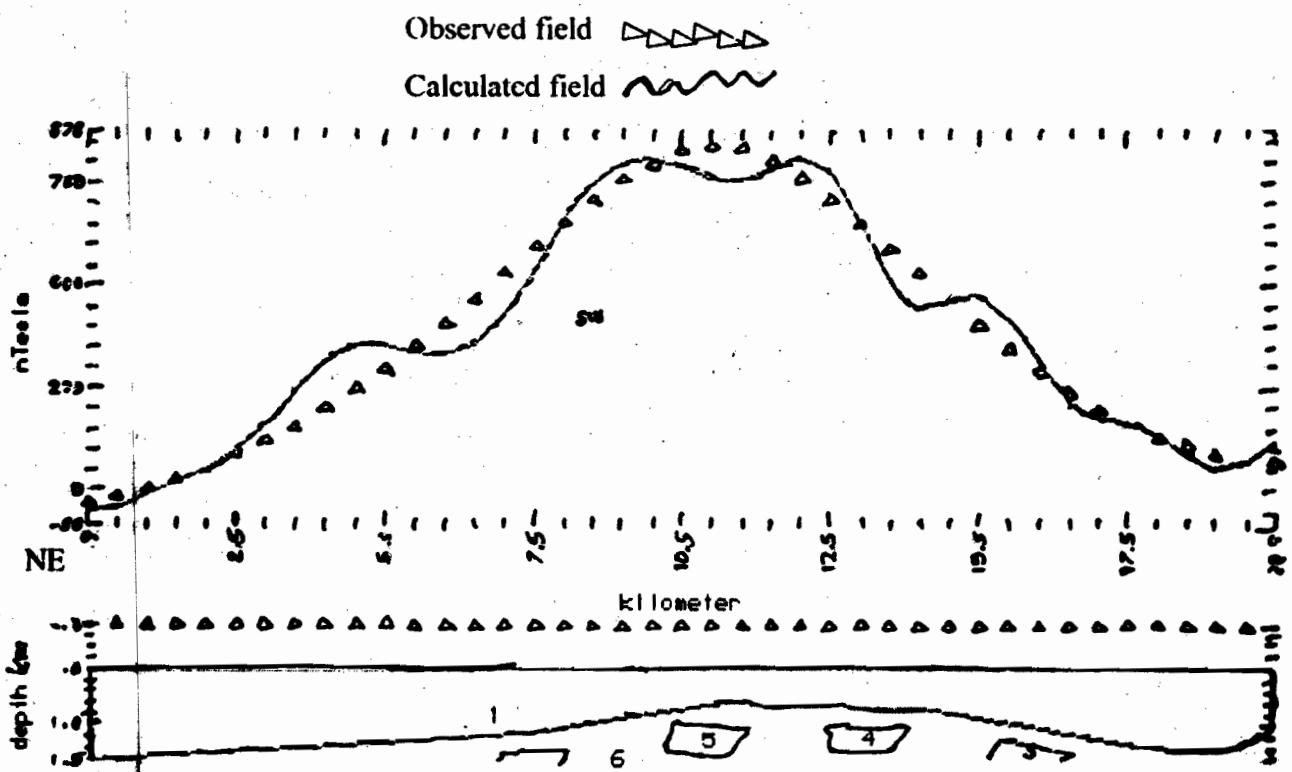

Fig 8c:

Legend: 1= Sedimentary Rocks
2, 3, 4, 5, 6, = basement rocks magnetics

2.5D Modelled profile 3 along Yanga Lau (vanga)

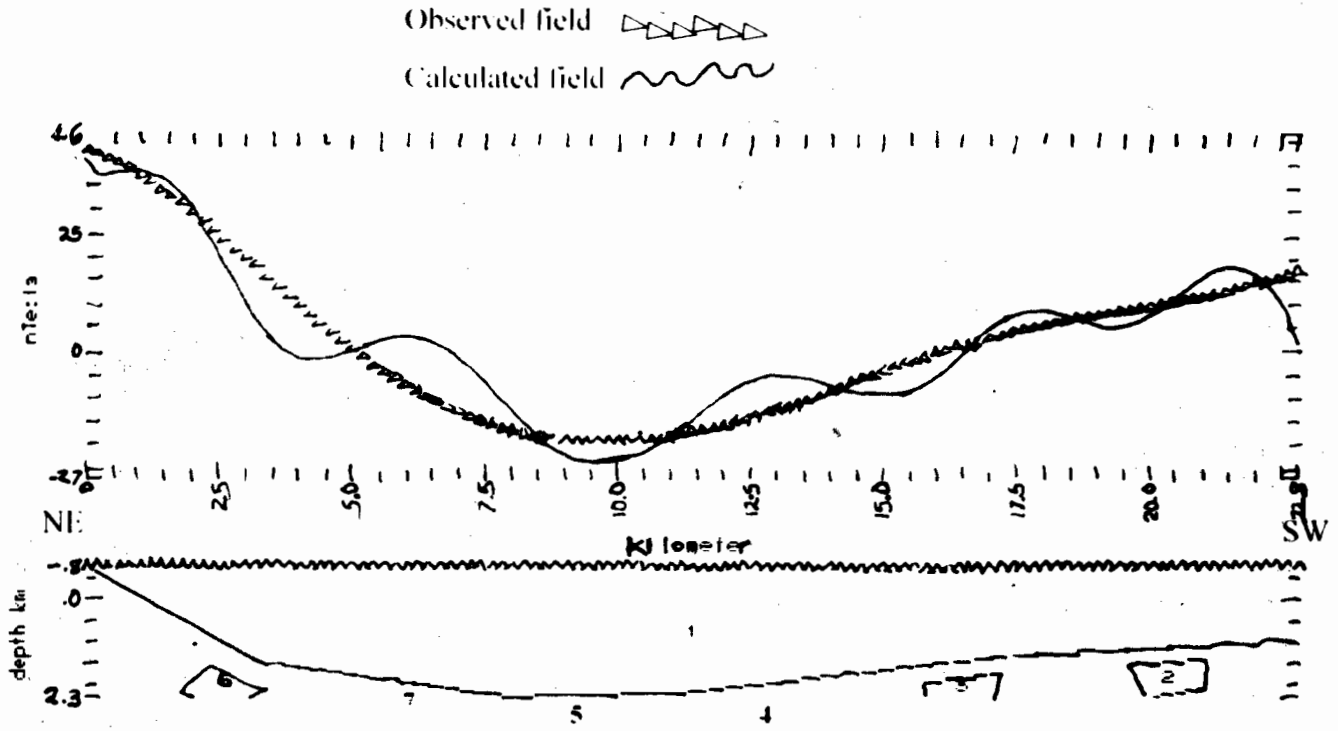

Fig 8d: Legend: 1 = Sedimentary Rocks
2, 3, 4, 5, 6, 7 = basement rocks magnetics

2.5D Modelled profile 4 along Barwa (Lau Basin subsector)

RESULTS

The residual anomaly map (Fig. 4) shows low magnetic contours of -20 to -40nT representing sedimentary rocks from Yola to Muleng axis trending NE – SW while the closely spaced positive anomaly at the NW of muleng represents probably exposed basement rocks. The Lau (Barwa) area also has low magnetic contour of -10 to -20nT of sedimentary origin which trends NW-SE and terminates towards Yanga area with high positive magnetic contours of +40nT. this trend runs from Yanga cutting between Lau (Barwa) and Yola. this is probably the Laminde Anticline

The upward continuation map (Fig 5) reveals two major lineament trends. The Yola to muleng axis indicates a NE-SW trend while the Lau (Barwa) to Yanga axis indicate a NW-SE trend. The deeper lineament trends are better revealed and their orientation expressed clearly since the upward continuation filtering technique has eliminated shallow seated lineament trends. Results from the spectral analysis and analytical signal depth maps (Fig 6 – 7) reveals two sub-basins which are the Lau sub-basin with an average sediment thickness ranging from 2.0 – 3.5km, and the Yola sub-basin whose sediment thickness ranges between 2.0 to 2.5 km. The above results correlate well with depth estimates from the modeled profile (Fig 8a –d), which indicates that the basin configuration is that Horst and Garben with normal faulting. Sediment thickness increases in the downthrown blocks (Graben) with total intensity field values of -10nT to -30nT and decreases in the upthrown blocks (Horst) with values from -5nT to +23nT. Intrusive rocks are characterized by higher values of total intensity field from +23nT - +44nT. The modeled profiles indicate that the Yola sub-basin is characterized by four intrusive bodies with a sediment thickness that ranges from 2.1 km along Muleng to 2.8 km at Yola (Fig. 8a – b).

The Lau area of Barwa to Yanga has no intrusions and indicates a sediment thickness of 1.6 km to 2.3km over the Grabens and 1.2 to 1.0 km on the Horst. The sediments increase in thickness from the Yanga towards the Barwa areas (Fig. 8c – d).

The above models gave a good match between the calculated and the observed curves thus yielding a good structural configuration of the subsurface features (Olagundoye, 2004).

DISCUSSION/CONCLUSION

The Yola arm of the Upper Benue Trough has been studied to some detail using aeromagnetic data to unravel the subsurface basin configuration. Prior to this work no detailed modeling of the subsurface structures was made. The result obtained in this study corroborates that of other workers in adjacent sub basins (Okereke and Ofoegbu 1989, Nur 2000, Shemarg *et al.* 1989) in terms of orientation of the lineaments trend and average depth estimates. This study however highlights structure and basin configuration that has never been revealed. The study reveals an anticlinal feature of a positive magnetic high within the area with latitudes 9°5' to 9°7' and longitudes 11°5' to 11°7'. This feature is prominent on residual and basement depth maps. The area with basement and intrusive rocks are generally shallower as a result of the tectonic upliftment/emplacement of these rocks

The result has identified two sediment filled Troughs which may have good hydrocarbon prospects given that the areas has an appreciable sediment thickness of 2.0 -3.5 km as revealed by the spectral analysis and analytical depth maps. However, the identified intrusives within the Yola – Muleng areas makes it less favourable for hydrocarbon prospecting than the Lau – Yanga axis which has no intrusives. The Yola area may generate hydrocarbons but with the presence of numerous intrusive bodies, such generated hydrocarbon is likely to be "Overcooked" or well pass the oil window to produce only gas. The Lau area remains the best area for hydrocarbon exploration given that it has no intrusive and has an appreciable depth of 2.0 – 3.5 km.

In conclusion the major lineaments are revealed along two directions - the NE-SW and the NW-SE and the modeled architecture reveals an increase in sediment thickness of 2.0 km to 3.5 km toward the South-west and South-eastern portions with a decreasing depth of 1.0 km to 1.5 km towards the Northeast and Southwest portions. The Basin thins Northwards and deepens Southwards.

REFERENCES

Burke, K. and Dewey, J. F., 1973. Plume Triple Junctions: Key Indicators in applying plate tectonics to old rocks. J. Geol 81: 406-436.

Corredor, F., Shaw, H. J. and Bilotti, F. D., 2005. Structural Styles in Deep Water Fold and Thrust Belts of the Niger Delta. American Association of Petroleum Geologist Bulletin, 89: 753-780.

Dobrin, M. B and Savit C. H., 1988. Introduction to Geological Prospecting (4th Ed) New York: Mc Graw – Hill book Company

Ferdi, M. Quarta, T. and Santis, D. A., 1977. Inherent Power-Law Behaviour of Magnetic Field Power Spectra from a spector and Grant ensemble. Geophyiscs, 62(4): 1143-1140.

Hahn, A. Kind, E. G. and Mishra, D. C., 1976. Depth Estimated of Magnetic Soures by means of Fourier Amplitude Spectra. Geophysical Prospecting 24 287-308.

Jacobsen, B. J., 1987. A case for upward continuation as a standard separation filter for potential field maps Geophysics 52(8): 1138 -1148

Nabighian, M. N., 1972. The analytical signal of two dimensional magnetic bodies with polygonal cross section; It's properties and use for automated anomaly interpretation Geophysics, 37(3): 507-517

Naidu, P. S., 1970. Fourier Transform of Large Scale Aeromagnetic Field Using a modified Version of Fast Fourier Transform. Fast Fourier Transform. PAGEOPH, 81:17-25.

Nur, A., 2000. Analysis of Aeromagnetic data cover the Yola arm of the Upper Benue Trough, Nigeria. Jour. Mining and Geol 36(1): 77-84.

Nwogbo, P. O. Ojo, S. B. and Osazuwa, T. B., 1991. Spectral analysis and Interpretation of aeromagnetic data over the Upper Benue Trough of Nigeria. Nigeria Journal of Physics, 3: 128-141.

Okereke, C. S. and Ofoegbu, C. O., 1989. Gravity and Magnetic data cover the Yola arm of the Upper Benue Trough (1989). In C. O. Ofoegbu (Ed) The Benue Trough: Structure and Evolution (pp. 161-169). Braun Schwelg: Vieweg and Sohn.

Olade, M. A., 1975. Evolution of Nigeria's Benue Trough (Aulacogen): A tectonic model, Geol Mag 112:575-583.

Olagundoye, O. O., 2004. Basin Structure in the Anambra Frontier Basin, SE Nigeria. Implications for hydrocarbon potential. Unpublished P.hD thesis University of Calabar, Nigeria.

Philips, J. D., 1987. Potential field geophysical software for the PC, Version 2.2 U.S. Geological Survey open-file report 97-725, 1-32.

Shemang, E. M. Ajayi, C. O. and Umego, M. N., 1988. The Structure of the Gongola arm of the Upper Benue Trough as revealed by gravity and magnetic studies. NAPE Bulletin, 13(1): 50-69.

Shuey, R. T., 1972. Application of Hilbert Transforms to magnetic profiles. Geophysics 37:1043-1045.

Webring, M., 1985. MINC; A gridding programme based on minimum Curvature U S Geological Survey open-file – report, 81-1224, 1-41.

Wright, J. B., 1981. Review of the origin and Evolution of the Benue Trough in Nigeria – Earth Evolution Sciences. 1(2) 98-103.